FABRIC

Feasibility analysis and development of on-road charging solutions for future electric vehicles

Report on effect of up scaling to vehicle fleet and energy grids

Deliverable No.		D 5.4.1	
Workpackage No.	WP 5.4	Workpackage Title	Integrating EV with ICT, transfer & grids
Authors		Hans Bludszuweit, Ezio Spessa, Mattia Venditti, Juan de Blas, Panagiotis Papadimitratos	
Status		Final	
Dissemination level		Public	
Project start date and duration		01 January 2014, 54 Months	
Revision date		2018 - 06 - 17	
Submission date		2018 - 06 - 18	

This project has received funding from the European Union's Seventh Framework Programme for research, technological development and demonstration under grant agreement no 605405

TABLE OF CONTENTS

LIST OF FIGURES

LIST OF TABLES

LIST OF SELECTED ABBREVIATIONS

ABBREVIATION	DESCRIPTION
AADT	Annual Average Daily Traffic
AER	All-Electric Range
BEC	Battery Energy Consumption
BES	Battery Energy Storage
BEV	Battery Electric Vehicle
BS-DWPT-EV	Battery-Shrink DWPT-EV
CO_2	Carbon Dioxide
CV	Compact Vehicle
DC-EV	Dynamic Charging EV
DX.X.X	Deliverable X.X.X
DWPT	Dynamic Wireless Power Transfer
LDV	European Commission
EER	Effective e-Range
EES	Energy Storage System
EV	Electric Vehicle
GDP	Gross Domestic Product
GEC	Grid Energy Consumption
HDV	Heavy Duty Vehicle
ICE	Internal Combustion Engine
ICT	Information and Communication Technology
LCA	Life Cycle Analysis
LCC	Life Cycle Cost
LCOE	Levelised Cost of Energy
LDV	Light Duty Vehicle
LDCV	Light Duty Commercial Vehicle (delivery van)
LHV	Lower Heating Value of the fuel
OEM	Original Equipment Manufacturers
PHEV	Plug-in Hybrid Electric Vehicle
RE-DWPT EV	Range-Extended DWPT-EV
RES	Renewable Energy Sources
SECC	Specific Energy Consumption Cost (c€/km)
SoC	State of Charge

ABBREVIATION	DESCRIPTION
SP	Sub-Project
SUV	Sports Utility Vehicle
TCO	Total Cost of Ownership
TEN-T	Trans-European Transport Network
TTW	Tank-to-Wheel
TX.X.X	Task X.X.X
UC	Use Case
V2G	Vehicle to Grid
VEC	Vehicle Energy Consumption
VMT	Vehicle Miles of Travel
WP	Work Package
WPT	Wireless Power Transfer
WTT	Well-to-Tank
WWT	Well-to-Wheel

REVISION CHART AND HISTORY LOG

REV	DATE	REASON
0.1	09/03/2016	CIRCE: Deliverable structure, Table of Contents (first draft)
1.0	31/03/2016	CIRCE: Agreed version of ToC
1.1	19/04/2016	QiE: Revised ToC with some more detail on section 3.7
1.3	16/05/2016	POLITO: Revised ToC with more detail on chapter 2
1.4	23/05/2016	Final ToC: QiE: More details on section 3.7
1.5	07/11/2016	Final ToC: minor modifications
2.3	05/09/2017	CIRCE: New content in Chapter3
2.5	29/09/2017	CIRCE: New content in Chapter3
2.6	06/11/2017	CIRCE: New content in Chapter3: section 3.6, integration of solar and wind.
2.7	10/11/2017	POLITO: New content in Chapter2 CIRCE: modified Chapter 3 according to 100 km/h reference speed.
2.8	28/02/2018	POLITO: New major content in Chapter2 (model results)
3.0	30/03/2018	CIRCE: First version for peer review (still to be completed: Chapter 2 and 4, Section 3.4.2, References, Conclusions)
3.1	27/04/2018	QiE: major contributions to Chapter 4 and document structure (Introduction and Chapter 3), Periurban Scenario added.
3.2	07/05/2018	CIRCE: Chapter 3 completed (additions/modifications in sections 3.4.2, 3.4.3, 3.6.4 and 3.6.5)
4.0	20/05/2018	POLITO: Revised Chapter 2, CIRCE: revised reference list from chapter 2 and conclusions; Second version for peer review (still to be completed: Chapter 4, Conclusions)
5.0	17/06/2018	Final revision after peer-review. Revised simulation results in chapter 2, modified assumptions for urban bus grid connection, completed chapter 4 and conclusions.
6.0	18/06/2018	Final version

EXECUTIVE SUMMARY

The main objective of FABRIC project was the assessment of feasibility of dynamic wireless power transfer (DWPT) for electric vehicles. The objective of this document is to present an estimation of possible effects of the up-scaling of DWPT systems to electric vehicle fleets and electricity grids. Three basic scenarios have been used as most probable for introduction of DWPT systems the motorway scenario (e-Corridor), the periurban scenario (e-Launcher) and the scenario about urban buses (e-Trench).

As a first step, based on previous work in FABRIC, effects of DWPT at vehicle level is analysed. A vehicle performance model has been developed to calculate well-to-wheel (WTW) energy consumption and CO_2 emissions comparing ICE drivetrains and battery electric vehicles (BEV) with the option of DWPT. The main conclusion of this exercise is that the introduction of DWPT increases WTW energy consumption and CO_2 emissions due to the currently 80% charging efficiency of DWPT systems. The gains due to reduced vehicle weight in the "battery-shrink" strategy are substantial for heavy vehicles and buses. The WTW energy consumption of electric vehicles depends very much on the electricity mix. The adopted EU-mix considers that for each kWh of electricity delivered to an EV, 2.95 kWh of primary energy are needed. As a result, BEVs only show slight advantages over ICEs (at most 30%) and electric heavy-duty vehicles even consume more energy than ICE ones. It is acknowledged that the transition to renewable energies will reduce WTW energy consumption considerably for electricity in general. Regarding CO_2 emissions, the advantage of all electric options will become more visible.

The effect on the electricity grid of upscaling DWPT has been assessed for the three scenarios selected. The main conclusions of the study are that the expected electricity consumption will be modest at European level (only 5% of expected EV demand), and will pose no significant problems for integration in the electricity grid. 10 GW of RES would provide annual zero net energy to cover this demand. Major advantages for solar integration have been identified in this deliverable, as demand occurs mainly during daylight hours (>50% self-consumption possible for motorway traffic patterns). Local energy storage is able to smooth out fluctuations on a 24-h horizon (0.25 kWh/client), while seasonal availability of renewable energy needs to be addressed otherwise (5.5 kWh/client). 60 million DWPT clients are estimated by 2050, representing 30% of all EVs.

CO_2 emissions of electrified traffic will tend to zero at the pace that emissions for electricity generation are reduced. On European level, there are currently huge differences between countries, although the EC roadmap suggests that by 2050 emissions from electricity generation will have diminished almost to zero.

The cost for additional grid infrastructure has been estimated to be approximately 900 million € for Europe in a period of 30 years. This amount would be 0.006 % of 2017 EU GDP which was 15.3 trillion €. It has been found that 10 GW of solar and wind power would be needed. Considering 2017 average costs of 1.3 Million €/MW for RES (onshore wind and solar), installing 10 GW would require investments of 13,000 Million € EU-wide in 30 years. In the light of the European policy against climate change, 10 GW is a very small number anyway.

1 INTRODUCTION

1.1 General

This deliverable presents an estimation of possible effects of the up-scaling of dynamic wireless power transfer (DWPT) systems to vehicle fleets and electricity grid. The work is based on other deliverables from the FABRIC project but considers also information from other projects. In Figure 1 the relationships are shown schematically. Also, the FABRIC deliverables which are fed by this report are included.

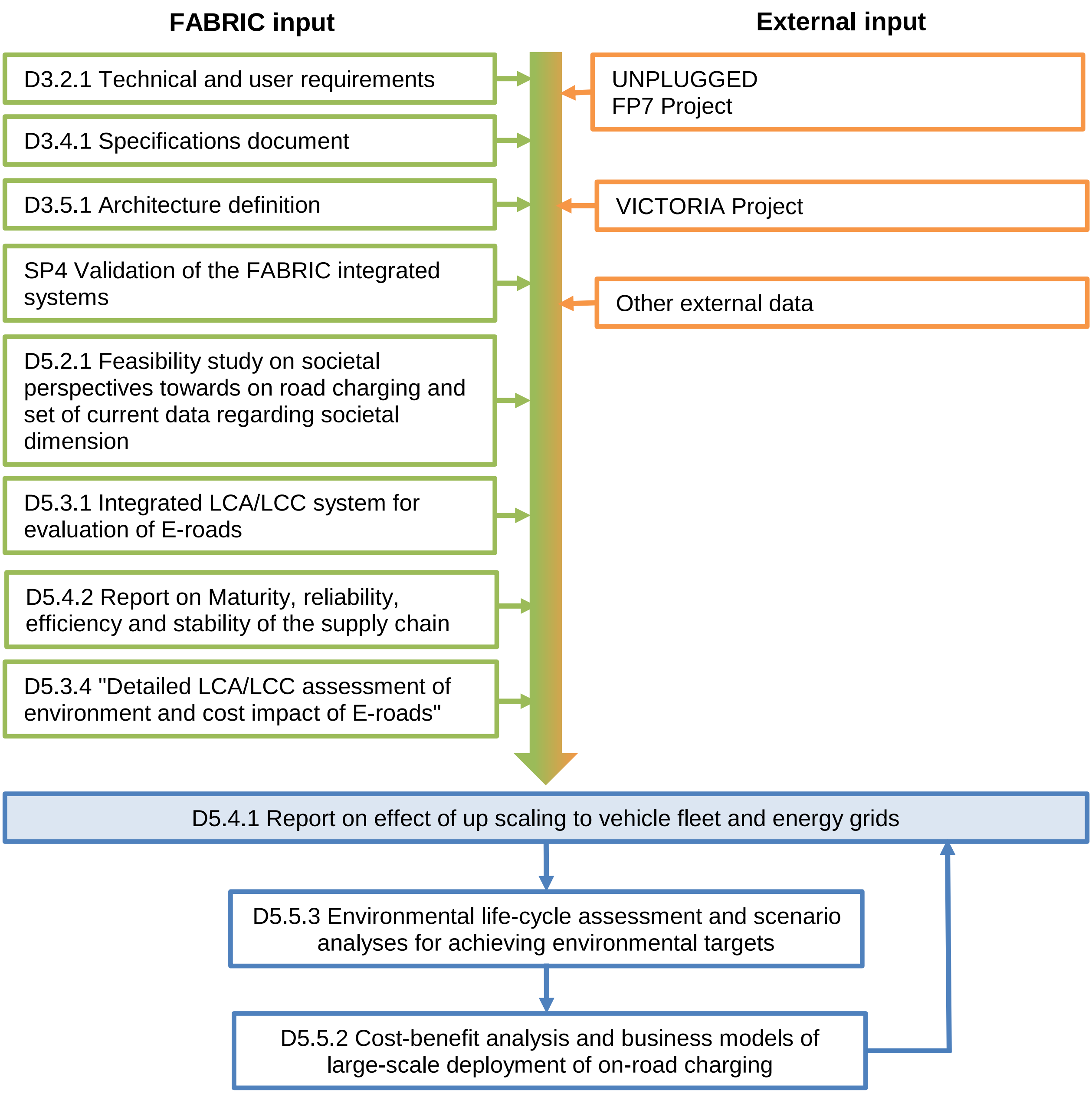

Figure 1: Relationship of the present deliverable D5.4.1 with FABRIC project and external sources of information

In the framework of the work presented in the deliverable, the requirements, specifications and architecture considerations obtained in SP3 of FABRIC are put in a wider context.

1.2 Contribution to FABRIC objectives

The main objective of FABRIC project was the assessment of feasibility of on-road charging solutions based on dynamic power transfer. The present D5.4.1 combines technical and economic information created in SubProjects 3, 4 and 5, in order to create a possible scenario to analyse the effects of an up-scaling of DWPT-EVs on the electricity grid.

Specifically, the main goal of D5.4.1 is to determine:

- the expected energy requirements at grid level in Europe considering the proposed deployment scenarios for DWPT EVs
- the impact on costs
- the environmental impact
- whether energy and power needs can be covered by renewable energies (on site or remote), and their impact at system level.

1.3 Deliverable structure and methodology

Chapter 1 is an introductory chapter that specifies the objective of the document, target audience and structure of the analysis.

In **Chapter 2**, a vehicle model is developed to assess the effect of dynamic power transfer on energy consumption, CO_2 emissions and costs.

Chapter 3 analyses the impact of dynamic charging on the electricity grid. Possible grid architectures are discussed for urban and extra-urban applications. Based on traffic density patterns and consumption per vehicle, consumption patterns are obtained and evaluated.

Chapter 4 determines the overall impact of the e-Corridors deployment at European level in terms of energy and power requirements, environmental footprint and costs.

Finally, **Chapter 5** is dedicated to the concluding remarks.

1.4 Initial assumptions for calculations

FABRIC has identified in its D5.3.4 three scenarios as most likely to occur in the near future in relation to the dynamic charging technology. They are described below:

1. **Motorway Scenario**. In 2030, we can expect dedicated external lanes (e-Corridors) of 25 km length (in both directions) for dynamic charging of light and heavy electric-vehicles in the most crowded motorways (gaining travel time) between two spots at about 400 to 600 km and

providing a range extension of 10% to 20%. The TEN-T infrastructure (larger motorways with 3 to 4 lanes per direction) will be the most appropriate for the **e-Corridors** set up. In 2050, the expertise gained along 20 years will lead to use one of the motorway lanes instead of one constructed externally, reducing costs (**e-Roads**).

2. **Periurban Scenario.** Dynamic charging of heavy vehicles and buses in areas with high density traffic, from periurban logistic centres, ports, etc. to the city centre or among close cities (intercity buses) travelling a daily distance of around 250 km with e-Corridors of 10 km length. It will be highly recommended to set up business contracts between Industry Service companies and the infrastructure owners to ensure a minimum number of daily charging events in the e-Corridors named here as **e-Launchers** due to its short extension (10 km).
3. **Urban Scenario**. This will likely be the first entry point in 2030 using bus stops as static charging points and some trenches ahead summing up 25 m for dynamic charging (**e-Trenches**). Cities with trolley lanes will be easily adaptable for dynamic charging if the number of e-buses is sufficient to justify the infrastructure investment.

According to D5.5.2, the deployment process will be as follows for a given very congested motorway with a daily traffic (AADT) per lane of 18.000 vehicles.

ASSUMPTIONS FOR THE MOTORWAY TRAFFIC	No.	Unit
Length e-corridors	25	km
Daily Traffic per lane in selected motorways (ADDT)	18,000	units
Number of lanes	3	units
Total number of daily traffic	54,000	units
Light vehicles	88	%
Total number of daily light vehicles	47,520	units
Total number of daily light vehicles/lane	15,840	units
Heavy vehicles	12	%
Total number of daily heavy vehicles	6,480	units
Total number of daily heavy vehicles/lane	2,160	units

Table 1. Main assumptions for a given congested motorway where an e-Corridor will be placed.

In Table 2, the expected number of EVs (light and heavy) crossing and charging at the e-Corridors in 2030, 2040 and 2050 are shown. Note that the number of e-Corridors in motorways in the last line of the table refers to number of units installed in each decade (2020-2030, 2030-2040 and 2040-2050), summing up to a total of 32 e-Corridors by 2050.

		BASIC SCENARIO (without e-Corridors)						FABRIC SCENARIO (with e-Corridors)					
	LIGHT VEHICLES IN MOTORWAYS	**2,030**		**2,040**		**2,050**		**2,030**		**2,040**		**2,050**	
1	Percentage of fleet that it is electric	25	%	44	%	58	%	25	%	44	%	58	%
	Light EVs	11,880	units	20,909	units	27,372	units	11,880	units	20,909	units	27,372	units/day
2	Nº electric vehicles that use motorways	50	%	60	%	70	%	70	%	80	%	100	%
	Light EVs in motorways	5,940	units	12,545	units	19,160	units	8,316	units	16,727	units	27,372	units/day
3.	No. Of light EVs equiped with WPT (dynamic charging)	0	%	0	%	0	%	60	%	75	%	100	%
	Light EVs-WPT in motorways	0	units	0	units	0	units	4,990	units	12,545	units	27,372	units/day
3	Users that recharge in motorway superchargers	20	%	20	%	20	%	20	%	30	%	40	%
	Light EVs charging in supercharger in motorways	1,188	units	2,509	units	3,832	units	1,663	units	5,018	units	10,949	units/day
4	Users that recharge in motorway e-corridors							10	%	20	%	30	%
	Light Evs-WPT charging in e-corridors in motorways							832	units	3,345	units	8,211	units/day
	% of users charging in e-corridors/EVs equiped with WPT							17	%	27	%	30	%
	HEAVY VEHICLES IN MOTORWAYS	**2,030**		**2,040**		**2,050**		**2,030**		**2,040**		**2,050**	
5	Percentage of fleet that it is electric	25	%	44	%	58	%	25	%	44	%	58	%
	e-HDVs	1,620	units	2,851	units	3,732	units	1,620	units	2,851	units	3,732	units/day
6	Nº electric heavy vehicles that use motorways	10	%	20	%	30	%	30	%	60	%	100	%
	e-HDVs in motorways	162	units	570	units	1,120	units	486	units	1,711	units	3,732	units/day
7	No. Of e-HDV equiped with WPT (dynamic charging)	0	%	0	%	0	%	60	%	75	%	100	%
	e-HDVs-WPT in motorways	0	units	0	units	0	units	292	units	1,283	units	3,732	units/day
8	Users that recharge in motorway superchargers	20	%	20	%	20	%	20	%	30	%	40	%
	e-HDV charging in supercharger in motorways	32	units	114	units	224	units	97	units	513	units	1,493	units/day
9	Users that recharge in motorway e-corridors							10	%	20	%	30	%
	e-HDV charging in e-corridors in motorways							49	units	342	units	1,120	units/day
	% of users charging in e-corridors/EVs equiped with WPT							17	%	27	%	30	%
10	Nº of e-corridors in motorways	0	units	0	units	0	units	10	units	10	units	12	units

Table 2. Deployment forecast in motorway scenario.

The assumption in D5.5.2 is that all EVs in 2030 will have the possibility for static/stationary wireless charging and will have autonomous driving features to support aligning. As a result, 80% DWPT efficiency will be achieved on average. End users will be willing to add the dynamic charging package (sold as an option) of approximately 1000 €/unit, provided that an e-Corridor exists close to their centre of operations and the cost-benefit analysis will be positive for them.

The same exercise was done for the periurban scenario only applied to heavy vehicles in motorways close to cities with a reduced e-Corridor length of 10 km (e-Launcher). The assumption here is that the drivers of such vehicles will be mostly professionals (service companies) and the price of electricity will be cheaper (no taxes and VAT). Therefore, the business model is more positive, and the number of e-Launchers will be higher (400). In Table 3 the deployment forecast for the periurban case (e-Launchers) is shown. Similar to the motorway case, the number of e-Launchers (last line of the table) refers to the number of units installed in each decade, summing up to a total of 400 e-Launchers by 2050.

PERIURBAN HEAVY VEHICLES	BASIC SCENARIO (without e-Launchers) 2,030		2,040		2,050		FABRIC SCENARIO (with e-Launchers) 2,030		2,040		2,050	
Percentage of fleet that it is electric	25	%	44	%	58	%	25	%	44	%	58	%
e-HDVs	1,620	units	2,851	units	3,732	units	1,620	units	2,851	units	3,732	units/day
Nº e-HDV that moves in urban and periurban areas	100	%	100	%	100	%	100	%	100	%	100	%
e-HDVs in periurban areas	1,620	units	2,851	units	3,732	units	1,620	units	2,851	units	3,732	units/day
No. Of light EVs equiped with DWPT (dynamic charging)	0	%	0	%	0	%	60	%	75	%	100	%
e-HDVs-DWPT in periurban areas	0	units	0	units	0	units	972	units	2,138	units	3,732	units/day
e-HDV Users recharging in headquarters or urban static c	100	%	100	%	100	%	100	%	100	%	100	%
e-HDV charging in supercharger in headquarters	1,620	units	2,851	units	3,732	units	1,620	units	2,851	units	3,732	units/day
e-HDVs users that recharge in periurban e-launchers							50	%	62	%	83	%
e-HDV charging in e-launchers in periurban							810	units	1,768	units	3,098	units/day
% of users charging in e-launchers/e-HDV equiped with WPT							83	%	83	%	83	%
Nº of e-Launchers in periurban areas	0	units	0	units	0	units	80	units	120	units	200	units

Table 3. Deployment forecast in periurban scenario (e-Launchers).

D5.5.2 concludes that the urban scenario applied to public bus fleets will be the most positive, if the considered assumptions are fulfilled. An exercise was done considering a base case scenario with 300 to 400 e-buses operating on forty routes in a city with around 750,000 inhabitants. The figures reflect that converting the whole fleet to DWPT e-buses (400 buses), considering 25 m of static and dynamic charging at each bus stop, 18 round trips and 1,080 bus stops in total, the system shall be sustainable at a cost equivalent to using a conventional bus fleet. In Table 4 the deployment forecast for the urban case (City Buses) is shown. As in the two cases above, the number of cities with DWPT bus systems (last line of the table) refers to the number of systems installed in each decade, summing up to a total of 200 cities in 2050.

URBAN SCENARIO (CITY BUSES)	BASIC SCENARIO (without e-trenches) 2,030		2,040		2,050		FABRIC SCENARIO (with e-trenches) 2,030		2,040		2,050	
Case study (200,000 inhabitants city). Nº buses	400	units	400	units	400	units	400	units	400	units	400	units
Conventional urban buses	200	units	100	units	0	units	100	units	50	units	0	units
No e-buses	200	units	300	units	400	units	300	units	350	units	400	units
Nº e-buses equipped with DWPT							300	units	350	units	400	units
Nº km of static/dynamic charging (25 m per bus stop * 1.080 stops)							27.0	km	27.0	km	27.0	km
Nº of e-buses charging in one e-trench per day (40 routes)							135	units	158	units	180	units
Nº of cities with dynamic/static charging at bus stops.							40	units	60	units	100	units

Table 4. Deployment forecast in urban scenario.

The bus scenario will have its best application in those cities with tramways or trolley buses in operation, as electricity at suitable power levels will be available close to the bus stops. In 2017 the number of EU cities with tramways reached 280, according to a recent press release from “Ecologistas en acción” [1]. We consider 200 of those cities as a possible scenario for the penetration of DWPT e-buses, with 40 in 2030, additional 60 in 2040 and finally, 100 more in 2040.

Additionally, a discussion is included in section 3.3.4 of the present deliverable regarding an additional deployment option for taxis in those cities where DWPT buses are introduced, in order to explore the possibility of taxis sharing the same charging infrastructure. Taxis use much less energy per unit and it can be considered that a similar number of taxis will be on the street compared to buses. It should be mentioned, that the taxi fleet might double bus fleet, but

according to the consulted literature, the effective number of vehicles circulating, is similar to the one of buses. An analysis of shared use of the infrastructure (taxis and buses) revealed an additional charging power of not more than 1 MW, compared to 7.5 MW peak demand of buses, as demand peaks do not coincide. As a conclusion, the same infrastructure might possibly be able to absorb additional demand from taxi charging, increasing only slightly its nominal power.

Despite positive feasibility from the infrastructure perspective, typical activity patterns of taxis are very different and this scenario is discarded here. Taxis normally do not stop at bus stops, so energy absorbed is too low to allow an efficient charging of the taxis. Additional static wireless charging infrastructure for Taxi stations would be needed. Some synergy with bus infrastructure might be found (dedicated electricity distribution grid might be shared), but a separate business case must be developed in order to assess feasibility. It is considered here that extra costs will not be acceptable for the very competitive taxi business, especially with the assumption that by 2030 expected autonomy for light vehicles will be 400 km. According to conversations with taxi drivers in several European cities this autonomy, will be able to cover their daily needs by a comfortable margin. In case taxis are shared in 3-shift service (operation 24/7), the option of ultrafast chargers located at strategic places of the city to be used in service breaks seems more likely. Also, the option of occasional charging at e-launchers on motorways around the cities is considered an incentive not strong enough to invest in the transformation of taxis to DWPT.

D5.5.2 concludes that only in 2050, with a critical mass of EVs on the road, the dynamic charging framework will be sustainable. Before that, some incentives from governments will be required. Although it is still unclear how the end-users may decide, it is considered here that they will be willing to pay for such service (dynamic charging) for the purpose of calculating the electricity requirements in the best case. The next tables summarise the main assumption presented above.

In Table 5 the assumed forecast for the number of installed infrastructures in Europe is shown until 2050. It is assumed that numbers are approximately doubled by each decade.

	2,030	2,040	2,050
Motorway	10	20	32
Periurban	80	200	400
Urban Bus	40	100	200
Total	**130**	**320**	**632**

Table 5. Forecast for cumulative installed e-Roads in Europe (e-Corridors, e-Launchers and e-Trenches).

Table 6 summarises for each scenario assumptions regarding the number of EVs, circulating on European e-Roads, based on assumptions on the number of installed DWPT infrastructure and AADT (Annual Average Daily Traffic) on the DWPT lane. While for Motorway and Periurban

scenarios, annual average daily traffic is relevant, for the Urban bus scenario, it is the bus fleet per city.

Horizon	**2030**	**2040**	**2050**
MOTORWAY			
E-Corridors	10	20	32
AADT DWPT-Light Vehicles	832	3,345	8,211
AADT DWPT-Heavy Vehicles	49	342	1,120
Total daily DWPT-EVs in Europe	**8,802**	**73,751**	**298,598**
PERIURBAN			
E-Launchers	80	200	400
AADT DWPT-Heavy Vehicles	810	1,768	3,098
Total daily DWPT-EVs in Europe	**64,800**	**353,549**	**1,239,183**
URBAN BUS			
Cities with E-Trenches	40	100	200
DWPT e-Buses in operation per city	400	400	400
Total DWPT e-buses in operation in Europe	**16,000**	**40,000**	**80,000**

AADT: Annual Average Daily Traffic (vehicles per lane)

Table 6. Total daily DWPT e-vehicles using e-Corridors, e-Launchers and e-Trenches in Europe.

2 VEHICLE LEVEL CONSEQUENCES OF DWPT REQUIREMENTS

2.1 Introduction

In this chapter, the impact of DWPT on well-to-wheel (WTW) energy consumption, CO_2 emissions and total cost of ownership (TCO) is analysed on vehicle level. Results are used as a reference for further projections within this deliverable and in WP55 of the FABRIC project. A simulation model is presented, which was developed specifically for this analysis, estimating energy consumption of different vehicles for a number of different drive trains and driving missions.

The model has been designed in order to provide results which go far beyond the scope of this deliverable, which focuses on the effect of up scaling to energy grids. This is due to the fact that the same model will also serve to give support to further studies in WP55, which include LCC, LCA, business models and sensitivity analyses.

In this report, results will be focused on the 3 reference scenarios: motorway, periurban and urban bus, which imply a reduction of vehicle typologies to passenger cars, heavy vehicles and buses. Nevertheless, the full model is described here in order to give insight into assumptions and complexity of the reference from which simplifications have been applied, in order to obtain a broad view of the effect of upscaling DWPT.

2.2 Overview of the vehicle performance model

Information is gathered from SP3 deliverables as starting point for the analysis. In this framework the vehicle requirements are intended to be expressed in terms of total costs of ownership, weight, energy consumption, CO_2 emissions, effective electric range, charging time at the end of specific driving missions and total time to drive long trips (up to 1000 km). Case studies have been identified based on WP5.1 outcomes.

Table 7 reports the list of the vehicle typologies that have been included in the vehicle performance model. A compact vehicle has been selected to represent an urban taxi, a Sport Utility Vehicle (SUV) as an individual passenger car, a Light-Duty Commercial Vehicle (LDCV) as a delivery van, a BUS as an urban bus and a Heavy-Duty Vehicle (HDV) as a Freight Logistics Truck.

Acronym	Vehicle typology	Vehicle application
CV	Compact vehicle	Taxi
SUV	SUV	Individual passenger car
LDCV	Light duty commercial vehicle	Delivery van
BUS	Bus	Urban bus
HDV	Heavy duty vehicle	Freight logistics truck

Table 7: List of vehicle typologies.

Three macro-categories of powertrains have been modelled for each vehicle class: the conventional vehicle equipped with either the compression-ignition (**Diesel**) or the spark-ignition (**Gasoline**) engine, the Battery Electric Vehicle (**BEV**) and the Dynamic Charging Electric Vehicle (DC-EV, in other FABRIC documents referred to as Dynamic Wireless Power Transfer EV or **DWPT-EV**). DWPT-EV is the solution that this project intends to investigate in terms of **energy consumption, CO_2 emissions, total costs, vehicle sizing, charging time and long-distance limits** (i.e., the vehicle performance), with respect to both the conventional and the BEV solutions. The DWPT-EV solution is equipped with a Wireless Power Transfer (WPT) system that allows the vehicle to receive energy from a dedicated electrified road (here forth it will be mentioned as **e-road**). The gasoline powertrain has been installed only in the SUV class. The performance of each vehicle is simulated with a kinematic model developed in the Matlab environment, over specific driving missions. Driving missions have been selected according to the vehicle class, since WTW energy consumptions and CO_2 emissions are significantly affected by driving conditions. In Table 8 driving missions are listed and Table 9 shows simulated driving missions per vehicle typology.

Acronym	Driving mission
NEDC	New European Driving Cycle
AUDC	Artemis Urban Driving Cycle
AMDC	Artemis Motorway Driving Cycle
J10-15	Japanese 10-15 driving cycle
RDM1	Real Driving Mission-1
RDM2	Real Driving Mission-2
WLTP	Worldwide Harmonized Light Vehicles Test Procedure
MBC	Manhattan Bus Cycle
SORT, SORTx3	Standardised On-Road Test cycle
ETC	European Transient Cycle
WHVC	World Harmonized Vehicle Cycle
HDUDDS	EPA Urban Dynamometer Driving Schedule for Heavy Duty vehicles
CBD	Central Business District
CSC	City Suburban Cycle
HWM	High-Way Mission

Table 8: List of employed driving cycles.

The NEDC, J10-15, AUDC and RDM1 missions have been selected to represent typical conditions for taxi vehicles in urban and suburban patterns. We have also added three extra-urban driving missions for the SUV case (individual car owners), namely the AMDC, WLTP, RDM2.

The driving scenarios for LDCVs are described with the NEDC, J10-15, AUDC, WLTP and RDM1 to represent more severe urban patterns for city logistics company, such as DHL and UPS, with a fleet of vans.

Driving mission	SUV	CV	LDCV	BUS	HDV
NEDC	●	●	●		
AUDC	●	●	●		
AMDC	●				
J10-15	●	●	●		
RDM1	●	●	●		
RDM2	●				
WLTP	●		●		
MBC				●	
SORT, SORTx3				●	
ETC					●
WHVC					●
HDUDDS					●
CBD					●
CSC					●
HWM					●

Table 9: Simulated driving missions per vehicle type.

The MBC and SORT missions can be used for describing the bus urban conditions, while the ETC, WHVC, HD-UDDS, CBD, CSC and HWM missions are suitable to simulating extra-urban and highway driving patterns for a fleet of freight logistics company heavy duty trucks.

We intend to calculate the three terms, namely well-to-tank (**WTT**), tank-to- wheel (**TTW**), well-to-wheel (**WTW**) of energy consumption and CO_2 emissions. We also estimate the weights of the vehicle and its components. In addition, we estimate the initial costs of the vehicle, the operating costs, and the total costs of ownership (**TCO**) as the sum of the two first terms.

Finally, we calculate the effective e-range (**EER**) for BEVs and DWPT-EVs, the time to charge these vehicles after a 100-km trip and the time to travel 1,000 km.

The DWPT-EV solution will be compared to the conventional and BEV ones with reference to the above defined output variables. The model is also prepared to perform a sensitivity analysis of:

1. **Market**: the price of the fuel, the electric energy and of the battery;
2. **E-road**: the maximum e-road charging power, the WPT efficiency, the e-road penetration;
3. **Usage**: the vehicle miles of travel (VMT) and the payload.

2.2.1 Input/output variables and system parameters

The input variables of the vehicle model are:

1. Vehicle class: Compact vehicle, SUV, Light-duty commercial vehicle, bus and heavy-duty vehicle;
2. Powertrain: Diesel, gasoline, BEV, DWPT-EV and RE-DWPT-EV;
3. Driving mission: The set of driving missions depends on the vehicle class.

The output variables of the vehicle model instead are:

1. **Energy consumption**: Three terms are considered, i.e., WTT, TTW and WTW. The TTW term depends on the fuel consumption for the conventional vehicle, on the battery energy consumption (BEC) for the BEV and on the sum of energy consumption at the battery and grid (GEC during dynamic charging) levels for the DWPT-EV solution;
2. **CO_2 emissions**: Three terms are considered, i.e., WTT, TTW and WTW.
3. **Total cost of ownership**: It is the sum of initial and operating costs;
4. **SECC**: Specific Energy Consumption Cost (c€/km) represents the costs per km due to fuel/electricity refilling and vehicle replacement, if necessary (BEV/DWPT-EV);
5. **EER**: effective e-range, i.e., the distance that each BEV/DWPT-EV can cover between two following static charging stages;
6. **Charging time**: It is the time required to fully recharge the battery at the end of a 100km long trip. Two time-estimates are provided in this project, one for the slow charge (1/10 of the fast charge power), the other for the fast charge (the charging power is equal to that available at the e-road for the DWPT-EV of the same class) case;
7. **Traveling time**: it is the time required to drive a 300 km (for CVs, LDCVs and Buses) or a 1000 km (for SUVs and HDVs) trip, considering specific constraints for rest and no-stop driving times.

The system parameters are grouped into four main categories:

1. **Market**: fuel price (€/kg), electricity price (€/kWh), and battery price (€/kWh);
2. **E-road**: e-road efficiency (%), e-road charging power (kW) and penetration (%);
3. **DWPT-EV**: the e-range target (km) and the battery sizing option (DWPT-EV if the battery is downsized according to the estimated energy available from the e-road, RE-DWPT-EV if the battery has as the same size as the equivalent BEV case);
4. **Usage**: Vehicle miles of travel (VMT, km) and payload (kg).

2.2.2 Vehicle powertrains

Table 10 reports the maximum power of each powertrain per vehicle types (kW).

Vehicle typology	Diesel	Gasoline	BEV	DWPT-EV
CV	70	-	70	70
SUV	90	90	110	110
LDCV	100	-	105	105
Bus	270	-	250	250
HDV	340	-	300	300

Table 10: Maximum power (kW) of each powertrain per each vehicle typologies.

One of the most important factor of a BEV powertrain is its battery size (as the maximum energy content available at the battery level), which determines the effective electric range (EER), i.e., the distance that the vehicle can cover starting from the full-charged battery condition. We therefore include this design parameter into the name of each BEV solutions, a BEV200 refers to a BEV that can drive through 200 km with its battery. The battery energy storage (**BES**) is, however, affected by the actual vehicle energy consumption (**VEC**) that depends on the driving conditions. In the “Battery sizing” section, we will explain our assumption required to design the battery.

The DWPT-EV solution can receive additional energy from the infrastructure while driving. There are two options to manage this energy content:

1. **Range extend**: this energy amount increases the EER, in a proportional way to the actual VEC. This solution is referred to as RE-DWPT-EV-X, where X is the obtained EER.
2. **Battery shrink**: the amount allows the energy storage required in the battery to be decreased in order to guarantee a given autonomy distance. This solution is referred to as BS-DWPT-EV-X, where X is the obtained EER.

In this project, the BS-DWPT-EV-X solution is the reference choice, so it is also referred to as DWPT-EV-X.

It should be mentioned here, that while battery-shrink (BS-DWPT-EV) is the reference choice, as it reduces vehicle weight and battery-related CO_2 emissions, the range-extender (RE-DWPT-EV) option has been identified as the most viable business case for the motorway-scenario. Especially for light vehicles, general EV adoption would be low, if autonomy is not increased. A range-anxiety threshold of 400 km has been identified, in order to make EVs main-stream competitors for conventional vehicles, even if realistically, over 90% of all trips are less than 100 km. Reduction of the battery size implies more investment in e-Corridors and there will not be sufficient critical mass of electric vehicles to justify such extra investment. Nonetheless, the battery-shrink option is possible in the peri-urban scenario (light delivery trucks) and definitely the choice for urban buses.

2.2.3 Driving missions

Table 11 reports the main specifications of the driving mission sets per each vehicle class, namely the duration (s), the length (km), the specific energy consumption (at the wheel level) in traction (SEC-tract) and braking (SEC-brake) stages (kWh/km), the average vehicle speed in traction (km/h), the average vehicle power demand in traction (kW), the maximum vehicle speed (km/h) and the average acceleration (m/s^2). Figure 2 shows the distribution of vehicle power demand vs vehicle velocity in traction (white) and braking (grey) stages for the driving mission sets of the SUV (top) and HDV (bottom) classes.

Vehicle Class	Name	Duration	Length	SEC-tract	SEC-brake	V-tract	P-tract	V-max	A-avg
		s	km	kWh/km	kWh/km	km/h	kW	km/h	m/s2
CV	NEDC	1180	10.9	0.09	-0.03	46.8	4.7	120.0	0.21
	AUDC	993	4.9	0.12	-0.08	25.3	4.9	57.5	0.61
	J10-15	660	4.2	0.08	-0.04	35.3	3.9	70.0	0.31
	RDM1	799	8.9	0.08	-0.02	52.5	5.4	92.7	0.19
SUV	NEDC	1180	10.9	0.13	-0.05	46.8	7.3	120.0	0.21
	WLTP	1800	23.3	0.15	-0.06	59.7	12.0	131.3	0.28
	AUDC	993	4.9	0.20	-0.15	24.9	8.7	57.5	0.61
	J10-15	660	4.2	0.14	-0.08	35.3	6.6	70.0	0.31
	RDM1	799	8.9	0.12	-0.04	51.8	8.4	92.7	0.19
	AMDC	1068	29.5	0.19	-0.04	107.1	24.1	148.0	0.19
	RDM2	4841	107.4	0.17	-0.04	89.9	19.7	136.6	0.22
LDCV	NEDC	1180	10.9	0.34	-0.11	46.8	18.5	110.2	0.20
	WLTP	1800	22.6	0.39	-0.12	58.3	28.9	115.1	0.26
	AUDC	993	4.8	0.49	-0.35	25.1	20.5	57.5	0.60
	J10-15	660	4.2	0.34	-0.17	35.3	16.5	70.0	0.31
	RDM1	799	8.8	0.32	-0.09	51.3	21.8	92.7	0.19
BUS	MBC	1089	3.3	1.41	-1.03	17.2	38.5	40.4	0.47
	SORT	545	2.9	1.16	-0.71	29.0	45.1	60.0	0.35
	SORTx3	1635	8.7	1.16	-0.71	29.1	45.2	60.0	0.35
HDV	ETC	1800	29.5	1.12	-0.10	63.8	76.4	91.0	0.08
	WHVC	1800	20.1	1.08	-0.23	50.8	66.6	87.8	0.18
	HDUDDS	1060	8.9	1.26	-0.37	49.7	78.1	93.3	0.26
	CBD	560	3.3	1.07	-0.65	26.6	31.3	32.2	0.31
	CSC	1700	10.7	1.05	-0.49	31.4	46.8	70.4	0.28
	HWM	1000	24.6	1.37	-0.04	90.0	125.5	92.0	0.03

Table 11: Main specifications of the driving mission sets per each vehicle class.

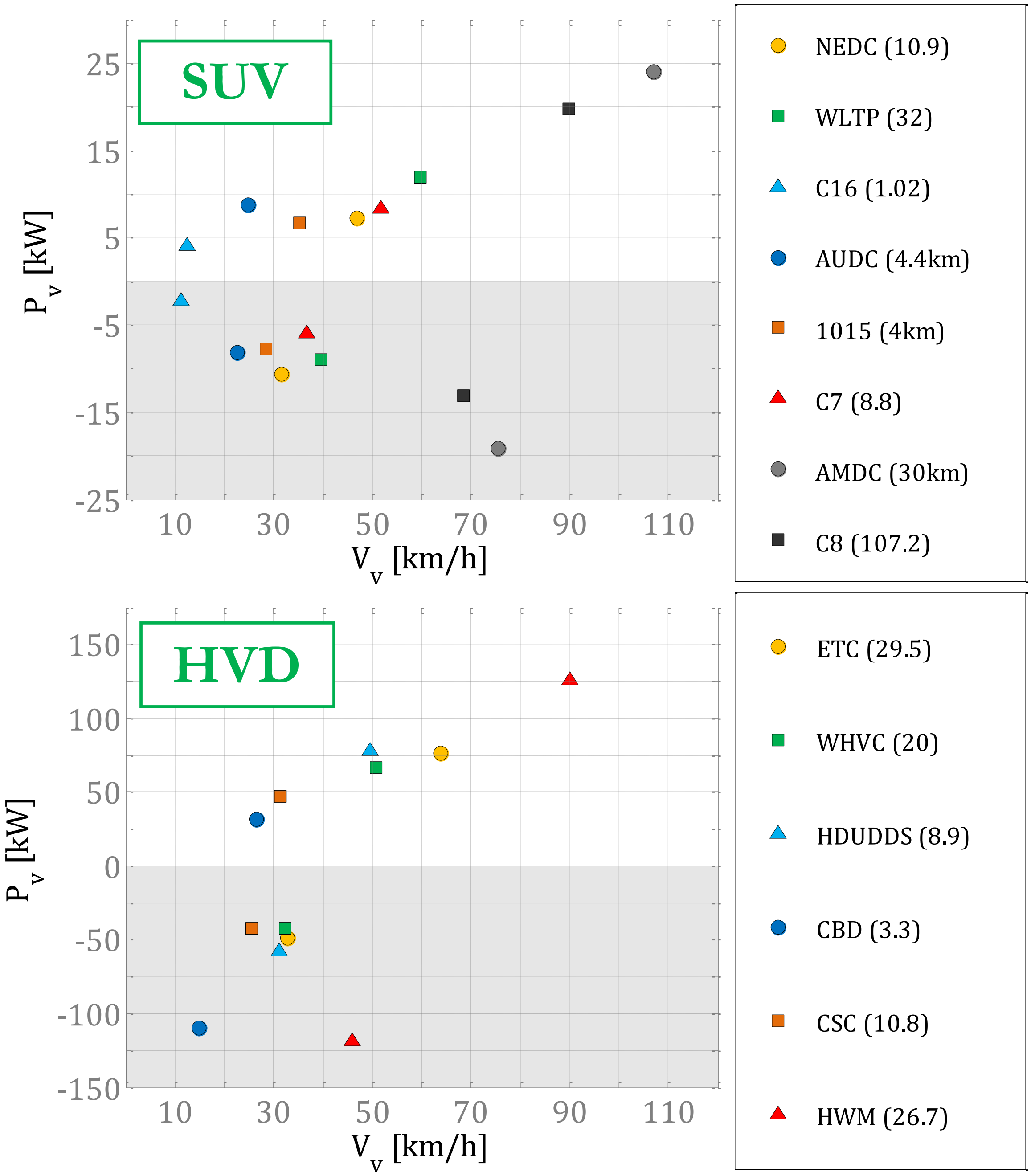

Figure 2: Distribution of vehicle power demand vs vehicle velocity in traction (white) and braking (grey) stages for the driving mission sets of the SUV (top) and HDV (bottom) classes.

2.3 Methodology of the vehicle performance model

2.3.1 E-road parameters

The main parameters of the e-road system have been identified as follows:

1. WPT efficiency, $\boldsymbol{\varepsilon_{er}}$ (%): it represents the power loss from the primary coil of the road and the secondary coils installed on the vehicle. It is mainly affected by misalignment and the air gap between the transmitter and the receiver, the vehicle velocity and the transmitted power;
2. E-road penetration, $\boldsymbol{\delta}$ (%): it is the share of the electrified road network with respect to the total road infrastructure;
3. E-road charging power, $\boldsymbol{P_{er}}$ (kW): it represents the available power at the primary coil to transfer to the vehicle;
4. E-road charging velocity, $\boldsymbol{V_{er}}$ (km/h): it is the average vehicle velocity during the dynamic charging stage;
5. E-road segment length, $\boldsymbol{L}$ (m), it is the length of each continuously electrified segment (it consists of several modules).

We therefore assume that the probability to encounter an e-road segment over a specific driving pattern is equal to the e-road penetration, $\boldsymbol{\delta}$.

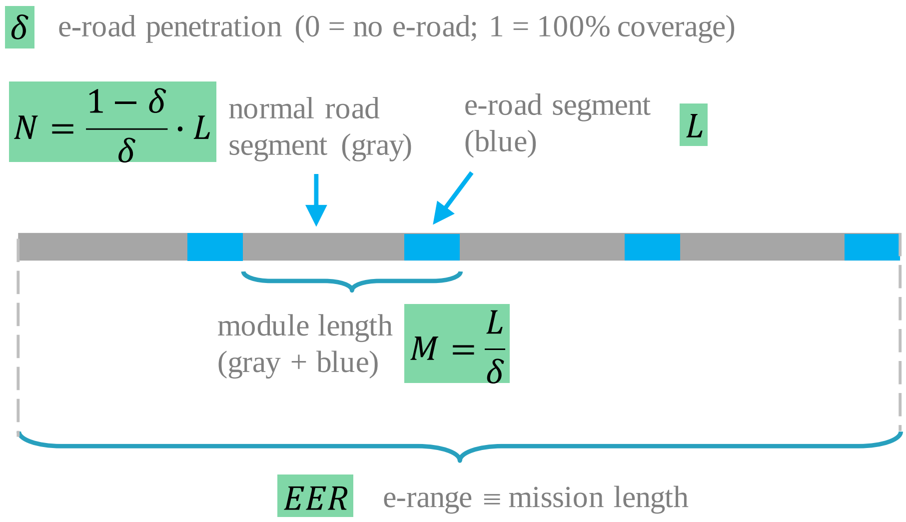

Figure 3: Scheme of the e-road segment distribution over a specific mission.

Figure 3 shows the scheme of the e-road segment distribution over a specific mission. The mission is a sequence of e-road segments (blue) with length $\boldsymbol{L}$ and normal road segments (grey), whose length N. The concatenation of an e-road and a normal road segments is referred to as a module, whose length is M. If we assume that the mission length is equal to the EER of the vehicle

and that the mission exactly contains N_{seg} modules, from the definition of e-road penetration, δ, it follows that:

$$\delta = \frac{L \cdot N_{seg}}{EER}, \qquad EER = (L + N) \cdot N_{seg},$$

and we obtain that:

$$N = \frac{1-\delta}{\delta} L, \qquad M = \frac{L}{\delta}$$

During the actual vehicle simulation over a specific driving mission, whose length is less than the EER of the vehicle, we need to determine the distribution of the e-road segments so that the effective penetration is exactly equal to the δ variable. The number of e-road segments is calculated as:

$$N_{seg} = \left\lceil \frac{D_{mis} \cdot \delta}{L} \right\rceil$$

where the operator $\lceil x \rceil$ rounds its input x to the nearest integer greater than or equal to that input. The length of the e-road segment is adjusted as follows:

$$L' = \frac{D_{mis} \cdot \delta}{N_{seg}}$$

We define two temporal arrays (which store values for each segment) of the starting (ers_{start}) and ending (ers_{end}) locations of the k segment, as follows:

$$ers_{start}(k) = k \cdot \frac{1-\delta}{\delta} \cdot L', \qquad ers_{end}(k) = ers_{start}(k) + L', \qquad \forall\, k = 1, \cdots, N_{seg}$$

The e-road distribution is determined by the variable, i_{er}, which is equal to 1 whenever the vehicle is over an e-road segment and to 0 otherwise:

$$i_{er}(t) = \begin{cases} 1 & if \;\; d(t) \geq ers_{start} \wedge d(t) \leq ers_{end} \\ 0 & otherwise \end{cases}$$

Where the cumulative vehicle distance $d(t)$ at time instant t is calculated as:

$$d(t) = \int_0^t V(t) \cdot dt$$

2.3.2 E-range of the reference BEV for each vehicle typology

One of the most critical design constraints for a BEV architecture is the required autonomy or e-range, i.e., the continuous distance that the vehicle can cover between two consecutive static charging phases. Since the vehicle application differs from one typology to another, we need to specify the reference BEV, in terms of e-road target, for every vehicle class (from CVs to HDVs).

The e-range target of the BEVs affects the total vehicle weight and its retail price, as well as the traveling time required to cover a given driving distance:

1. a 300 km long urban trip for CVs, LDCVs and buses;
2. a 1,000 km long extra-urban trip for SUVs and HDVs.

Each trip is a sequence of sub-trips and rest times. Each trip ends due to one of the following reasons:

1. The battery is drained;
2. The sub-trip time exceeds the admissible time to travel (2 hours for CVs, LDCVs and buses, 4 hours for SUVs and HDVs);
3. The vehicle reaches the end of the trip.

During the rest time, which is defined by the input parameter t_{ch} (h), the vehicle receives power P_{ch} from the station and its battery energy content increases by:

$$\Delta BES = P_{ch} \cdot t_{ch} \cdot \varepsilon_{ch} \cdot \varepsilon_{bat}$$

Where ε_{ch} is the charger efficiency (97%) and ε_{bat} is the battery efficiency when it recharges at P_{ch}.

We have analysed the trade-off between the e-range, the static charging requirements and the traveling time to select the reference BEV for each vehicle typology.

In Figure 4 we report the travel time as a function of the BEV e-range (km) for LDCV (a), BUS (b), SUV (c), HDV (d). The horizontal dashed grey line is reference time of the conventional vehicle, while the travel time of the BEV depends on the charging power P_{ch} (P in the legend) and the charging time t_{ch} (CT in the legend) at the station. Table 12 reports the increment in travel time and vehicle weight of the BEV solution, with respect to the conventional powertrain, and the battery weight share to the vehicle weight, as a function of the e-range (km) per each vehicle class. This allows the reference e-range to be identified as the AER (All-Electric Range) that gives the same "long-trip time" of the reference vehicle (increment equal to 0% in Table 12) and the minimum increment in vehicle and battery weight. The reference e-range has been highlighted in a black box for each vehicle class in Table 12. It is worthwhile observing that for HDV over a long-trip of 1000 km this would lead to 800 km AER with a significant increase in vehicle weight (+33%

with respect to conventional powertrain) and of Total Cost of Ownership (TCO) (more than 3 times with respect to conventional powertrain solution). Therefore, a shorter reference e-range has been selected, considering a trade-off between long-trip time, increment of vehicle weight and of TCO. A more detailed discussion is reported in what follows.

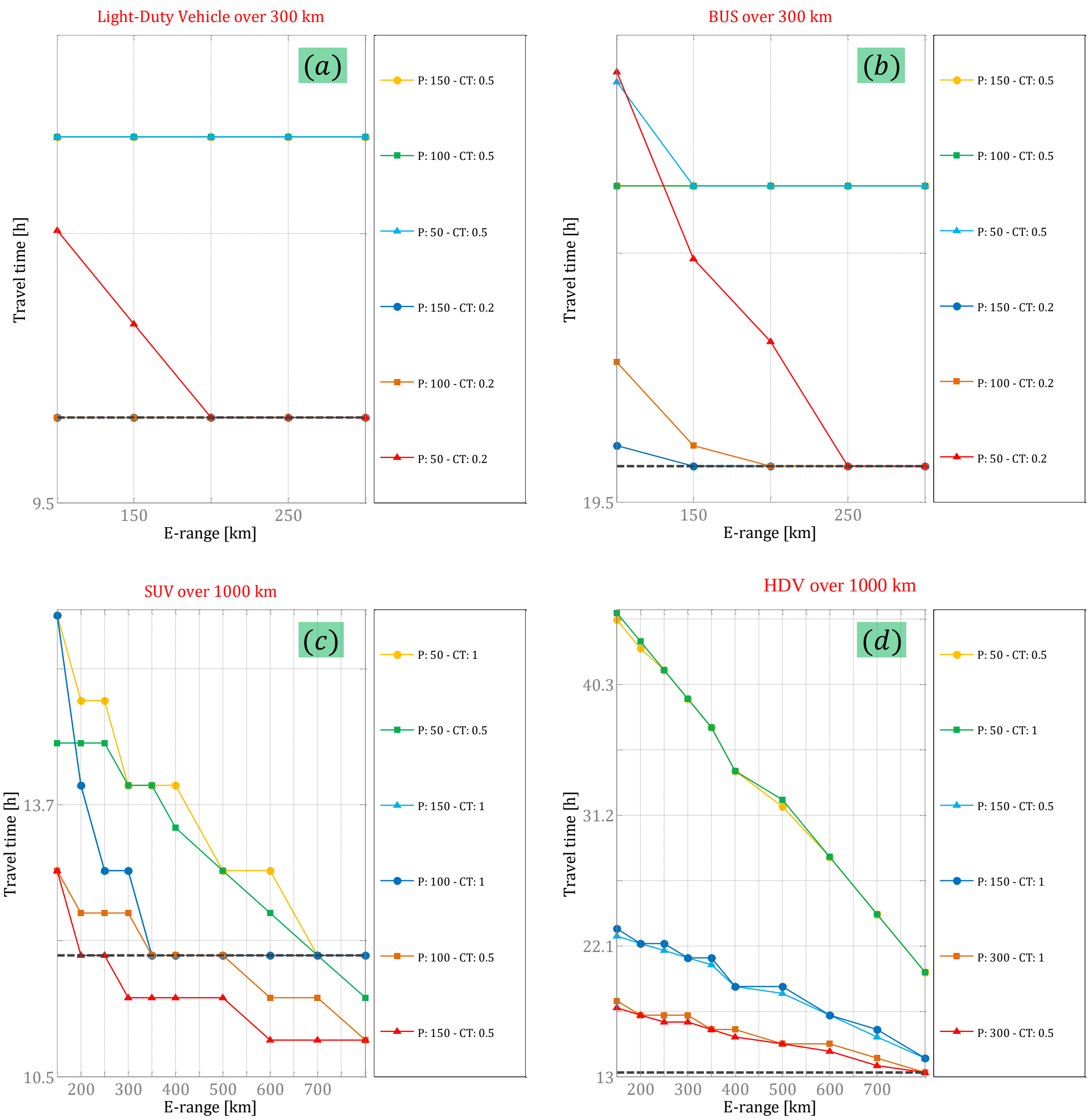

Figure 4: Travel time as a function of the BEV e-range (km) for LDCV (a), BUS (b), SUV (c), HDV (d).

Vehicle Class	AER	Long-trip time	Vehicle weight	Battery weight
	km	%	%	%
CV	100	0.00	-5.61	6.76
	150	0.00	-2.44	9.80
	200	0.00	0.74	12.64
	250	0.00	3.92	15.31
	300	0.00	7.10	17.82
SUV	150	8.38	-0.49	7.08
	200	0.00	1.86	9.22
	250	0.00	4.20	11.26
	300	-4.19	6.54	13.21
	350	-4.19	8.88	15.08
	400	-4.19	11.23	16.87
	500	-4.19	15.91	20.23
	600	-8.38	20.60	23.33
	700	-8.38	25.28	26.19
	800	-8.38	29.97	28.86
LDCV	100	0.00	-1.38	3.61
	150	0.00	0.40	5.32
	200	0.00	2.17	6.96
	250	0.00	3.95	8.56
	300	0.00	5.73	10.09
BUS	100	1.01	0.97	3.63
	150	0.00	2.63	5.35
	200	0.00	4.63	6.99
	250	0.00	6.45	8.59
	300	0.00	8.28	10.13
HDV	150	33.91	3.96	6.98
	200	30.14	6.38	9.09
	250	26.37	8.79	11.11
	300	26.37	11.21	13.04
	350	22.60	13.62	14.89
	400	18.84	15.67	16.71
	500	15.07	20.87	19.99
	600	11.30	25.70	23.07
	700	3.77	30.53	25.91
	800	0.00	35.36	28.56

Table 12: Travel time and vehicle mass increment (%), with respect to the conventional powertrain, of the BEV solution and the share of battery weight to the vehicle weight, as a function of the e-range (km) per each vehicle class.

In the LDCV case (300 km urban trip), the vehicle average speed is 33 km/h. If the station charging power P is 50 kW and charging time CT is 0.2 h (red line with triangle marks in Figure 4a), with BEV150 the travel time to drive 300 km increases from 9.86 h (conventional vehicle) up to 10.5 h (+6%). If the charging power increases to 100 kW, the travel time of the BEV is equal to that of the conventional vehicle for all considered e-range values, i.e. the travel time is not affected by vehicle e-range if we assume that a conventional LDCV vehicle also stops for 12 min every 2 hours of non-stop driving ($t_{ch} = 0.2$). In the LDCV case, we chose 150 km of e-range, since 100 km could be too restrictive for some other driving missions and keeping in mind that

environmental conditions could limit vehicle e-range in real driving conditions. The 150 km e-range does not affect the vehicle weight.

In a similar way, we have also chosen the 150 km e-range for the CV and BUS solutions. CV outcomes are reported in Table 12, BUS results are shown in Figure 4: Travel time as a function of the BEV e-range (km) for LDCV (a), BUS (b), SUV (c), HDV (d).Figure 4b and Table 12.

In the SUV case (1000 km highway trip), the vehicle average speed is 101 km/h. If the station charging power is 100 kW and charging time is 30 min (orange line with square marks in Figure 4c), with BEV e-range of 200 km the travel time to drive 1000 km increases from 11.9 h (conventional vehicle) up to 12.9 h (+8.4%). If the charging power increases to 150 kW, the travel time of the BEV200 is equal to that of the conventional vehicle if we assume that a conventional SUV also stops for 30 min ($t_{ch} = 0.5$) every 4 hours of non-stop driving. Vehicle weight is affected to a limited extent (less than +2% in Table 12).

In the HDV case (1000 km highway trip), the vehicle average speed is 88.7 km/h. An e-range of 800 km with charging power of 300 kW and charging time of 30 min is required to have a travel time which is equal to that of a conventional powertrain (red line with triangles in Figure 4d). However, this leads to an increment of vehicle weight by 36% and requires large batteries on-board, thus significantly limiting payload capacity. Therefore, a penalty on travel time has to be accepted for the reference BEV in this specific case. We chose 400 km of e-range with a 20% penalty in travel time and +16% increase in vehicle weight with respect to a conventional vehicle (Table 12). It is worthwhile observing that the 600 km e-range solution would lead to a 25% increment in the total vehicle weight with respect to a conventional vehicle, with a small benefit only in terms of travel time with respect to BEV400 (the travel time increment reduces to 11% for BEV600 as reported in Table 12), giving a TCO of BEV600 that is almost three times higher than that of a conventional powertrain.

2.3.3 Battery sizing

In this section we present in detail the estimate of the total battery energy storage (BES) required to satisfy the e-range target. The BEV and RE-DWPT-EV (range extender) solutions require a battery that can provide the energy demand for the e-range, as follows:

$$BES = \frac{SVEC^* \cdot EER_0}{SOC_w}$$

where EER_0 is the EER target of the vehicle, $SVEC^*$ is the average specific vehicle energy consumption (kWh/km) and SOC_w is the SOC window (90% in this project).

The BS-DWPT-EV (battery shrink) architecture instead can exploit the energy available from the e-road and its battery size can therefore be decreased. The procedure to estimate its effective BES is reported below.

Starting from the definition of e-road penetration, we obtain the number of segments.

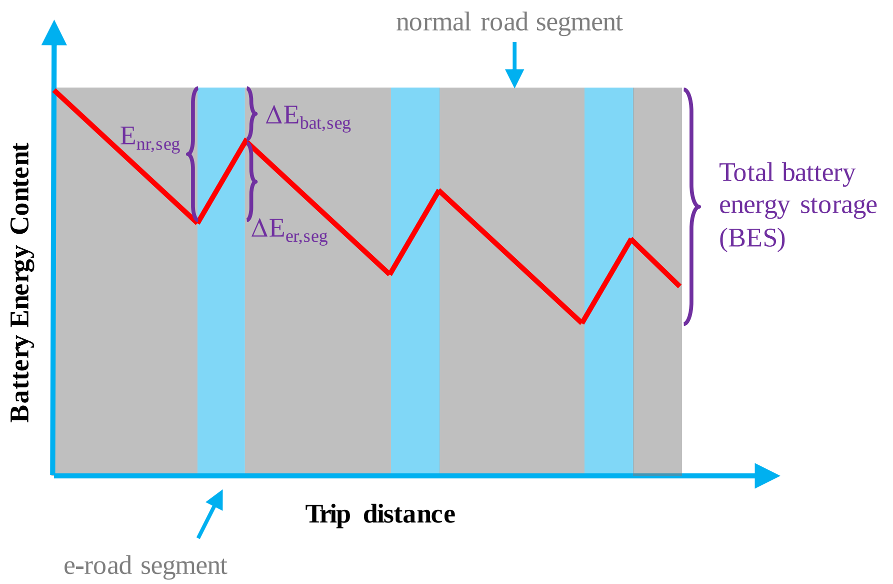

Figure 5: Scheme of the energy flow through the battery over the sequence of modules, used to determine the minimal battery size.

We calculate the energy consumption of the vehicle over the normal road segment, as the energy consumption at the battery level, which counts for the driveline and powertrain efficiencies, averaged over several driving conditions. The energy consumption of the vehicle over the e-road segment is the difference of the energy from the e-road grid and the energy consumed to drive.

Figure 5 shows the battery energy variation (solid red line) over the mission. It decreases over the normal segment and it increases over the e-road segment (in the figure it is assumed that the amount of energy that the vehicle receives from the grid is greater than the amount it has to consume to drive through the e-road segment). The effective energy consumption, $\Delta E_{bat,seg}$, of the battery over the overall module is the positive difference of the energy consumed in the normal segment and the energy recovered over the e-road track. The quantity $\Delta E_{bat,seg}$ represents the actual battery energy consumption over a module. The battery size will therefore be affected by this term and the number of modules to cover the EER. The battery energy consumption (BEC) at the end of N_{seg} modules is $N_{seg} \cdot \Delta E_{bat,seg}$. However, we consider the case where distance of the N_{seg} modules is less than the target trip distance, EER_0. The vehicle either (a) partially covers the normal segment or (b) complete the normal section but partially drives through the e-road one. In this framework, the maximum BEC value can occur at the end of the normal road segment

of the penultimate module (third normal segment in Figure 5), or in the last module (at the end of the trip in the case a, or at the end of the normal segment in the case b). The final battery size is determined from the maximum value of the two options.

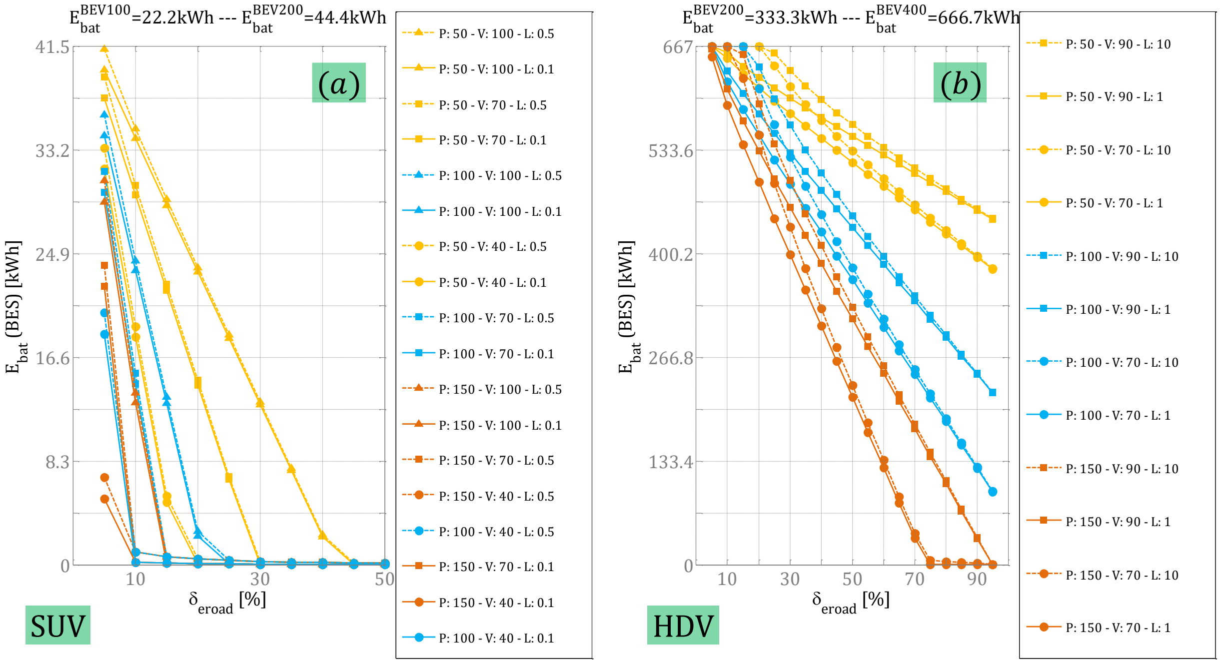

Figure 6: Battery Energy Storage of the DWPT-EV as a function of the e-road penetration (%) for several combinations of dynamic charging power (kW), average speed (km/h) and module length (km), for the SUV (a) and HDV (b) classes.

Figure 6 shows the battery size of the DWPT-EV solution for the SUV (a) and the HDV (b) cases, as a function of the e-road penetration (%) for several combinations of dynamic charging power (P: kW), average speed (V: km/h) and module length (L: km). The legend has been sorted in descent order with respect to the BES values at penetration δ of 10% and 50% for the left and right plots, respectively.

Example SUV: If the e-road module is 100 m long, the penetration δ is 10% and the charging power is 50 kW @ 40km/h, it is possible to install an 18.2 kWh battery to guarantee 200km of e-range (yellow circle), while a 44.4 kWh battery is required for the BEV version to guarantee the same e-range.

Example HDV: If the e-road module is 1 km long, the penetration δ is 50% and the charging power is 150 kW @ 90km/h, it is possible to install a 316.5 kWh battery to guarantee 400km of e-range (orange square), while a 666.7 kWh battery is required for the BEV version.

Number of battery cells

The number and type of battery cells depend on the required BES and maximum power $P_{b,max}$.

The maximum current $I_{c,max}$ that can flow through the cell is calculated as a function of the cell capacity C_c, the C-rating of the cell (see Table 13) and PE is the power-energy ratio of the battery. The total number of cells is determined from the power balance of the equivalent circuit model. We select the cell type that minimize the battery weight. Table 13 also reports the cell mass (kg) for several cell types. In the battery model the mass is calculated as a function of the cell capacity (Ah).

Capacity	Ah	0.72	1.7	2.9	9.3	24	33	50	60	94	200	500	700	1000
C-rating	A/Ah	5	5	5	5	4	4	4	4	4	3	2	2	2
Weight	Kg	0.04	0.042	0.045	0.3	0.57	0.8	1.2	1.4	1.9	5.5	15	17	26

Table 13: Maximum C-rating and weight as a function of cell capacity.

The battery package weight consists of the total cell weight and the battery management system (BMS) weight. In this work the BMS weight is assumed to be 20% of the total cell weight.

2.3.4 Grid power demand

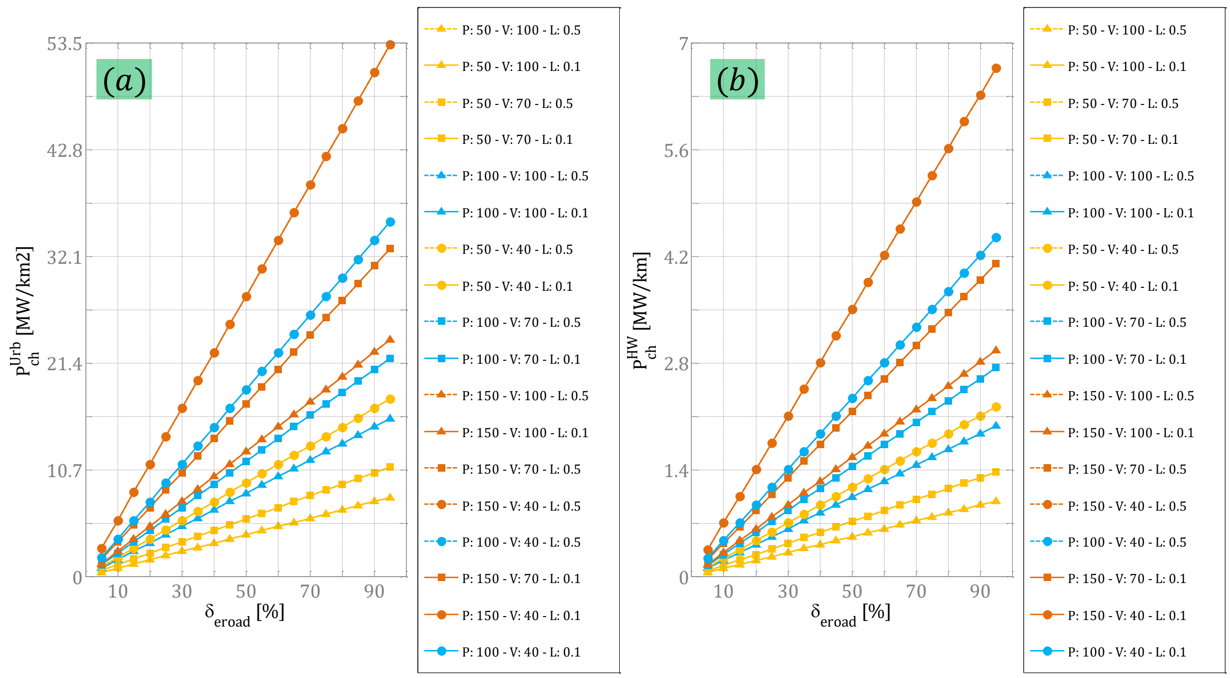

Figure 7: Grid power demand density for the urban area (a) and the highway line (b) as a function of the e-road penetration (%) for several combinations of dynamic charging power (kW), average speed (km/h) and module length (km), for the SUV class.

The maximum feasible charging power that the vehicle can receive from the e-road, $P^*_{er,max}$, is determined by the infrastructure. As it is mentioned in detail in Chapter 3, the maximum required grid power density, ρ_P^U, in the city-centre context is constrained to be less than 20 MW/km^2, which is a reasonable value for a medium sized low-voltage distribution substation. The maximum

required grid power density, ρ_P^{HW}, in the highway scenario, instead, is expressed as a linear density and is constrained to be less than 5 MW/km. We consider the number of vehicles per km N_{veh} as follows:

$$N_{veh} = \frac{1000}{t_s \cdot V_{veh} + l_{veh}}$$

where t_s is the temporal security distance between two consecutive vehicles(s), V_{veh} is the average vehicle speed (m/s) and l_{veh} is its length (m). In this project we assume that the entire vehicle lot consists of the same vehicle class. The number of vehicles is therefore homogenous.

The charging power, $P^*_{er,max}$, in the urban and highway contexts is therefore obtained as follows:

$$P^U_{er,max} = \frac{\rho_P^U}{\delta \cdot N_{veh} \cdot \rho_R \cdot}, \qquad P^{HW}_{er,max} = \frac{\rho_P^{HW}}{N_{veh}}$$

where ρ_R is the road density in an urban centre, i.e., km of road per km^2 of area. It usually ranges from 3 to 10 km/km^2. The nominal value here is 8 km/km^2 for passenger cars and LDCVs, and it is 2 km/km^2 for buses. In this project we have investigated the set [5, 100, 150] kW as possible values of the charging power, P_{er}. During the battery sizing of each vehicle, we check that the selected value for the charging power does not exceed the maximum admissible charging power, $P^*_{er,max}$, in the vehicle context (urban for CVs, LDCVs and buses, urban+highway for SUVs and highway for HDVs).

Figure 7 reports the grid power demand density for the urban area (a, MW/km^2) and the highway line (b, MW/km) as a function of the e-road penetration δ (%) for several combinations of dynamic charging power (kW), average speed (km/h) and module length (km), for the SUV class.

As far as the SUV is concerned, if the e-road penetration is 10% and the charging power is 50 kW, the fleet travels at 40km/h and the road density is 8 km/km^2, the urban grid power demand density is about 1.9 MW/km^2. If the e-road penetration is 10% and the charging power is 50 kW and the fleet travels at 40km/h, the highway grid power demand density is about 233 kW/e-km. If the e-road module is 100 m long, the grid power demand to each highway station is 233 kW. (The distance between two following stations would be 1 km).

As far as the HDV is concerned, if the e-road penetration is 10% and the charging power is 150 kW and the fleet travels at 90 km/h, the highway grid power demand density is about 1.49 MW/e-km. If the e-road module is 1 km long, the grid power demand to each highway station is 2.98 MW. (The distance between two following stations would be 10 km).

2.3.5 Vehicle sizing

The weight of the engine, the e-machine and the transmission is a function of the maximum power of the component. The battery weight is calculated as described in the "Battery sizing" section. The weight of the wireless power-transfer (WPT) system installed on the vehicle is related to the vehicle type and varies from 60 kg for the CV to 150 kg for the HDV.

Table 14 reports the vehicle weight for each powertrain and each vehicle type (kg). The battery weight is reported with respect to the vehicle weight in brackets (%). The second column lists the minimum e-range that each powertrain solution has to guarantee, while the final column lists the vehicle payload (kg).

The vehicle weight is defined as the sum of vehicle curb weight and payload. The default payload values for the five vehicle typologies are 150 kg, 300 kg, 1250 kg, 4000 kg and 7500 kg, respectively.

From Table 14 it is clear for the LDCV case that the WPT system weight counterbalances the battery weight reduction.

Vehicle typology	E-range	Curb Vehicle Weight			Payload
		Diesel	BEV	DWPT-EV	kg
CV	150	950	923 (11.4%)	912 (3.7%)	150
SUV	200	1690	1726 (10.8%)	1716 (4.5%)	300
LDCV	150	3000	3488 (7.2%)	3487 (4.9%)	1250
BUS	150	11302	11704 (7.2%)	11642 (5.1%)	4000
HDV	400	6970	9230 (30%)	7740 (14.8%)	7500

Table 14: E-range, vehicle curb weight and payload per each vehicle typologies.

Conventional powertrain

Since the specification of the engine hugely varies from passenger cars to heavy duty vehicles, a sample engine map has been required for each segment. Engine map extrapolation techniques can be reasonably adopted to estimate fuel consumption at the boundaries of the map, i.e. at idle and full-load conditions, using the Willian's line method [2].

Each conventional vehicle is equipped with a multiple speed transmission. The CV and SUV solutions are equipped with a 6-speed transmission, the LDVs with an 8-speed transmission, while the BUS and HDV classes with a 12-speed transmission.

Electric powertrain

The efficiency map of each electric machine can be derived from a baseline map of the selected machine type and scaled as a function of the e-machine power. A baseline e-machine is required

for each vehicle typology, since the specification of the e-machine might significantly vary from passenger cars to HDVs. E-machine map scaling techniques can be reasonably adopted for different machines, if the output power of the new machine is comparable to the baseline engine.

Based on the maximum power and power-to-energy ratio of the battery system and on the cell technology (such as lithium ion, NiMH) available in the dataset, the model determines the number of cells in parallel and in series, the cell capacity and voltage.

From the specific energy (Wh/kg) vs specific power (W/kg) correlation and from the power-to-energy ratio of the battery, given as input, the actual specific power and energy values are obtained.

Each electric vehicle is equipped with a 2-speed transmission to optimize the powertrain efficiency at low vehicle speeds, without sacrificing the maximum vehicle speed.

2.3.6 Energy and CO_2 emissions model

The energy model uses a kinematic vehicle approach, derived from the one described in [3] and [4], where the operating conditions of the system and the control variables are directly obtained with respect to the kinematic state of the system itself. This approach has been implemented in the Matlab environment. This methodology is believed to be consistent with the purpose of this framework, where different vehicle typologies equipped with several powertrains are compared in terms of energy consumption, total costs of ownership and CO_2 emissions.

Two different vehicle models have been developed, one for the conventional vehicles (Diesel and Gasoline), the other for the electric vehicles (BEV and DWPT-EV).

The power demand to the powertrain is calculated from the vehicle velocity patterns, which is an input to the kinematic model, considering the driveline efficiency chain and the efficiency of each machine (engine, e-machine and battery) as a function of the operating points.

The total power required at the powertrain level, which is the engine for the conventional vehicles and the e-machine for the electric vehicles, is the sum of several components: rolling resistance, grade resistance and drag resistance. Vehicle data adopted in this project are reported in Table 15.

Vehicle typology	Unit	CV	SUV	LDCV	BUS	HDV
Drag coefficient	-	0.27	0.24	0.58	0.7	0.96
Front area	m^2	2.19	2.59	3.8	8.15	9.96
Rolling resistance	-	0.008	0.008	0.008	0.008	0.008
Wheel radius	m	0.3	0.32	0.35	0.48	0.52
Wheel inertia	kg m^2	1.05	1.16	1.56	2.3	2.5
# of wheels	-	4	4	4	6	12
Vehicle length	m	4	4.5	4.5	11	13

Table 15: Main vehicle specifications per each vehicle typology.

Figure 8 shows the scheme of the kinematic approach to estimate energy consumption and CO_2 emissions (WTT and TTW).

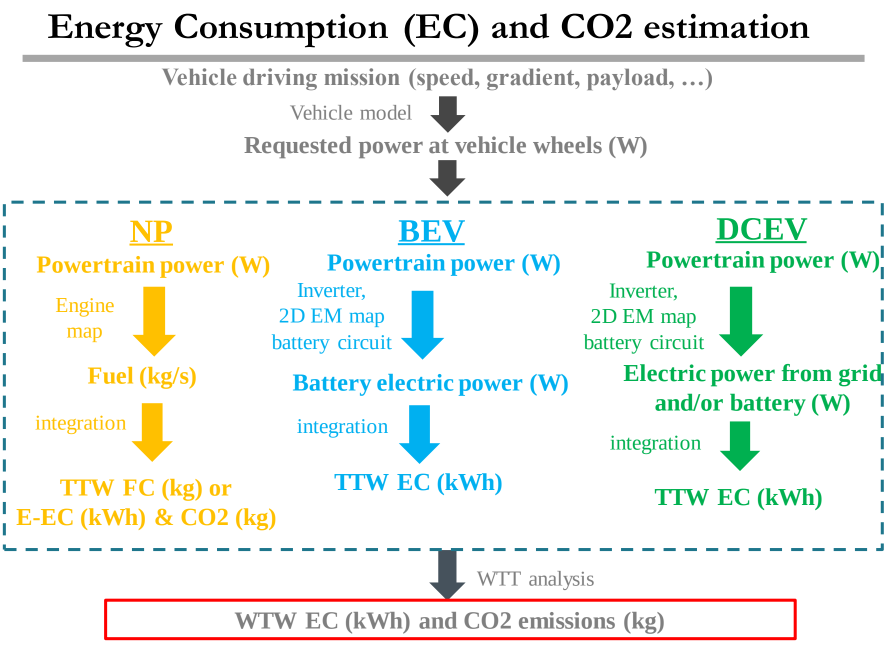

Figure 8: Scheme of the kinematic approach to estimate energy consumption and CO_2 emissions (WTT and TTW).

2.3.6.1 Conventional powertrain

From the vehicle power demand, the vehicle model calculates the engine power and speed using the driveline model, and interpolates an experimentally-derived quasi-static 2D map as a function of engine speed and torque, to evaluate the mass flow rate of fuel. The fuel consumption, FC (kg), is then determined by integrating over the driving mission time horizon [5]. The corresponding tank-to-wheel (TTW) CO_2 emissions [6] have instead been determined linearly using the coefficient $\mathrm{k}_{co2,ttw}$ (see Table 16).

Parameter k	Unit	Diesel	Gasoline
TTW CO2	[CO_2 pound/Fuel BTU]	161.3	157.2
TTW CO2	[CO_2 kg/Fuel kg]	3.006	2.997
LHV	MWh/kg	12.05	12.30
WTT EC	MJ/MJ	0.20	0.18
WTT CO2	[CO_2 g/energy kWh]	55.4	49.7

Table 16: TTW CO_2 conversion factor, LHV, WTT EC and CO_2 conversion factors for different fuels ([7]).

The corresponding TTW energy consumption has been determined using the lower heating value of the fuel (LHV).

The impact of the electric energy production is of fundamental importance to properly compare the effective performance in terms of energy consumption and CO_2 emissions of any electric vehicle to that of a conventional vehicle. The well-to-tank (WTT) energy consumption is a linear function of TTW energy consumption, using the $\mathrm{k}_{EC,wtt}$ factor. Similarly, the well-to-tank (WTT) CO_2 emissions is obtained from TTW energy consumption using the $\mathrm{k}_{CO2,wtt}$ factor. See Table 16 for more details.

2.3.6.2 Electric powertrain

Battery power demand from vehicle

From the vehicle power demand, the vehicle model calculates the electric machine power and speed using the driveline model, and it simulates the power conversion from the mechanical to the electric form, considering the energy losses of the e-machine by means of efficiency maps, which are functions of the machine torque and speed. The electric power demand to the battery, $P_{bat,el}$, is determined considering the efficiency of the inverter.

Dynamic charging

However, if the vehicle has the opportunity to recover energy from the e-road, it is necessary to determine the amount of charging power that the battery can receive from the grid. The battery demand should account also for this contribution as follows:

$$P'_{dem} = P_{bat,el} - P_{er} \cdot \varepsilon_{er} \cdot \varepsilon_{inv} \cdot i_{er}(t)$$

where i_{er} indicates whether the vehicle is over an e-road segment, $i_{er} = 1$, or not ($i_{er} = 0$).

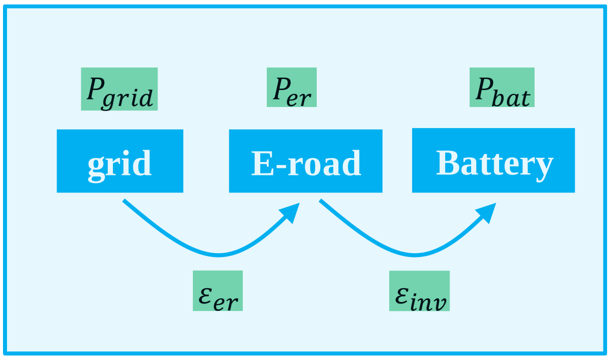

Figure 9: Scheme of the power flow from the grid to the battery.

If the powertrain has to provide tractive power, the model checks that P'_{dem} does not exceed the maximum power that the battery can handle. The actual battery power demand is then saturated according to the minimum and maximum battery power values. The actual power demand to the grid, P_{grid}, is therefore obtained from the vehicle power demand and the actual battery power.

Grid and battery energy consumption

The battery power losses are modelled using an equivalent resistance circuit, in which the resistance and the open-circuit voltage of the battery are SOC-dependent. The battery temperature is assumed constant and the temperature effect is therefore disregarded.

The battery energy consumption, BEC (kWh), is determined by integrating the battery chemical power $P_{bat,chem}$ over the driving mission time horizon. The dynamic grid energy consumption, DGEC (kWh), is instead determined by integrating the grid electric power P_{grid} over the driving mission time horizon. This quantity is obviously zero for every BEV.

The TTW energy consumption is the sum of the two contributions, BEC and DGEC. The WTT energy consumption has been determined using the TTW energy consumption and the $\mathrm{k}_{EC,wtt}$ coefficient (1.95 MJ/MJ, see JRC WTT report [7]). Similarly, the well-to-tank (WTT) CO_2 emissions have been determined from the TTW energy consumption using the $\mathrm{k}_{CO2,wtt}$ factor (489 g CO_2/kWh, see [7]).

It should me mentioned here, that 489 g CO_2/kWh is an average value for electricity generation, considering a large share of fossil fuels (only 15% renewable fraction). As shown in section 3.5 of this document, in European countries, CO_2 emissions per kWh of electricity generation range from values far below 100 to above 1000 g/kWh. The target of the European Commission until 2050 foresees a 100% reduction of electricity-related CO_2 emissions. Therefore, WTT emissions should be revised and replaced by a coefficient which reflects a 100% renewable energy mix.

Well to wheel analysis

The total well-to-wheel (WTW) energy consumption, EC_{wtw}, and CO_2 emissions, $\mathrm{CO}_{2,wtw}$, are obtained as a sum of the two contributions (WTT+TTW).

2.3.7 Cost model

The cost model aims at estimating the production vehicle costs from an OEM point of view and the total costs of ownership (TCO) for the final-end user. Procedure and parameters for estimating costs have been derived from the literature [8], [9], [10] and [11].

2.3.7.1 Initial costs

Retail price

The cost of the electric machine and the engine is estimated as linear functions of their rated power, while the cost of the transmission is represented by suitable functions of the power to be transferred and the number of gears. The cost of the battery is expressed as the product of the energy content [kWh] and the specific cost (€/kWh), calculated as a function of the power-to-energy ratio. In this project the maximum ($PE_{bat} = 40$) and minimum ($PE_{bat} = 2$) specific costs have been set equal to 400 and 200 €/kWh, respectively.

Table 17 reports the vehicle base price (chassis, wheels and other components) and the OEM powertrain cost for each powertrain and each vehicle type (k€). The battery cost is reported with respect to the powertrain cost in brackets (%). The second column lists the vehicle base price.

The vehicle retail price is defined as the sum of vehicle base price $P_{veh,base}$ and powertrain cost, C_{pwt}, weighted by the retail mark-up of the OEM, μ_{OEM}. The vehicle base costs (chassis, wheels and other components) can be estimated from several manufacturer's suggested retail price data of different vehicle segments.

Vehicle typology	Vehicle base price (k€)	Powertrain cost (k€)		
		Diesel	BEV	DWPT-EV
CV	10.4	2.1	7.3 (71%)	5.1 (42%)
SUV	14	2.3	12 (75%)	8.1 (51%)
LDCV	21.5	2.7	14.9 (81%)	12.3 (68%)
BUS	50	5.2	45.5 (87%)	40.2 (73%)
HDV	122	6.1	135.2 (95%)	64.8 (83%)

Table 17: Vehicle base price and powertrain cost per each vehicle typology; percentage share of battery cost in brackets.

Incentives and additional costs

It has been assumed that each BEV/DWPT-EV solution receives an incentive I_{veh} to prompt its purchase. It represents 15% of the original retail price. However, any solution of that kind requires a dedicated charging station (or charger) for slow static recharging. Its price, $C_{ch,station}$, has been set to 1 k€ for each BEV/DWPT-EV.

2.3.7.2 Operating costs

Maintenance

Table 18 lists the maintenance costs per year, C_{maint}, (k€/year) for the three powertrain types and each vehicle class.

Vehicle typology / Powertrain	Maintenance costs (k€/year)				
	CV	SUV	LDCV	BUS	HDV
Diesel	1.3	3	10	15	15
BEV/DWPT-EV	0.6	1	3.3	5	5

Table 18: Maintenance costs k€ per year.

Energy consumption costs

The total cost due to recharging/refilling is calculated from the total energy consumption per trip and the electricity/fuel price trends over the time. The cost, c_{EC} (€/trip), related to the vehicle energy consumption to drive over a given driving mission is estimated from the TTW energy consumption of the vehicle and the price of the electricity (0.211 €/kWh) or the price of fuel, according to the powertrain type.

The overall energy consumption costs, which is estimated considering the number of trips that the vehicle has to drive over the entire life of the vehicle, is obtained as follows:

$$C_{EC} = \frac{c_{EC} \cdot (VMT - VMT_{RV})}{D_{mis}} \cdot L_{life}$$

where VMT is the vehicle mile travel, i.e., the total distance covered by the vehicle during its life, VMT_{rv} is the distance covered with the replacement vehicle (see "Vehicle replacement" section), D_{mis} is the length of the driving mission and L_{life} is the expected life of the vehicle, set to 10 years for all the vehicles in this project. The default vehicle miles of travel (VMT) is assumed to be 25,000 km per year for the CV, SUV and LDCV cases and to be 75,000 km per year for the BUS and HDV cases.

Vehicle replacement cost

For the two passenger cars (CV and SUV) we have assumed that the final user owns at least a conventional vehicle (referred to as the replacement vehicle) and he might favour to the alternative vehicle whenever the trip distance exceeds the e-range (EER) of the BEV/DWPT-EV solution. The distribution of the number of trips per year, $\varphi(\rho)$, as a function of their distance, ρ, is adjusted to guarantee the input VMT, starting from a reference distribution per each vehicle class. The total distance VMT_{RV} (km) covered by the replacing vehicle is obtained from the distribution and the vehicle replacement cost, C_{VR} (€), as $\mathrm{C}_{VR} = \mathrm{c}_{VR} \cdot VMT_{RV} \cdot L_{life}$, where c_{VR} is the cost per km of the replacing vehicle.

The effective e-range (EER) of the BEV/DWPT-EV is estimated over each driving mission, according to the specific vehicle energy consumption.

$$EER_{BEV} = \frac{E_{bat} \cdot SOC_w}{BEC \cdot \varepsilon_{ch}} \cdot D_{mis}, \qquad EER_{DCEV} = \frac{E_{bat} \cdot SOC_w}{BEC \cdot \varepsilon_{ch} + DGEC \cdot \varepsilon_{er} \cdot \varepsilon_{inv}/\varepsilon_{bat}} \cdot D_{mis}$$

where E_{bat}, SOC_w and BEC are the energy content (kWh), the SOC window (-) and the energy consumption (kWh) of the battery over the mission, respectively, GEC is the grid energy consumption (kWh), D_{mis} is the distance of the mission itself, ε_{ch}, ε_{er}, ε_{inv} and ε_{bat} are the efficiency of the static charger, the e-road, the inverter and the battery, respectively.

Battery replacement costs

The total cost due to battery replacement is calculated from the total number of additional batteries required over the life of the vehicle and the battery price. The number of additional batteries is estimated considering the number of trips per year that each vehicle has to drive over their associated set of driving missions. We consider the battery aging phenomenon as a constant process in which the battery capacity drops as a function of the number of complete charge/discharge cycles that the battery has to overtake (see [3] and [12]). The number of charge/discharge cycles depends on the actual distance per year covered by the BEV/DWPT-EV and the energy flow through the battery. We assume a "*battery buy-buy*" scenario, so that the final-user pays entirely for the new required batteries. Whenever the capacity k_b reaches the

lower bound of 80%, final-user purchases a new battery, whose energy content has to compensate the loss in capacity of the original battery.

Additional costs

It has been associated a tax cost, C_{tax}, to the CV and SUV classes. A social cost related to the global warming, i.e., the cost to repair the damage done by global warming (CO_2 emissions) has been considered to every vehicle.

Total cost of ownership

The final total cost of ownership is calculated as the sum of the initial and operating costs:

$$\mathrm{TCO} = \overbrace{\mathrm{RP}_{veh} - I_{veh} \cdot \mathrm{RP}_{veh} + C_{ch,station}}^{INITIAL} + \overbrace{C_{maint} \cdot L_{life} + \mathrm{C}_{EC} + \mathrm{C}_{VR} + C_{BR} + \mathrm{C}_{CO2} + \mathrm{C}_{tax}}^{OPERATING}$$

2.4 Simulation Results

In this section, results of the vehicle performance model are summarised. In the first sub-section, main results of the detailed comparison of all vehicle typologies and driving scenarios, as described in section 2.3 are reported. In the following sub-sections, specific results for the three FABRIC DWPT scenarios are shown. These results are fundamental inputs for further studies in WP55 of FABRIC, where feasibility is analysed. Finally, some comments on WTW energy consumption are added, in order to clarify outcomes of the vehicle performance model, which is based on current European electricity mix, while FABRIC scenarios are looking forward to the years 2030, 2040 and 2050.

2.4.1 Results of the detailed model

In this section, main results of the detailed comparison of all vehicle typologies and driving scenarios, as described in section 2.4 are summarised.

For **passenger cars application (SUV and CV)**, DWPT-EV solutions enable a dramatic reduction of CO_2 WTW with respect to conventional vehicles (ranging from 40% to 50%). TCO is also significantly reduced (13-25%, depending on vehicle class and ICE adopted for conventional powertrain), mainly due to lower maintenance costs and energy consumption that compensate higher initial costs. It is worthwhile recalling that for DWPT-EV, calculations have been carried out assuming a 10% e-road penetration, an e-road charging power equal to 50 kW (see 2.2.4) and an 80% WPT efficiency.

As far as comparison with reference BEV is concerned for passenger car applications, TCO of DWPT-EV is 2% lower than BEV (thanks to battery shrinking), and average EER of DWPT-EV is significantly longer than that of reference BEV (2-6 times longer, depending on vehicle class and driving mission). However, DWPT-EV show 13-20% higher WTW CO_2 emissions than reference

BEV (depending on vehicle class). Such an increase of CO_2 emission is more apparent in urban driving missions (AUDC, +21% for SUV) than in motorway missions (AMDC, +5% for SUV) and is mainly due to lower efficiency of WPT systems with respect to conventional charging systems.

For **heavy duty truck for freight logistics (HDV)**. For dynamic charging solutions, calculations have been carried out assuming a 50% e-road penetration, an e-road charging power equal to 200 kW (see 2.3.4) and an 80% WPT efficiency. DWPT-EV shows 13% reduction in CO_2 WTW with respect to conventional vehicles. TCO of DWPT-EV is 5% less than conventional diesel solution and also 6% lower than BEV (due to battery shrinking). Average EER for DWPT-EV is about 25% longer than reference BEV. However, DWPT-EV show 10% higher WTW CO_2 emissions than reference BEV. This penalty in terms of CO_2 emission is less apparent in highway driving conditions (HWM, +2%).

With reference to **urban bus applications (BUS)**, DWPT-EV calculations have been carried out assuming a 10% e-road penetration, an e-road charging power equal to 150 kW (see 2.3.4) and an 80% WPT efficiency. WTW CO_2 emissions and TCO of DWPT-EV solutions are better than an equivalent diesel solution but worse than reference BEV (+14% CO_2 WTW, + 7% TCO with respect to reference BEV). EER is significantly extended, up to 900 km, but this might not be a tangible advantage for an urban bus.

For **delivery van for urban logistics (LDCV)**, DWPT-EV calculations have been carried out assuming a 10% e-road penetration, an e-road charging power equal to 50 kW (see 2.2.4) and an 80% WPT efficiency. WTW CO_2 emissions and TCO are better than an equivalent diesel solution but worse (+12% CO_2, +1% TCO) than reference BEV. EER is not significantly extended with respect to reference BEV.

Based on these outcomes, additional simulations have been carried out to address the three scenarios introduced in section 1.4 (motorway, periurban and urban scenarios).

2.4.2 Motorway scenario

A stretch of 25-km e-road every 400 km on motorways (e-road penetration: 6.25%) has been considered. Vehicle types are mostly passenger cars (88%), whereas the remaining part is made up of heavy duty trucks. Different charging speeds (V_{er}) and e-road charging powers (P_{er}) have been considered. Table 20 reports the changes of primary energy consumption (E_c WTW), CO_2 WTW, TCO, battery weight and battery capacity (BES) with respect to a reference BEV, i.e. BEV400 for passenger cars and BEV250 for heavy duty trucks, according to discussion reported in section 3.2.1. Results for reference BEV and for reference conventional vehicles are reported in Table 19.

Vehicle type	Reference vehicle	Ec WTW [Wh/km]	CO2 WTW [gCO2/km]	TCO [k€]	Battery mass [kg]	BES [kWh]
Passenger cars	BEV400	735	122	55.0	373	89.0
	Gasoline	710	176	51.0	-	-
	Diesel	691	175	49.0	-	-
Heavy duty trucks	BEV250	5491	910	604.2	2156	514.2
	Diesel	4001	1016	571.1	-	-

Table 19: Motorway, simulation results for reference vehicles.

For the battery-shrink-scenario, a significant reduction in battery size is apparent for DWPT-EV passenger cars with respect to BEV400, thus contributing to a reduction in TCO ranging from 2% to 5%, depending on the recharging speed. A slight deterioration of CO_2 WTW is estimated, in line with previous discussions (see table below).

As far as heavy-duty trucks are concerned, DWPT-EV solutions allow battery weight to be reduced by 3-5% with respect to BEV250. TCO is slightly reduced and a reduction of 13 g CO_2/km (WTW) has been estimated, confirming that DWPT-EV solutions can be suitable to long-haul freight logistics.

Vehicle type	P_{er} [kW]	V_{er} [km/h]	ΔEc WTW [Wh/km]	ΔCO2 WTW [gCO2/km]	Δ TCO [%]	Δ battery mass [%]	Δ BES [%]
Passenger cars	50	60	18	3.0	-5.0	-24.3	-24.3
		80	22	3.6	-3.0	-18.1	-18.1
		100	24	3.9	-1.8	-14.4	-14.4
Heavy duty trucks	100	60	-79	-13.1	-0.8	-4.6	-4.6
		80	-76	-12.7	-0.6	-3.2	-3.2

Table 20: Motorway, Battery-Shrink – Variations for DWPT vs. reference BEV).

For range-extension, simulation results show that TCO is increased slightly in all cases (3.7% for passenger cars and 0.8% for heavy vehicles). Regarding WTW energy consumption, passenger cars show increased demand due to DWPT, while for heavy duty trucks, DWPT is beneficial.

Battery weight is not changed, according to the definition of the range-extending scenario.

Vehicle type	P_{er} [kW]	V_{er} [km/h]	ΔEc WTW [Wh/km]	ΔCO2 WTW [gCO2/km]	Δ TCO [%]	Δ battery mass [%]	Δ BES [%]
Passenger cars	50	60	63	10.4	3.7	0	0
		80	63	10.4	3.7	0	0
		100	63	10.4	3.7	0	0

Heavy duty trucks	100	60	-45	-7.5	0.2	0	0
		80	-45	-7.5	0.2	0	0

Table 21: Motorway, Range-Extender – Variations for DWPT vs. reference BEV).

2.4.3 Periurban scenario

This scenario investigates the application of dynamic charging to heavy duty vehicles in areas with high traffic density, for example from periurban logistic centres or ports to the city centre or among close cities. Travelling a daily distance of around 250 km with e-road of 10 km length has been considered (4% e-road penetration). An e-road charging power (P_{er}) of 100 kW has been considered, whereas different charging speeds (V_{er}) have been investigated.

Table 23 reports the changes of primary energy consumption (E_c WTW), CO_2 WTW, TCO, battery weight and battery capacity (BES) with respect to reference BEV, i.e. BEV250 (see Table 22). Results are very similar to the Motorway scenario, showing slight reductions in battery sizes and as consequence of this, reduced WTW energy consumption and CO_2 emissions. Overall reductions are smaller, as the e-Launcher is shorter and less energy is obtained from DWPT.

Vehicle type	Reference vehicle	Ec WTW [Wh/km]	CO2 WTW [gCO2/km]	TCO [k€]	Battery mass [kg]	BES [kWh]
Heavy duty trucks	BEV250	4524	750	530.6	1850	441.2
	Diesel	3596	913	541.6	-	-

Table 22: Periurban, simulation results for reference vehicles.

Vehicle type	P_{er} [kW]	V_{er} [km/h]	ΔEc WTW [Wh/km]	ΔCO2 WTW [gCO2/km]	Δ TCO [%]	Δ battery mass [%]	Δ BES [%]
Heavy duty trucks	100	60	-48	-7.9	-0.3	-3.5	-3.5
		80	-45	-7.5	-0.1	-2.5	-2.5

Table 23: Periurban scenario, Battery-Shrink – Variations for DWPT vs. reference BEV).

DWPT-EV solutions allows battery weight to be reduced by 3-4% with respect to BEV250. TCO is virtually unchanged and a gain of 7-8 g CO_2/km (WTW) has been estimated. This shows the benefit of DWPT-EV in heavy duty trucks in motorway conditions.

For range-extension, compared to the Motorway scenario, TCO is increased slightly more (1.3% compared to 0.2%) and demand is increased due to DWPT, which results also in increased CO_2 emissions.

Vehicle type	P_{er} [kW]	V_{er} [km/h]	ΔEc WTW [Wh/km]	ΔCO2 WTW [gCO2/km]	Δ TCO [%]	Δ battery mass [%]	Δ BES [%]
Heavy duty trucks	100	60	46	7.6	1.3	0.0	0.0
		80	46	7.6	1.3	0.0	0.0

Table 24: Periurban scenario, Range-Extender – Variations for DWPT vs. reference BEV).

2.4.4 Urban scenario

This scenario investigates the application of dynamic charging to urban buses. Travelling a daily distance of 324 km, made up of 18 round-trips (9 km route one way, 18 km route and return). The 9-km trip results from the SORT driving cycle, described in detail in chapter 3 of this report. Two use cases have been considered:

- E-road stretches of 25 m at each one of the 27 stops over the one-way route (7.5% e-road penetration). And e-road charging power (P_{er}) of 100 kW has been considered, along with a charging speed of 3 km/h (only charging while the bus stops and accelerates after the stop)
- E-road stretches (e-trenches) of 11 m at each one of the 27 stops over the one-way route (3.3% e-road penetration). An e-road charging power (P_{er}) of 150 kW has been considered, along with a charging speed of 2.26 km/h (only charging while the bus stops, average speed is obtained from average stop time and e-trench length)

Results for reference BEV and for reference conventional vehicles are reported in Table 25 and Table 26 reports the changes of primary energy consumption (E_c WTW), CO_2 WTW, TCO, battery weight and battery capacity (BES) with respect to reference BEV, i.e. BEV330, capable of driving the whole daily-trip before recharging.

Vehicle type	Reference vehicle	Ec WTW [Wh/km]	CO2 WTW [gCO2/km]	TCO [kEuro]	Battery mass [kg]	BES [kWh]
Bus	BEV325	3415	566	400.8	1818	433.6
	Diesel	3584	910	417.7	-	-

Table 25: Urban Bus, simulation results for reference vehicles.

Vehicle type	P_{er} [kW]	V_{er} [km/h]	ΔEc WTW [Wh/km]	ΔCO2 WTW [gCO2/km]	Δ TCO [%]	Δ battery mass [%]	Δ BES [%]
Bus	50	18	-258	-42.8	-17.2	-89.7	-89.7
	100	3	-206	-34.1	-16.5	-89.7	-89.7
	150	2.26	-233	-38.6	-16.9	-89.7	-89.7

Table 26: Urban bus scenario, Battery-Shrink – Variations for DWPT vs. reference BEV).

For battery-shrink DWPT-EV solutions allow battery weight to be reduced by 90% with respect to BEV325. TCO is reduced of about 17% and a reduction of 34-43 g CO_2/km (WTW) has been estimated. Reductions of energy consumption are obtained due to the reduced vehicle weight.

Results regarding battery reduction are less than obtained from calculations carried out in chapter 3, where battery size was reduced by approximately 97% regarding required energy capacity. The difference can be explained with the battery model used in POLITO's vehicle performance model. In chapter 3, the model was based on energy balance, without any constraint for the storage system. The aim was to define requirements regarding power and energy for the storage system on board. The vehicle performance model starts from the assumption that a specific battery technology will be used (Li-Ion battery in this case). This assumption means that this battery will have a power constraint. Typically, it is recommended that Li-Ion batteries should not be recharged at higher rates than 1C. In this case, 10C was considered, which resulted in a minimum battery size of 45 kWh and battery reduction of 90%.

As a conclusion, it can be stated here, that for the urban bus case, reduction of battery size is so dramatic, that actually a different storage technology should be considered: supercapacitors. As this technology-switch is outside the scope of the vehicle performance model, is could not be reflected properly. In any case, this is an important outcome of this study, which will lead to an important improvement of the model in the future.

2.4.5 Comments on WTW energy consumption

Simulation results have shown elevated WTW consumption for BEV and DWPT-EV options compared to Diesel and Gasoline. BEV consumption was reduced to 60-75% of reference Diesel

option for SUV and compact vehicles. In the case of Heavy-duty vehicles and buses, WTW energy consumption of the electrified options were found to be even higher than for the Diesel reference. This result is at least surprising for those who expected electric transport to be much more energy efficient than the internal combustion engine. The reason for this surprising result is the extremely low energy efficiency of the electricity system, which was assumed in this study, according to the JRC WTT Report [7]. The applied factor of energy expended per unit of final fuel (electricity in this case), has been 1.95 MJ/MJ. In other words, assumed fuel efficiency of the EU-28 electricity mix is approximately 34% (1/(1+1.95)). This is in line with standard thermal power plant efficiency in the range of 30-40%.

Therefore, if results from this study are to be projected into a future with a radically different electricity mix, this factor must be adjusted. It was not the objective of this deliverable to re-calculate this factor in detail, but with some simple assumptions, an estimate will be given here below, how this factor might evolve from here to 2050. In Figure 10 a possible projection is given for energy expended to deliver final fuel for EU-28 electricity mix. Data has been elaborated based on JRC values (1.95 MJ/MJ for EU-28 mix in 2010) and projections on the EU-28 electricity mix given by the EU reference scenario.

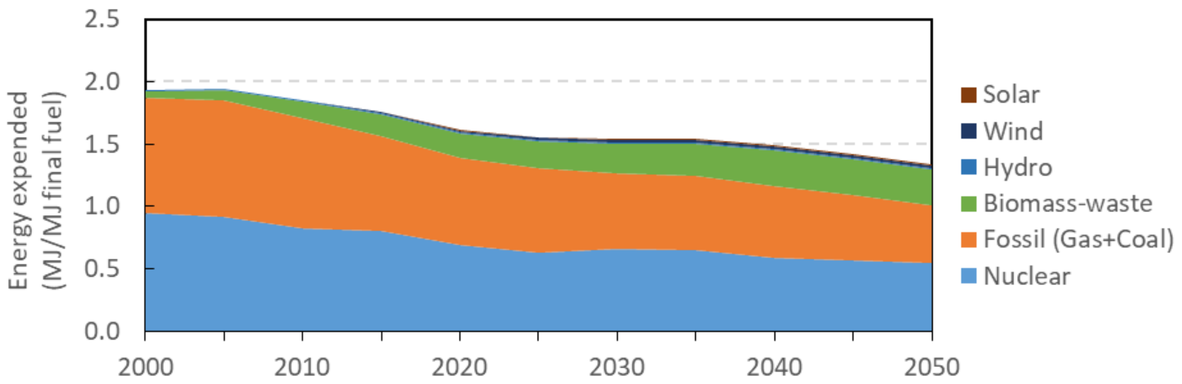

Figure 10: Projection of energy expended to deliver final fuel for EU-28 electricity mix.

Individual values for each technology have been estimated from available data of the JRC study [7] and are shown below in Table 27. These values are obtained from a rough estimate which was elaborated adjusting values in order to reach the reference of 1.95 MJ/MJ for EU-mix 2010. Therefore, values might be disputable, but the general message is clear. Renewable energies, except biomass, have virtually zero additional energy expenditure and thus, will increase system efficiency dramatically.

	MJ/MJ
Solar	0.12
Wind	0.12
Hydro	0.12
Biomass	3.00
Nuclear	3.01
Fossil	1.71

Table 27: Individual values of energy expended to deliver final fuel from WTT analysis.

Applying coefficients from Table 27, in Figure 11 the electricity mix 2015 according to EU reference scenario has been compared with 2050 projections from the same study and the proposal from Greenpeace Energy [R]evolution scenario [13]. The Greenpeace scenario is shown here, in order to give an example of 100% renewable energy generation without nuclear power, which in turn is a scenario of particularly low energy expenditure for each MJ_e delivered.

It has to be noted here, that the value of expended energy per MJ_e has the following relationship with electricity conversion efficiency $\eta_{conversion}$ regarding primary energy source:

$$\eta_{conversion} = \frac{1}{1 + MJ/MJ_e}$$

As a result, the WTT energy coefficient to obtain WTW energy consumption from TTW consumption is $1+MJ/MJ_e$. This value is represented in Figure 11 (below), as it directly shows the impact of conversion efficiency on WTW energy consumption.

Compared to the reference value of 2.95 for the WTT energy coefficient which was employed in the WTW analysis of this report, it is foreseeable that WTW energy consumption of electric transport will be reduced significantly, just due to the transition from fossil/nuclear to mainly renewable energy mix. The EU-reference scenario might be taken as a conservative estimate, representing 20% reduction, while the Energy [R]evolution scenario might be the most aggressive scenario with 44% reduction.

Main conclusion from these considerations is, that with a 33% reduction in WTT energy coefficient (reduction from 2.95 to 1.97), all electric scenarios will show lower energy consumption on a WTW basis than the Diesel reference, including heavy vehicles, which turned out to consume up to 50% more energy in the case of range-extending DWPT.

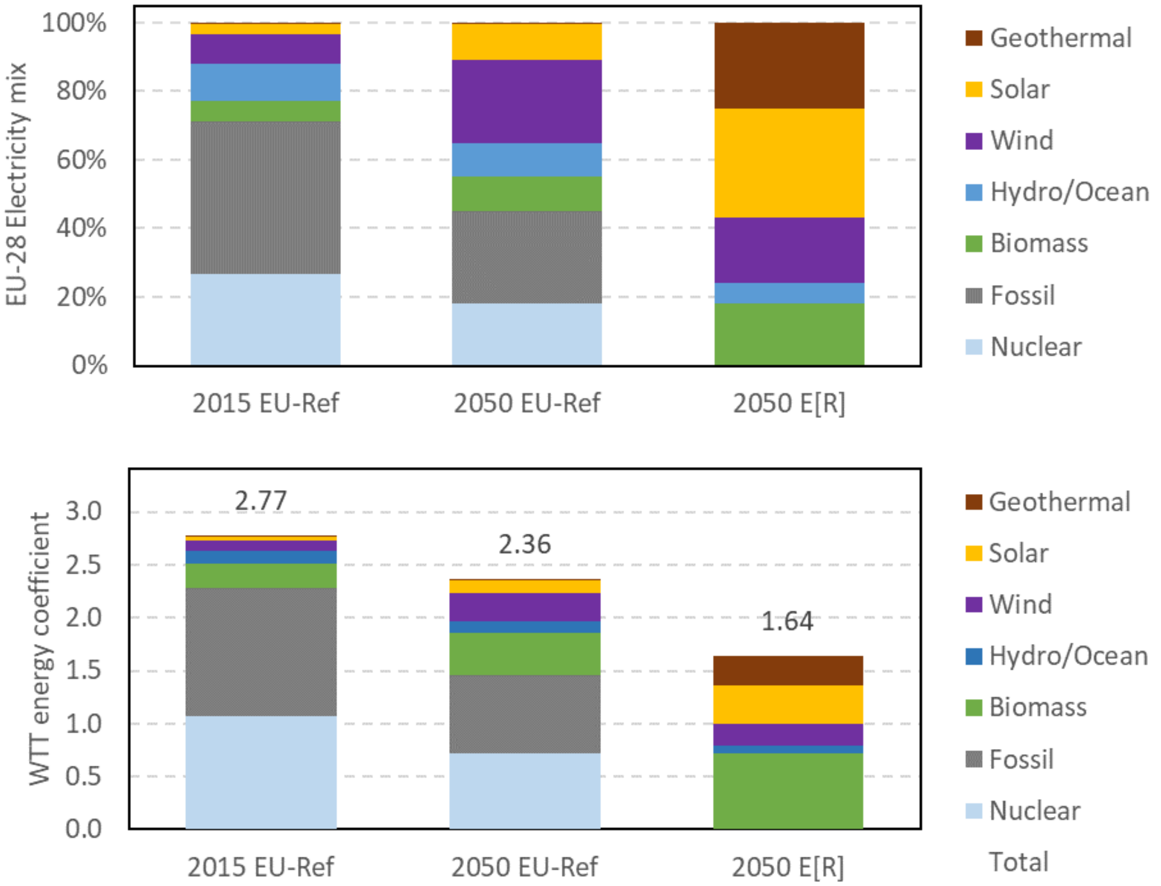

Figure 11: EU-28 electricity mix (above) and WTT energy coefficient (below) for 2015 and different scenarios in 2050.

2.5 Conclusions

In this section, the vehicle impact has been analysed in terms of WTW energy consumption and CO_2 emissions, total costs of ownership (TCO), weight, effective electric range, charging time at the end of specific driving missions and total time to drive long trips (up to 1000 km). Case studies have been identified based on WP5.1 outcomes.

The investigation was carried out by simulation and a specific model has been developed and applied within this activity (see section 2.3). Capabilities of this model go beyond this report and include:

- comparison of dynamic charging solutions (DWPT-EV) with the other vehicle typologies in a way that any model assumption has the same impact for all configurations;
- sensitivity analysis for some key-parameters related to market (prices of fuel, electric energy and batteries), e-road (maximum e-road charging power, WPT efficiency, e-road penetration) and usage (vehicle miles of travel and payload).

Two main options have been considered for DWPT-EV solutions:

- **Range extension:** the additional energy received from the e-road while driving has been exploited to increase the EER, in a proportional way to the actual VEC.
- **Battery shrink:** the energy received from the e-road allows the energy storage required in the battery to be decreased in order to guarantee a given autonomy distance.

Five vehicle classes have been investigated:

- Two types of passenger cars:
  - CV, representative of a compact car mainly used for urban driving, like a taxi
  - SUV, mid-size vehicle representative of a private car used for urban and longer extra-urban trips
- LDCV: Delivery van for urban logistics
- BUS: Urban bus
- HDV: Heavy duty truck for freight logistics

Several driving missions have been considered in order to reproduce typical usage of each vehicle class (see section 2.2.3 for details).

DWPT-EV results have been reported with reference to both conventional vehicles (equipped with ICE only) and BEV. Reference BEV and electric range for each driving scenario and vehicle class have been discussed and identified in 2.3.2.

For the motorway scenario, passenger cars show slightly increased CO_2 emissions compared to the BEV reference, despite important reductions in battery size.

For heavy duty trucks, DWPT improves all indicators (reduced battery size, TCO and CO_2 emissions). Here, battery-shrink is the fundamental advantage of DWPT. The same conclusions apply for the periurban scenario, as only heavy vehicles are considered.

For urban buses, DWPT is found to be key for important reductions in battery size. In this case, range-extension is not justified. As a result, costs and environmental impacts of e-buses can be reduced which gives positive results for both, environmental and economic criteria. In this case, battery reduction is so dramatic, that a switch from battery to supercapacitors is probably indicated. This technology switch was not foreseen in the vehicle performance model, which resulted in much less battery reductions than actually would be possible.

In general, battery shrink DWPT-EV has shown to give better results regarding environmental criteria (reduction of energy consumption and CO_2 emissions) than range-extend DWPT-EV for all considered vehicle class and driving scenarios. However, a sensitivity study carried out by reducing the battery price, shows that range extend DWPT-EV can be very promising in terms of

TCO (economic criteria) if battery price is going to be significantly reduced in the future. In addition, we should keep in mind that vehicle TCO figures reported in this section do not include the investment costs for infrastructure (e-road). Reduction of the battery size (according to battery shrink option) might imply more investment in e-roads and, especially at early stage of deployment, there could not be sufficient critical mass of DWPT-EV to justify such an extra investment. This means that range-extension DWPT-EV results should not be disregarded.

3 ASSESSMENT OF UP-SCALING ON ELECTRICITY GRID

This chapter deals with the wider impact on electricity grids. Basically, this chapter takes results from the studies of SP3 and takes them to a higher level. While models in SP3 focus on local grid impact (fast high-power peaks), using power flow analysis, in this chapter regional, national and EU-wide impacts are studied. These studies are based on energy balances. Annual mean values are used for assessment of CO_2 emissions and daily patterns (aggregated load curves) are studied in order to assess integration with renewable generation and storage, with special focus on solar photovoltaics.

3.1 Grid connection architectures

In FABRIC deliverable D3.5.1 [14] a generic grid connection architecture has been proposed, which has been confirmed by further findings as the project has been evolving. In order to remind this architecture, it is reproduced here in the following Figure 12 (from Figure 99 of D3.5.1).

In this report we are considering one road converter station for each km for the extra-urban solution (e-road) and a slightly different approach for the urban solution, as depending on the power transfer level (50, 100 or 150 kW) different solutions are practicable. For lower power levels (50 kW) a continuous WPT track similar to the e-road is needed to provide sufficient energy to the vehicle. But when power is increased, a discontinuous solution is possible.

According to existing layouts for tramways, a 750-V DC line can be conceived with feeding converter stations spaced 1 km or more (see D3.5.1 section 4.4.4).

As mentioned already in FABRIC deliverable D3.5.1 [14], it is most reasonable to conceive the e-road more like railways rather than highways. Historically, railway systems have been using DC distribution (up to 3 kV DC), but recently the trend is to use MV AC distribution.

There are many possible grid connection scenarios, but here only some examples will be provided, which were obtained from the expertise of the FABRIC consortium and related to the estimate of e-corridors demand (see also D5.4.2 [15]).

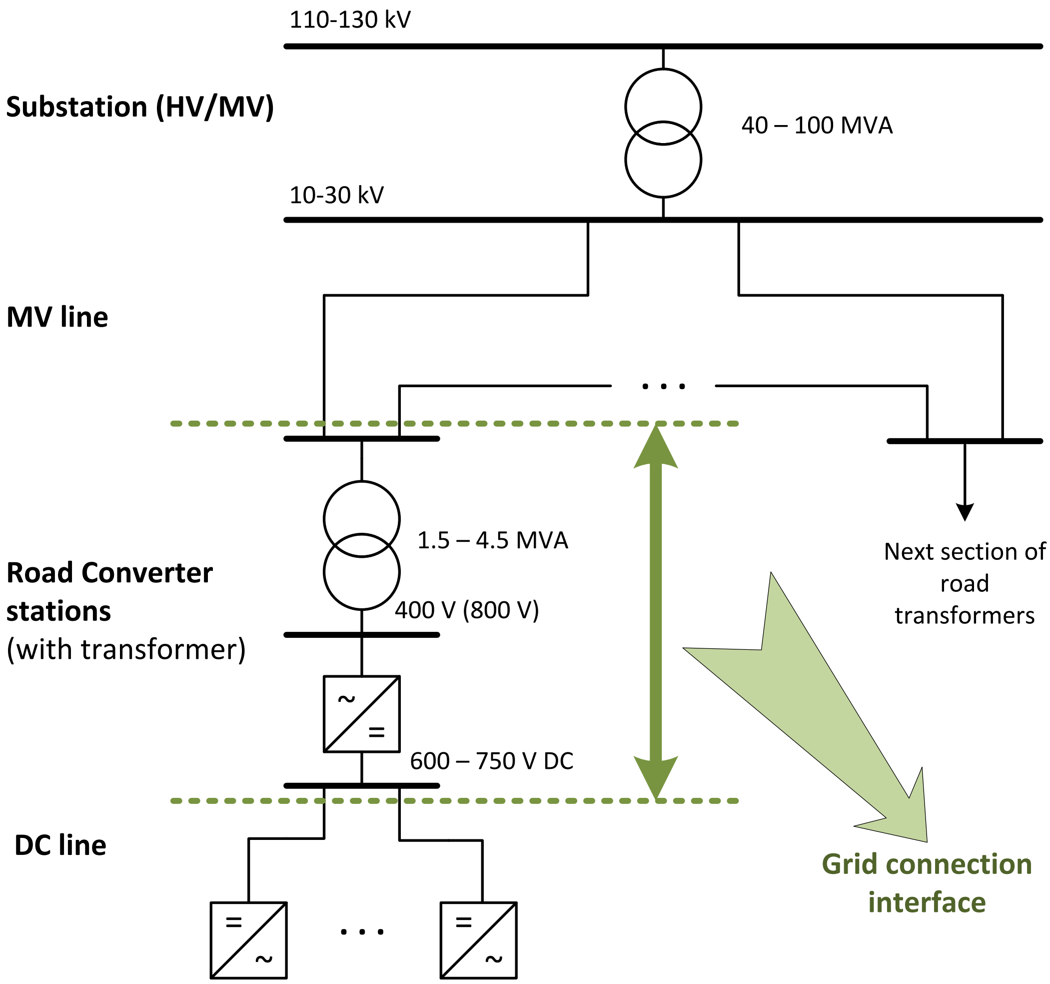

Figure 12: Generic grid connection design from HV down to the 750-V DC line.

According to the viable business cases, which were identified in D5.2.1 [16], different grid connection scenarios are considered. Two main grid-connection options have been identified, one for urban and one for extra-urban application:

- Extra-urban application:
  - Motorways (LDV and HDV)
  - Periurban areas (HDV charging near logistic centres)
- Urban application:
  - Urban (buses)

3.1.1 Power requirement

A major concern regarding grid connection architecture is the required power levels or the question, how much power per km will be needed. Therefore, two parameters need to be defined:

- Charging power per vehicle

- Number of vehicles per km

If charging power per vehicle and number of vehicles per km is known, the power requirement for the grid connection can easily be obtained from the formula below:

$$P_{km}[kW] = N_{vpk}\, P_{ch}\; [kW]$$

With $P_{km}[kW]$ being the power requirement per km, N_{vpk} the number of vehicles per km and P_{ch} the charging power per vehicle.

3.1.1.1 Charging power per vehicle

Charging power depends on the available technology. In the FABRIC project power levels of 25-50 kW have been demonstrated for early prototypes. To be useful as effective range extending technology, it is assumed that 50 kW of charging power need to be considered in the up-scaling scenario for small vehicles with just one receiver coil. Larger vehicles such as delivery vans, buses and trucks may have several receivers and thus, increase the received energy by a factor two or three, without the need of larger ground coils. In this study, power levels of 25-100 kW are considered for continuous charging (e-road concept) and 50-150 kW are considered for the special case of urban buses, which might recharge only at the stops. For economic analysis, one power level has been chosen for each scenario (Motorway, Periurban and Urban), as shown in the table below.

Scenario	Motorway E-Corridors/E-Road	Periurban (E-Launchers)	Urban (Bus)
Power per vehicle	50 kW	100 kW	100 kW

Table 28: Selected power levels per vehicle for Motorway, Periurban and Urban scenarios.

It should be mentioned here that in D3.3.3 “Interoperability considerations” it has been shown that existing low-power systems for passenger vehicles are not compatible with high-power systems for buses and trucks, mainly due to different voltage levels of the on-board system. On the other hand, there is a trend for higher voltages in line with larger battery packs and higher power for fast charging. Currently, a 50-kW static charger is still considered a fast charger. Nevertheless, for the Californian car maker Tesla this was not enough, as these cars have battery packs of up to 100 kWh. Therefore, Tesla developed and installed their own fast chargers called “Superchargers”. The first version had 120 kW, the second (current) version has 145 kW and the “Supercharger V3” was announced in December 2016 with a power level of 350 kW. This number is in line (probably not by accident) with the plans of other car manufacturers. In March 2016 started the European Ultra-E project [17], which aims to develop and install 350-kW ultra-fast chargers for electric vehicles along the trans-European transport network (TEN-T), which will be compatible with Tesla’s cars. These chargers are announced to have a voltage level of 800 V DC,

which is very similar to the one proposed for the DWPT system. Therefore, it is considered here that the problem of different voltage levels might be overcome in the time horizon of this study (around 2030 first commercial dynamic wireless power transfer tracks). Together with the voltage level, it is also assumed here that common battery packs by 2030 will be able to receive recharge power of 50-100 kW from the dynamic power transfer system without problems.

3.1.1.2 Vehicles per km – Motorway

To obtain the maximum number of vehicles which might be charging at the same time on a given track, vehicle length and security distance must be taken into account. A well-established rule is to define the security distance in terms of time, the vehicle would pass it at its current speed.

With this, the following formula can be used to calculate the vehicles per km:

$$N_{vpk} = \frac{1000}{t_{secure}\,[\mathrm{s}] \cdot \frac{v_{veh}}{3.6}\,[\mathrm{km/h}] \ + l_{veh}\,[\mathrm{m}]}$$

$$N_{vpk} = \frac{3600}{t_{secure}\,[\mathrm{s}] \cdot v_{veh}\,[\mathrm{km/h}] \ + 3.6\, l_{veh}\,[\mathrm{m}]}$$

With N_{vpk} the number of vehicles per km, t_{secure} [s] the security rule, v_{veh} [km/h] the speed of the vehicle and l_{veh} [m] the length of the vehicle.

Assuming t_{secure} = 2 s and a vehicle length l_{veh} = 4 m, vehicles per km can be calculated for different vehicle speeds, as shown in the figure below. As can be seen from this chart, depending on which vehicle speed is considered, the number of vehicles per km covers a wide range from 100 down to 10 vehicles or less. Therefore, for practical reasons, a design speed should be defined in order to be able to finally calculate the power rating per km of e-corridor. For 100 km/h design speed, a maximum of 17 vehicles/km can circulate on the e-road. As explained in POLITO traffic model in D3.2.1 of FABRIC project [18], 30 vehicles per km is considered a critical traffic density for freeways under basic conditions [19]. This would correspond to a vehicle speed of 50 km/h (according to Table 29, which was obtained from the formula above, it is 31.5 vehicles per km). As a conclusion, for further considerations traffic densities of 10 and 15 vehicles will be considered, which are considered realistic and far enough away from the critical traffic density.

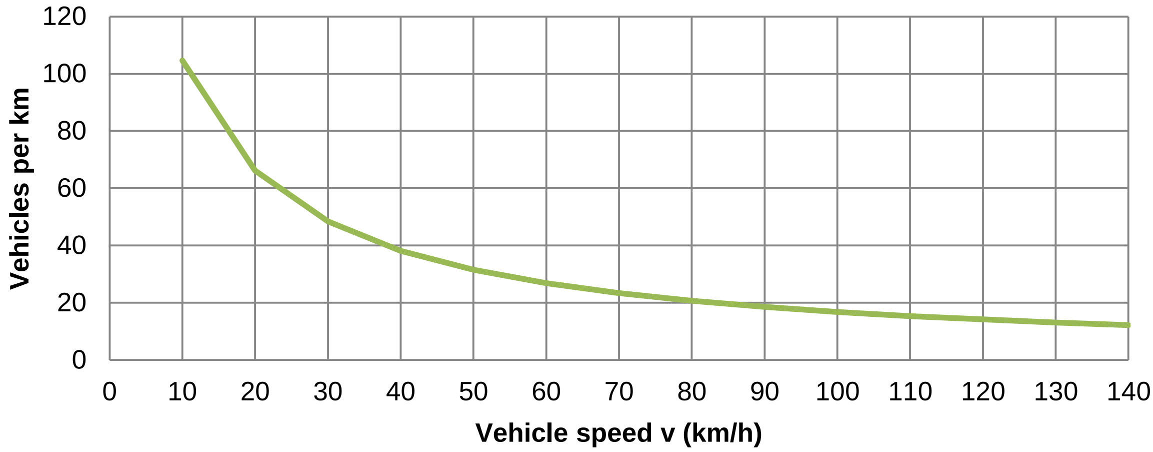

Figure 13: Vehicles per km with a security distance of 2 seconds and vehicle length of 4 m.

Vehicle speed v_{veh} (km/h)	Number of vehicles per km N_{vpk}	Distance between cars (m)
10	104.7	9.6
30	48.4	20.7
50	31.5	31.8
60	26.8	37.3
80	20.6	48.4
90	18.5	54.0
100	16.8	59.6
110	15.4	65.1
120	14.2	70.7
130	13.1	76.2

Table 29: Number of vehicles per km and distance between cars assuming 2s security rule.

Of course, it might be argued that the charging system should be able to serve also a larger number of vehicles, in case vehicle speeds are lower. Nevertheless, in this case the charging system might reduce individual charging power, as at lower speeds, there is more time available to recharge the desired amount of energy. For early systems, overall system power might even be further reduced, assuming that such dense vehicle flows will never be reached.

3.1.1.3 Vehicles per km – Periurban

For the Periurban scenario ("e-Launcher"), the same approach as for the Motorway scenario has been applied. The only difference consists in the fact that only heavy vehicles are assumed to use e-Launchers. As a result, another vehicle length must be considered. For the case of a speed of 80 km/h, in Table 30 resulting numbers of vehicles per km are shown for different vehicle lengths. As can be seen, the difference is rather small between the 4 m assumed in the Motorway scenario and 15 m considered for the Periurban scenario. It will also be shown, that expected

traffic density on e-Launchers will be much lower than the theoretical limit obtained from the 2-s rule.

Vehicle length	4 m	8 m	12 m	15 m
N_veh/km	20.6	19.1	17.7	16.8

Table 30: Number of vehicles according to the 2-s rule at 80 km/h and different vehicle lengths.

3.1.1.4 Vehicles per km – Urban bus

In Figure 14 an example of bus density is shown for the city of London, expressed in bus stops per squared km.

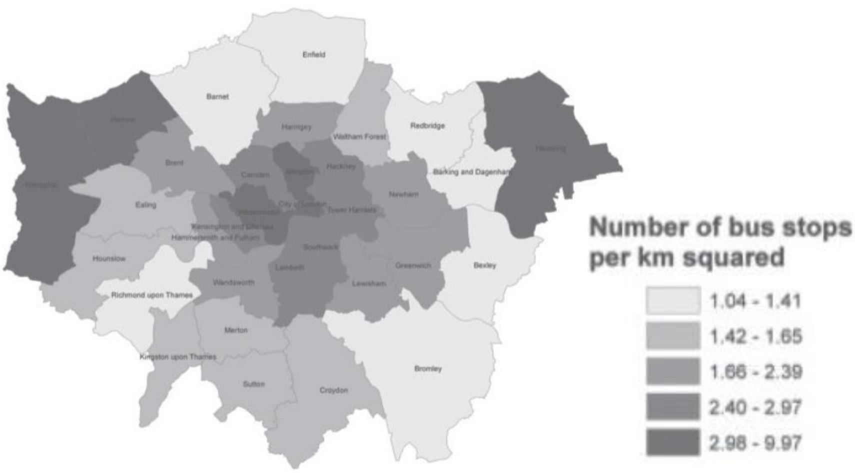

Figure 14: Bus density in London 2010. Source: Green 2014 [20].

Here, as a simplified way to estimate the number of charging buses per km² the range of density of bus stops from 1 – 10 is adopted as a reasonable guess. This means that for each bus stop, there is one bus on the road. This assumption seems reasonable, as considering a bus fleet of 400 buses for a service area of 100 km² gives an average bus density of 4 vehicles per km².

From the UNPLUGGED project (example city of Florence) and from comparison with other cities, the following assumptions are derived here for a medium-sized European City:

- City:
  - Service area: 100 km²
  - City centre with highest service density: 10 km²
- Buses:
  - 400 buses
  - Average traffic density: 4 buses per km² (assuming service area of 100 km²)
  - Energy consumption: 2 kWh/km
  - Max. power: 150-200 kW (on the bus)

    - Recharge power: 50 – 100 – 150 kW
- Routes:
    - Approx. route length: 10 km (20 km round-trip)
    - Bus density bus stops per km² (equal to buses charging): 1 – 10
        - Suburb: 1 bus per km²
        - City Centre: 10 buses per km²
    - Linear density (buses per km)
        - 1 bus per km (suburb, assuming 1 km bus lane per km²)
        - 5 buses per km (city centre, assuming 2 km bus lane per km²)

In addition, it is considered, that lager Cities will have similar indicators such as bus density per km², which will vary depending on the city district, but will always stay within the range of 1-10 stops per km².

3.1.1.5 Power per km – Motorway

For the extra-urban application, it is assumed that one e-corridor will have a length of 25 km and will be installed every 400-600 km in the motorway scenario. The objective in the motorway scenario is a range extension between 10%-20%, using the TEN-T infrastructure (larger motorways with 3 to 4 lanes per direction) with 88% light vehicles and 12% heavy vehicles.

Considering the boundary condition of 30 vehicles per km, if each vehicle is demanding 20 kW, 18.8 MW will be required at each substation (including 80% power transfer efficiency). If the requirement is reduced to 10 vehicles per km, the substation should still be able to provide 6.3 MW. If charging power is increased to 100 kW (in a scenario more in the future), the power requirement can reach up to 94 MW each 25 km (assuming 30 vehicles per km and 100 kW power transfer per vehicle). It should be mentioned here that 30 vehicles per km is an extreme scenario with a heavily saturated road. Here the implementation of an e-road might case issues with additional traffic congestions, so these roads are not suitable. It should be mentioned here that at 100 km/h and applying the 2-s security rule, only 17 vehicles can be present on one km.

In the table below, the required power supply from the grid is shown assuming 10 and 15 vehicles per km and different charging power levels per vehicle. Finally, power levels for a 25-km e-corridor are provided too, which would be able to feed a maximum of 375 vehicles simultaneously.

Charging power (per vehicle) $P_{ch}\ [kW]$	Grid power per km (Road converter station) $P_{km}\ [MW]$		Grid power per 25 km (HV/MV substation rating) $P_{25km}\ [MW]$	
	$N_{vpk} = 10$	$N_{vpk} = 15$	$N_{vpk} = 10$	$N_{vpk} = 15$
20	0.25	0.38	6.3	9.4
50	0.63	0.94	15.6	23.4
100	1.25	1.88	31.3	46.9

Table 31: Motorway scenario: power requirement for grid supply assuming values of N_{vpk} of 10 or 15 vehicles per km and different charging power levels.

These values (7.5 – 50 MVA) are reasonable values for HV/MV substation transformers. A doubly fed, dedicated MV line would be a practical solution here. In fact, in an early phase, only one 7.5-MVA connection to the HV grid would be sufficient, considering lower charging power and less than 10 vehicles per km during rush hours. The system can be upgraded later on, adding a second feeding substation and in a final step, upgrading each substation until the final capacity of 2x 25 MVA is reached.

One 250 kVA transformer is capable of providing power to 10x 20 kW chargers (assuming 80% transfer efficiency and 20 kW at the vehicle). Every 1-km section of the e-road is connected to MV by a road converter station which feeds 1 km of 750-V DC cable which runs along road side providing power to DC/DC converters every 100 m. Finally, another DC line distributes power from each DC/DC converter to the individual chargers, where the DC/HF converters are located.

If transfer power is increased, the concept remains identical, only the road converter stations would require higher power ratings, as shown in Table 31 (Grid power per km).

Nevertheless, it should be mentioned here that HVDC technology is improving continuously due to evolving power electronics [21]. Cost reductions make HVDC applications more and more interesting also for shorter distances and in the future power system, even MV DC grids might emerge. In this scenario, even 25-MW converter stations, which would be needed for the scenario with 100 kW power transfer might be a promising option.

Therefore, as this report is giving an outlook for a future technology, it cannot be discarded that MV distribution could be also a DC line (for example 10 kV DC), which might be doubly fed from HV AC grid. With this configuration, intermediate road converter stations are not needed any more, as power can be extracted locally directly by the DC/DC converters. In addition, this configuration would be beneficial for integration of renewable energy.

3.1.1.6 Power per km – Periurban

In the same way as for the Motorway scenario, the power requirement can be obtained for the e-Launcher, only with different power levels and numbers of vehicles per km. For the periurban business case, 10-km section is considered, but applied only to heavy vehicles.

A summary of resulting power requirements is given in Table 32. Comparing to the e-Corridor of 25 km length, the power requirement is reduced by a factor 2.5. This is due to the reduced length of the charging section (10 km compared to 25 km). Traffic density is half, but power level per vehicle is double the one considered for e-Corridor, thus, these two compensate each other.

Charging power (per vehicle) P_{ch} $[kW]$	Grid power per km (Road converter station) P_{km} $[MW]$		Grid power per 10 km (HV/MV substation rating) P_{10km} $[MW]$	
	$N_{vpk} = 5$	$N_{vpk} = 7.5$	$N_{vpk} = 5$	$N_{vpk} = 7.5$
50	0.31	0.47	3.1	4.7
100	0.63	0.94	6.3	9.4
150	0.94	1.41	9.4	14.1

Table 32: Periurban scenario: power requirement for grid supply assuming values of N_{vpk} of 5 or 7.5 vehicles per km and different charging power levels.

3.1.1.7 Power per km – Urban bus

For urban environment, the electrification of bus lanes was identified in D5.2.1 as the most likely business case. Mainly for urban buses, the same system might also be used by delivery trucks and taxis. Within the UNPLUGGED project, a showcase was presented for Florence City buses [22]. In the same report, also data from London (MILLBROOK LONDON TRANSPORT BUS) was presented. These showcases will be used here to create a scenario which will demonstrate the feasibility of grid connection of this urban application. Later in this report, the assumptions will be scaled to a higher level and introduced in the consideration for regional and European level.

In order to estimate required grid connection capacity, the density of buses per km² is the most relevant parameter. For example, for the city centre, with 10 buses per km² and simultaneous recharging at 100 kW, a power density of 1 MW/km² is obtained (ignoring power transfer efficiency for the moment). For metropolitan areas, this value corresponds to the lowest power densities, as can be observed in Figure 15. In this example, power densities for the City of Helsinki are shown, where maximum load centres are found with more than 40 MW/km². In the UNPLUGGED report cited above, it was stated that the whole power required by all charging stations (for recharging the entire bus fleet) represents less than 1% of the network capacity of the City of Florence.

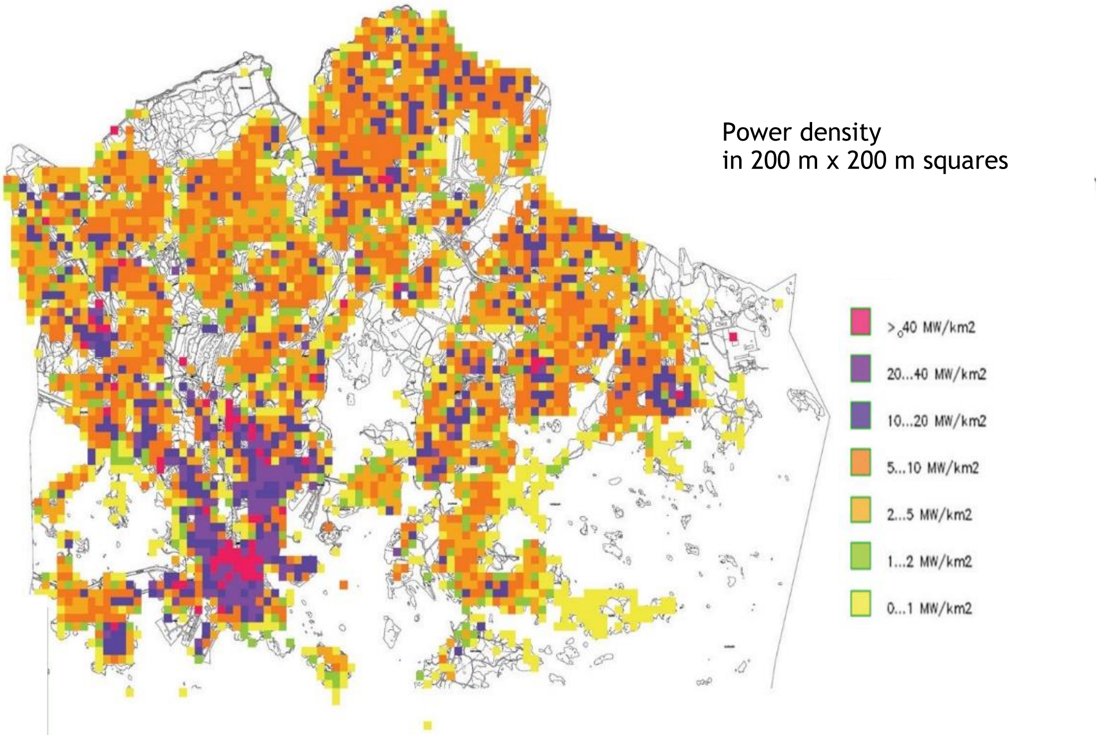

Figure 15: Load density distribution in Helsinki city (data 2007 Helen Electricity Network Ltd). Source: Hyvärinen 2008 [23].

Although load density per city area is the most relevant parameter for distribution network planning, dynamic charging lanes should be treated as linear objects, similar to the e-road concept. Therefore, in the following Table 33, charging lanes are considered and power per km is defined and compared with the values obtained per city area. The given range considers low densities for suburbs and high densities for city centres. In addition, a power transfer efficiency of 80% is considered.

As can be observed, for the highest charging power and density levels, required grid power per a one-km segment is 0.94 MW, which is a reasonable value for a medium sized LV distribution substation. Regarding load density per city area, even considering a charging power of 150 kW and power transfer losses, highest required grid power density is still below 2 MW/km².

Charging power P_{ch} $[kW]$	Grid power per km² P_{sqkm} $[MW]$		Grid power per km bus lane P_{km} $[MW]$	
	$N_{vpk} = 1$	$N_{vpk} = 10$	$N_{vpk} = 1$	$N_{vpk} = 5$
50	0.06	0.63	0.06	0.31
100	0.13	1.25	0.13	0.63
150	0.19	1.88	0.19	0.94

Table 33: Urban bus scenario: power requirement for grid supply assuming different values of N_{vpk} per km² and per km for different charging power levels.

For distribution system design, of a spatially distributed load, such as a bus-line system, it is more adequate to transform linear stops (per km) in stops per surface (per km²).

Notice the fact that the relationship between service area (km²) and bus lane length (km) is different for suburbs and city centres. It is assumed here, that route density, measured in km per km², is by a factor 2 higher in urban areas than in suburban, which is a reasonable guess at the light of the available data and might be discussed.

According to the SORT driving cycle, distance distribution between SORT1, SORT2 and SORT3 is 1/6, 1/3 and 1/2, assuming a typical bus route of 9 km (1.5 km SORT1, 3 km SORT2 and 4.5 km SORT3). With these assumptions and the total service area and bus lane length, the following equation can be developed, in order to obtain km/km² ratios for each SORT type which respects both, the proportion of route km and the total covered service area A.

$$A\,[\mathrm{km}^2] = L[\mathrm{km}]\left(\frac{\omega_1}{2a} + \frac{\omega_2}{1.5a} + \frac{\omega_3}{a}\right)$$

Where A is the service area in km², L is the total length of bus lanes in km, ω_1, ω_1 and ω_1 are the weights of each SORT cycle and a is the km-to-km² ratio for suburban area. Mixed and Urban are expressed as multiples of a, in order to model a linear progression.

Transforming the equation above, an expression for a can be obtained straight-forward, as a function of service area, total bus-line length and the weight of each SORT cycle in the overall driving cycle.

$$a = \frac{L[\mathrm{km}]}{A\,[\mathrm{km}^2]}\left(\frac{\omega_1}{2} + \frac{\omega_2}{1.5} + \omega_3\right)$$

From this expression, it can be seen, that if a constant km-to-km² ratio is considered, it will be just the quotient between total service length and service area. In our case this ratio would be 3.6 km/km² (360 km / 100 km²). For the considered linear progression, a value of $a = 2.9$ km/km² has been calculated for suburban areas. The resulting values for the other areas and covered area in km² are given in Table 34.

Driving cycle	Weight ω (Proportion of km)	Distance ωL (km)	Ratio (km/km²)	Covered area (km²)
Urban (SORT1)	1/6	60	5.8	10.3
Mixed (SORT2)	1/3	120	4.35	27.6
Suburban (SORT3)	1/2	180	2.9	62.1

Table 34: Relationship between served bus lane length and service area.

With the relationship of served km per km², bus stops per km² can be calculated and with this, the number of buses per km², considering that there is a ratio of 2.7 stops per bus (27 stops and 10

buses for each route). Results are shown in Table 35. Obtained stops per km² are sensibly higher than those reported above (1-10 stops per km²). This is due to the fact, that each bus line is treated separately, in order to represent actual buses circulating on this line. In reality, bus lines are sharing stops. In this study, it has been preferred to consider stops separately, in order to add a security margin and to avoid additional complexity, defining another parameter which would give the number of lines per bus stop.

Driving cycle	Stops per km	Buses per km	Stops per km²	Buses per km²
Urban (SORT1)	6	2.22	35	12.9
Mixed (SORT2)	3	1.11	13	4.8
Suburban (SORT3)	2	0.74	9	2.1

Table 35: Assumptions of spatial distribution of bus stops and buses for grid design.

Depending on the power transfer level, different road-side infrastructure is needed:

50 kW: continuous WPT lane

For this case, number of bus stops is irrelevant, as all buses are assumed to be charging continuously, but power requirements are obtained from the number of buses per km².

One 630 kVA road converter station is capable of providing power to 10x 50 kW chargers (assuming 80% transfer efficiency and 50 kW at the vehicle). As a result, 40 transformers are needed to feed 400 buses simultaneously, with a total power is 25 kVA. Average density is 1 transformer every 2.5 km².

Due to different traffic densities, transformer density varies accordingly, between 0.8 – 4.7 km² per transformer. The average density means that there should be one LV transformer for an entire route of 9 km. Nevertheless, cable lengths will not surpass 900 m, considering radial feeding possibility. This means that one transformer station might feed several different DC cables (different e-Trenches), through different feeders. In the suburban case, feeders from existing transformers might be used due to the low demand. Findings are summarised in Table 36.

Driving cycle	Power density (kW/km²)	Service area per 630-kVA road-converter station (km²)	Power per service area (kVA)	Required road-converter stations
Urban (SORT1)	805	0.8	8.33	13.3
Mixed (SORT2)	302	2.1	8.33	13.3
Suburban (SORT3)	134	4.7	8.33	13.3
Total			**25**	**40**

Table 36: Assumptions of spatial distribution of bus stops and buses for grid design.

In urban areas, 13 buses per km² are considered (approximately 3 times the average density), which results in an area of 0.8 km² which can be covered. The equivalent length of e-Trenches fed by this transformer is therefore also 1/3, which means 3 km. E-Trenches are fed by a 750-V DC cable which runs along road side providing power to DC/DC converters every 100 m. In mixed and suburban areas, the spacing of MV connections is increased, as demand decreases. In this configuration, in suburban areas, one MV connection might feed up to 136 DC/DC converters (13.6 km of DC lines), of 50 kW each, but it is assumed that never more than 10 will be powered simultaneously. Finally, another DC line distributes power from each DC/DC converter to the individual chargers, where the DC/HF converters are located.

With the 100-m spacing, with this configuration there would be 90 DC/DC converters on the 9-km route considered above.

100 kW: 25-m WPT tracks at each stop

Spatial distribution of transformers is identical to the 50-kW continuous case, as it is assumed that higher DWPT power transfer level is compensated by lower number of simultaneous charging. This means, the same transformer will feed the same area, but serve only half of buses at the same time. Total system power is also 25 kVA.

One 630 kVA transformer is capable of providing power to 5x 100 kW chargers (assuming 80% transfer efficiency and 100 kW at the vehicle). A 750-V DC cable which runs along road side providing power to DC/DC converters. Subsequent DC distribution is limited to the 25-m WPT tracks at each stop. The spacing of the DC/DC converters depend on the stops. According to SORT 1 and SORT2, distances between 100 – 600 m can be expected. In suburban areas, the spacing of MV connections is increased, as demand decreases. As in the case of 50-kW chargers, it is assumed that no more than 5 buses will recharge at the same time connected to the same road converter station. In this configuration, the number of DC/DC converters is drastically reduced (one per stop) compared to the continuous track in the first case. The number falls from 90 to 27 converters per route.

150 kW: stationary charging at each stop

As for 100 kW, spatial distribution of transformers is maintained. In this case, the same transformer serves only one third of buses at the same time.

One 630 kVA transformer is capable of providing power to 3x 150 kW chargers (assuming 80% transfer efficiency and 150 kW at the vehicle). As in the case for 100-kW chargers, the DC cable runs along road side providing power to the DC/DC converters. In this case, subsequent DC distribution is limited to the individual coils of the stationary charging configuration (might be 1-3 coils).

3.1.2 Energy requirement

Apart from the power level the vehicles are charged, an important design parameter is the energy consumption of the vehicle. For simplicity reasons, and attending the two use cases described here, two different consumption levels are considered in this report:

- Passenger car: 0.2-0.3 kWh/km (average 0.25)
- 12-m city bus: 1.0-2 kWh/km (average 1.5)

3.1.2.1 Motorway – E-Corridors

The consumption mentioned above is of course the overall average consumption. For the e-road application, assuming fluid traffic, a rather constant speed can be considered, and mean consumption will be a good estimate also for instantaneous power. However, the relationship between transferrable energy and vehicles speed needs some more attention, in order to justify some of the assumptions, such as typical traffic density of 10 vehicles per km.

As shown in the section 3.1.1.2 (Vehicles per km – Motorway), maximum number of vehicles per km (N_{vpk}) depends on the vehicle speed, if a security rule (for example 2 seconds) is established. However, traffic density is often given as vehicles per time (per hour or per day). Both numbers are related to each other by the vehicle speed as follows:

$$N_{vph} = N_{vpk} \cdot v_{veh} \text{ [km/h]}$$

Being N_{vpk} the number of vehicles per km and v_{veh} the vehicle speed.

Introducing this formula into the one of N_{vpk} the following expression is obtained:

$$N_{vph} = \frac{3600 \cdot \; v_{veh} \text{ [km/h]}}{t_{secure} \text{ [s]} \cdot v_{veh} \text{ [km/h]} \; + 3.6 \; l_{veh} \text{ [m]}}$$

$$N_{vph} = \frac{3600}{t_{secure} \text{ [s]} + \frac{3.6 \; l_{veh} \text{ [m]}}{v_{veh} \text{ [km/h]}}}$$

Being t_{secure} the security distance and l_{veh} the vehicle length.

From the resulting formula for N_{vph}, it can be seen easily that if vehicle speed v_{veh} tends to infinite, the number of vehicles per hour tends to 3600/t_{secure} [s]. In Figure 16 both parameters, N_{vph} and N_{vpk}, are depicted for the 2-s security rule and vehicle length of 4 m. In this case, N_{vph} tends asymptotically towards 1800 for higher vehicle speeds, while N_{vpk} (vehicles per km) tends towards zero.

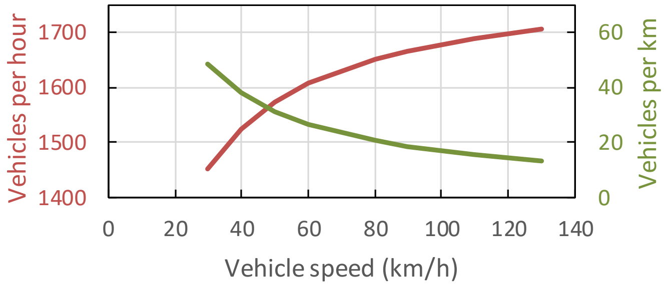

Figure 16: Relationship of vehicle speed and traffic density assuming 2-s security rule.

The only reason why the number of vehicles passing in one hour is not constant at 1800 vehicles (one vehicle every 2 seconds), is that a car length (in this case 4 m) is considered.

However, it is the number of vehicles per km (N_{vpk}) and not the number of vehicles per hour (N_{vph}), which finally defines the required power (N_{vpk} x transfer power) and also the transferrable energy. Considering a stationary traffic flow, it becomes clear that the more vehicles are being recharged simultaneously, the more energy is transferred in a given period of time. In this case, it is not relevant how much energy each individual vehicle receives, but the sum of all energy transferred to all vehicles which pass in a certain time interval. The formula to calculate the aggregated energy transfer of a 25-km stretch E_{25km} shows direct proportionality with N_{vpk}:

$$E_{25km}[\text{kWh}] = 25\ N_{vpk}\ P_{WPT}\ [\text{kW}]\ \cdot \Delta t\ [\text{h}]$$

Being P_{WPT} the transfer power and Δt the time interval considered.

Typical highway traffic patterns

Traffic on highways can show a wide range of patterns, depending on the location, time of day, direction and season. For example, in the morning, commuters will drive towards their working places and will come back in the evening. Seasonal variations can be expected, especially on highways which lead to highly frequented holiday locations, such as beaches or ski resorts. In D5.4.2, A first approach in order to identify suitable highways was a selection according to its average daily traffic per line. The survey of the TEN-T network showed that a typical range can be given between 4,000 and 12,000 vehicles per day and lane, being the higher number obtained from intensely used highways in The Netherlands and UK. Higher traffic density is considered problematic for DWPT integration (risk of traffic increased jam) and lower traffic is not relevant as expected income cannot justify investments.

In order to have an idea of average traffic densities per km, values of daily average traffic (4,000 – 12,000) can be converted into vehicles per km (N_{vpk}), employing the following formula (results are shown in Table 37):

$$N_{vpk} = \frac{N_{vpd}}{24\ v_{veh}\ [km/h]}$$

Being N_{vpd} the average number of vehicles per day and lane and v_{veh} the vehicle speed in km/h.

N_{vpd}	4000	8000	12000
N_{vpk}	1.7	3.3	5.0

Table 37: Daily traffic and corresponding vehicles per km for vehicle speed of 100 km/h.

The required design traffic density is obtained from the ration between average and peak traffic. Therefore, daily and seasonal traffic pattern need to be assessed, in order to obtain an estimate of a reasonable value for this ratio.

Of course, on highly congested roads, the probability of accidents is high and traffic jams occur almost daily. However, this case is not considered in this simplified case study.

In conclusion, with the premise that normal traffic is well below our reference maximum, it can be considered that energy consumption will increase proportionally with increased number of vehicles per day, assuming that vehicles per km also increase proportionally and all vehicles will stay the same time over the 25 km stretch of WPT lane.

There are extremely congested spots where up to 30,000 vehicles per day and lane are observed routinely. Such an example is A86 highway close to Paris urban area (measurement station A86E71.3000).

In Figure 17 hourly average distribution of working day traffic for this spot is shown in vehicles per hour and lane. Peak values near or above 1800 veh/h are observed between the 17th and 20th hour of the day. This means that on that highway, the 2-s safety distance is not respected during several hours of the day. According to the curve shown in Figure 16, 1800 veh/h should never be reached, if 2-s distance is considered and 1700 veh/h correspond to approximately 130 km/h vehicle speed. These extreme spots are definitely to be avoided for installation of e-corridors, as recharging service would be challenged during most of the day.

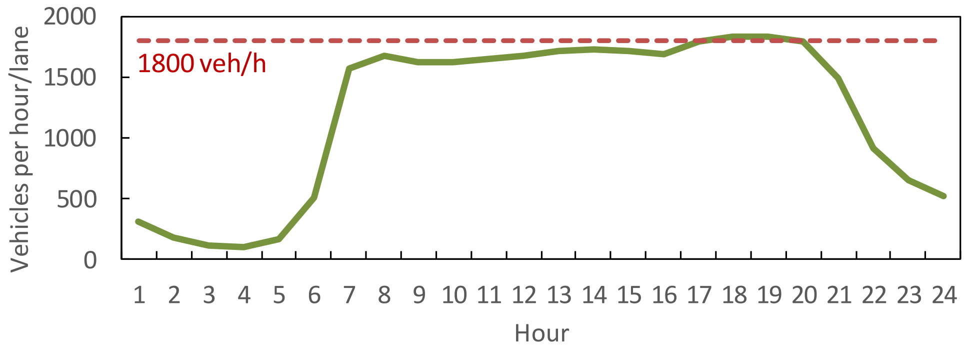

Figure 17: Average hourly working day traffic on A86 highway near Paris (measurement station A86E71.3000), Source: VEDECOM.

In order to obtain a more typical reference of possible traffic patterns which might be suitable for e-corridors, data from an exhaustive report on all Spanish toll highways [24] has been analysed and the results are shown hereafter.

In order to keep the scope of this report in a reasonable extent, in the end only one reference curve will be selected in order to showcase a typical demand pattern which might appear on an e-road. Traffic patterns are obtained in a normalised form, so different traffic density scenarios can be applied, as for example 4,000, 8,000 and 12,000 vehicles per day and lane. As we have seen that extreme traffic can reach up to 30,000 veh/day/lane, it is considered here that the value of 12,000 is still sufficiently far away from this extreme case, that linear scaling of the extracted patterns from the Spanish case can be considered a reasonable guess. The main difference between this southern example compared to northern countries might be a shorter summer peak. However, seasonal effects are much less important than daily patterns.

In the Spanish report mentioned above, 28 toll roads are described which represent a length of approximately 2,500 km. Overall average daily traffic is given with 16.65 thousand vehicles. Considering that the vast majority has 4 lanes (2 in each direction), the average daily traffic per lane is with 4,000 veh/day relatively low. However, 4 highway stretches have been identified which are considered suitable examples due to traffic density and length. Highway length was an important selection criterion, as short pieces of highway often show very specific traffic patterns which cannot be generalised.

The following 4 highway stretches have been selected:

- AP-2: Zaragoza-Mediterráneo (section I, until Lleida)
- AP-4: Sevilla Cádiz
- AP-68: Bilbao-Zaragoza

- AP-7: Barcelona-Tarragona

The table below contains main parameters of these highways. As can be observed from this table, traffic densities are relatively low, ranging from 2,500 up to 7,600 vehicles per lane and day, being the AP-7 near Barcelona the one with highest traffic and also highest percentage of heavy vehicles, which both can be explained by the industrial region of Tarragona and the sea ports in this area.

	AP-2	AP-4	AP-68	AP-7
Length (km)	215.5	93.8	294.4	96.6
Nº of lanes (sum of both directions)	4	4	4	6
Average hourly traffic (veh/h)	514	740	975	2273
Average daily traffic (1000 veh/d)	10.18	19.60	22.98	45.53
Light vehicles	9.06	18.53	20.31	37.78
Heavy vehicles	1.12	1.07	2.67	7.75
% of heavy vehicles	11.0%	5.5%	11.6%	17.0%
Average hourly traffic (veh/h/lane)	129	185	244	379
Average daily Traffic (1000 veh/d/lane)	3.1	4.4	5.9	9.1

Table 38: Main parameters of 4 selected Spanish toll highways.

Apart from average values, the most interesting information from this report was the fact that daily, weekly and yearly profiles were given (see Figure 18). Absolute values for each highway have been normalised by the daily, weekly and yearly average, so patterns are comparable and the percentage variation between average and peak traffic become more visible.

The daily pattern shows most of the variation, showing two very typical peaks: one morning peak and one evening peak. Highest traffic can reach almost 200% of the average. Weekly variation is much lower, showing a Friday-peak of 120% (20% over average). Finally, seasonal variation (monthly averages) depends very much on the highway, although all with a clear summer peak between July and August. The highest summer peak is observed for AP-2 (Zaragoza – Mediterranean) with 170%. Interestingly, the higher the overall traffic density, the lower the summer peak. AP-7 (Barcelona – Tarragona) which has highest traffic density, only shows a summer peak of 126%.

Important conclusions from Figure 18 are:

- Strong daily pattern with morning and evening peak
- Slight weekly peak on Friday (almost negligible)
- Traffic is significantly higher in summer than in winter
- Seasonal variations tend to be larger on highways with lower average traffic

For general conclusions, an average of these 4 curves is considered appropriate (see section 3.3.1 25-km E-road).

For generalization, it is important to know how far the observed traffic densities are from theoretical maximum traffic, which is calculated from vehicle speed and applying the 2-s safety rule. Especially important is to see if observed traffic peaks (i.e. Friday afternoon in August) might reach maximum densities. If this would be the case, saturation effects must be expected and linear scaling of daily patterns would not be advisable. A good example is the example of heavy traffic near Paris (see Figure 17) where the daily pattern shows a plateau, due to the fact that maximum capacity of the road is reached or even surpassed, considering safety aspects, such as minimum distance between cars.

In order to create a reference, theoretical traffic parameters are shown in the table below, assuming a typical vehicle speed of 100 km/h, 2 s security distance and 4 m average car length (see section 3.1.1.2 Vehicles per km – Motorway).

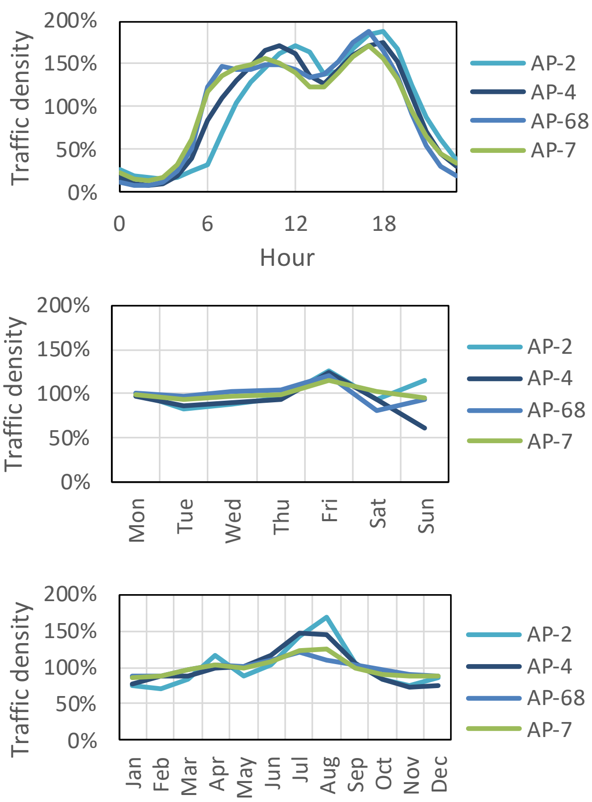

Figure 18: Average daily, weekly and yearly traffic profiles from 4 selected Spanish toll highways.

Safety distance (s)	2
Vehicle speed (km/h)	100
Number of vehicles per 25km	425
Time to cross 25 km (h)	0.25
Number of Vehicles per hour	**1700**

Table 39: Reference values for maximum traffic.

In Table 40 average and peak traffic values are compared with theoretical maximum traffic from Table 39. Values of maximum vehicles per hour are obtained multiplying the observed daily peak with weekly peak deviation percentage (Friday, around 120%) and seasonal peak deviation (depending on the road between 125-170%).

From Table 40 several conclusions can be drawn. Firstly, the ratio between maximum and average traffic (max/avg.) varies between 3.7 and 2.5 and decreases with increasing absolute traffic density (see Figure 19).

	AP-2	AP-4	AP-68	AP-7
Number of lanes (both dir.)	4	4	4	6
Maximum vehicles per hour	1,883	2,191	2,690	5,645
Average vehicles per hour	514	740	975	2,273
Maximum per h / lane	471	548	672	941
Average per h / lane	129	185	244	379
Average vehicles per day / lane	3,084	4,440	5,850	9,092
Ratio max/avg.	3.7	3.0	2.8	2.5
Ratio max/theor.max	0.28	0.32	0.40	0.56
Equiv. daily hours	1.8	2.6	3.5	5.4

Table 40: Selected variability parameters from 4 Spanish toll highways.

This means that expected peaks might be 3 times (or more) higher than reported average if that average is relatively low. An intermediate value (for example for 10 thousand vehicles per day) would be a ratio of 2.5 and a ratio of 2.0 might be expected if the annual average is 15 thousand vehicles per day. For the extreme case of A86 highway near Paris (30 thousand vehicles per day) a ratio of 1.5 was observed. This fact is due to saturation effects, as soon as the transit capacity of the road is reached.

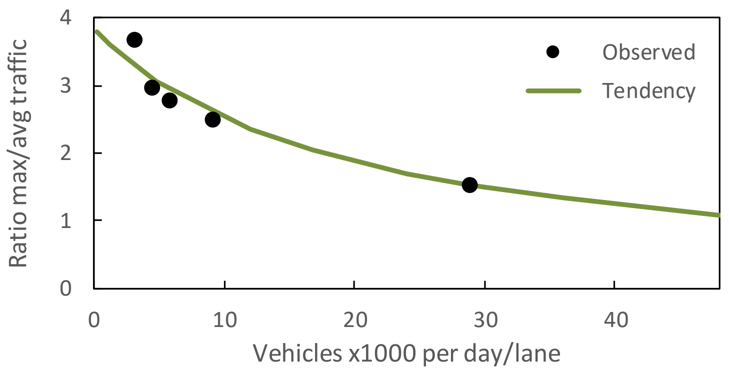

Figure 19: Ration between maximum and average hourly traffic versus average traffic density.

The second conclusion regards the ratio between observed maximum and theoretical maximum (max/theor.max). It can be seen here, that even the highest traffic peaks (AP-7) merely reach 56% of the theoretical maximum calculated with the premises from Table 39. This is the confirmation that these patterns are far away from saturation and a 50% increase for linear extrapolation up to 15,000 vehicles per day and line is acceptable with a reasonable margin of error.

Expected range extension: Example Nissan Leaf EV (data from 2016)

In order to give an estimate regarding the range extension which can be obtained from a 25-km stretch of e-road, an example is given here, which shows some key parameters to bear in mind:

- Recharged energy
    - Transfer power
    - Transfer efficiency
- EV energy consumption
    - Vehicle speed
    - Vehicle weight
    - External conditions (wind, slope, air temperature)
    - Auxiliary consumption on board (air-conditioning, lights)

Although “e-road as range extender” is a good concept, the quantification of the actual range which can be extended is complex and only estimates can be given, assuming a series of premises. For example, Transfer power might vary greatly if the vehicle is not perfectly aligned. Also, extreme weather might have important impact on vehicle consumption and thus, on the actual extended range.

In order to be able to give a number, the following assumptions are taken:

- Nominal power transfer (given in kW at the vehicle DC bus
    - Transformation and transfer efficiency is assumed at 80%
- Average vehicle consumption is considered (mixed city / highway driving)

Vehicle consumption is a critical issue to be discussed. In a first approach, it seems logical to calculate range extension based on certified average EV consumption (i.e. 0.15 kWh/km for a typical EV, such as the Nissan Leaf). Nevertheless, one could argue that the range extender which is proposed here is intended to give additional range under highway conditions, which imply a significantly higher consumption than the standard reference. As a result, highway range extension will always be lower than the one expected from average consumption.

In Figure 20, energy consumption of the Nissan Leaf EV (model 2016) is shown, considering a number of parameters. Consumption is considered as to be delivered by the battery and the evaluation is established at stabilised speed. Several parameters have been studied which can increase energy consumption, which are: speed, auxiliary power for inside comfort, slope, load on board (vehicle weight).

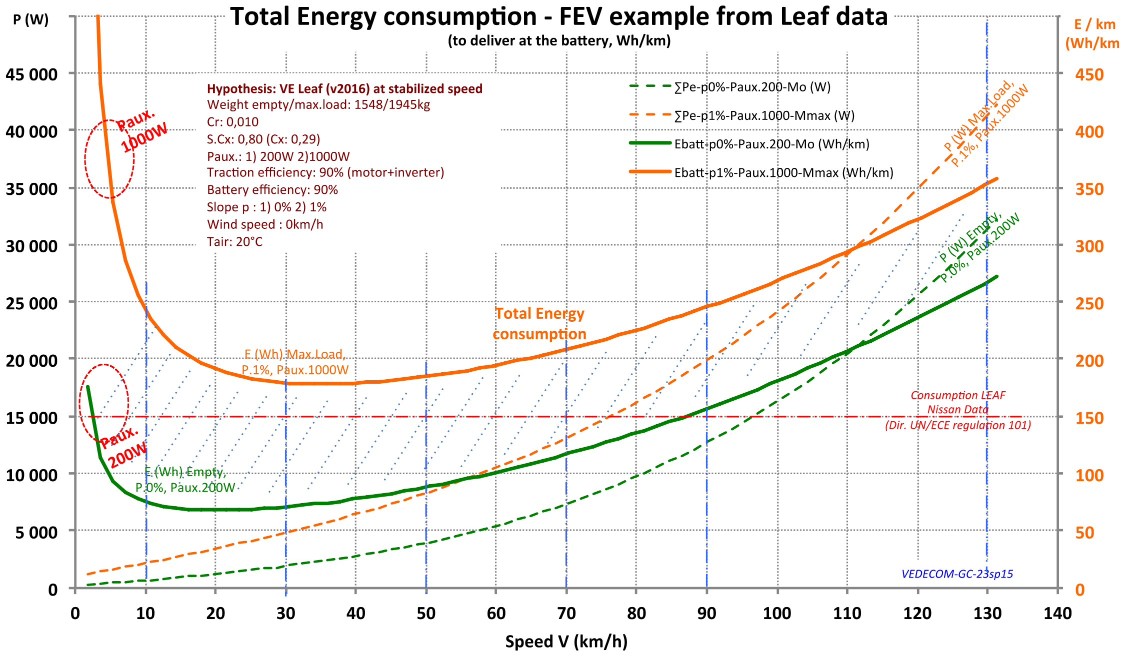

Figure 20: Energy consumption of Nissan Leaf EV, Source: Elaboration by VEDECOM.

In order to identify the boundary conditions which defines the range of energy demand which typically can be expected, 2 limit cases have been examined:

- Minimum consumption
  - Low auxiliary consumption: Paux = 200 W
  - No slope
  - Minimum weight: 1548 kg (only driver no passengers, no cargo)
- Maximum consumption:
  - High auxiliary consumption: Paux = 1000 W
  - Slope 1%
  - Maximum load: 1945 kg

Dashed lines are representing instantaneous power (left y-axis) and solid lines are representing energy consumption per km (right y-axis).

A main conclusion from this graph is that auxiliary power is most relevant for consumption at low speeds, while vehicle weight is decisive for higher speeds. It becomes also clear that there is an important difference between highway consumption and average consumption. As important result two typical driving conditions can be distinguished:

- **Urban driving:** 0.1 to 0.2 kWh/km
- **Inter-urban or highway driving:** 0.15 to 0.3 Wh/km

It can be concluded that the certified consumption of 0.15 Wh/km is most suitable for urban driving, but not suitable for highway driving. Therefore, it is proposed here to give two different values for range extension:

- Standard range extension: based on 0.15 kWh/km
- Highway range extension: based on 0.25 kWh/km

The following table shows the results for range extension for the three transfer power levels (20, 50 and 100 kW) considering standard and highway conditions. Recharged energy is calculated considering vehicle velocity of 100 km/h while recharging.

Dynamic and static power transfer level	20 kW	50 kW	100 kW
Energy recharged per vehicle over 25 km (at 100 km/h)	5.0	**12.5**	25.0
Range extension (km)			
Standard (assuming 0.15 kWh/km)	33	**83**	167
Highway (assuming 0.25 kWh/km)	20	**50**	100

Table 41: E-road range extension for different power levels of WPT and 100 km/h while recharging.

From Table 41 it can be seen that range extension capability is rather low for the scenarios of 20 and 50 kW power transfer, especially if highway extension is desired. At the current state of development of DWPT, 100 kW power transfer is considered as a possible technological limit.

For safety reasons, even 50 kW might be preferred. Therefore, higher range extension can only be obtained with lower vehicle speeds while recharging. In Table 42 results are presented assuming 50 kW power transfer and different vehicle speeds while recharging.

An important conclusion is that even at 60 km/h speed during recharge only 83 km of range extension is achieved (38 km gain compared to 110 km/h reference), considering highway conditions. In this calculation, energy savings (i.e. additional range extension) due to reduced speed are not included.

Apart from the discussion if recharge speed should be reduced to 80 km/h for example, time losses are equivalent to the time which would be required for conventional fast recharging at the same power level as for dynamic driving (50 kW in the example in Table 42). However, additional time spent for access of conventional recharging and possible waiting times in queues is avoided.

So, in summary, even at reduced speeds, considerable time is saved compared to conventional fast charging at the same power level. Of course, this advantage is reduced if fast charging levels are significantly higher than DWPT levels as foreseen by the European Ultra-E project and TESLA, which are preparing for 350 kW ultra-fast chargers (see discussion in section 3.1.1 Power requirement).

Vehicle speed while recharging	60 km/h	80 km/h	100 km/h
Energy recharged per vehicle over 25 km (kWh)	20.8	15.6	12.5
Range extension (km)			
Standard (assuming 0.15 kWh/km)	139	104	83
Highway (assuming 0.25 kWh/km)	83	63	50
Comparison with reference speed of 100 km/h			
Range gain (standard) (km)	56	21	0.0
Range gain (highway) (km)	33	13	0.0
Energy gain (kWh)	8.3	3.1	0.0
Time loss (min)	10.0	3.8	0.0

Table 42: E-road range extension for 50 kW transfer power different vehicle speeds while recharging.

3.1.2.2 Periurban – E-Launchers

In principle, the same considerations from the Motorway Scenario can be applied to the Periurban Scenario, with the only difference of charging power levels, expected traffic density and length of e-Corridor. Results for range extension for different DWPT levels are shown in Table 43. Compared to the motorway scenario, absolute km of range extension is significantly lower. Nevertheless, the same vehicle will probably cross the e-Launcher several times during a day and thus, obtain a higher range extension, which finally will result in an important time gain.

Notice that assumed consumption levels of 0.75 kWh/km for e-Trucks and e-Buses and 0.3 kWh/km for e-Vans are low values if highway consumption is considered. Nevertheless, these vehicles will mostly be circulating in city traffic, during delivery. Therefore, the average consumption and not highway consumption was considered for calculation of range extension, as this is the most relevant indicator in this case. Regarding consumption of e-Trucks, manufacturers are claiming a wide range of values, which cannot be verified by now. For example, for the urban bus scenario, 2 kWh/km were assumed, based on numbers of the UNPLUGGED project. If it turns out that promises from manufacturers were too optimistic, range extension of buses and trucks might be half of those stated in the table below.

Dynamic power transfer level	50 kW	100 kW	150 kW	
Energy recharged over 10 km				
One vehicle (kWh)	6.3	**12.5**	18.8	kWh/veh
Total on average day (MWh)	23	**45**	68	MWh/day
Range extension (km)				
e-Trucks/Buses (assuming 0.75 kWh/km)	8	**17**	25	km
e-Vans (assuming 0.3 kWh/km)	21	**42**	63	km

Table 43: E-Launcher range extension for different power levels of WPT and 80 km/h while recharging.

3.1.2.3 Urban bus

For the urban application (city bus), a driving cycle must be considered, in order to obtain a realistic picture of power demand along the route. As a result, a suitable recharging architecture can be derived (see section 3.1.1.7 "Power per km – Urban bus"). While for the e-road a continuous charging lane is practical, buses might need another configuration with shorter recharging tracks, spread over the bus route. Which configuration might be more suitable depends very much on the driving cycle. Therefore, in the following pages, an exercise is done considering some results from the UNPLUGGED project and applying data on our case.

In the UNPLUGGED project (among others) a "Firenze driving cycle" and MLTB (Millbrook London Transport Bus) driving cycle for buses were considered (see D3.2 of UNPLUGGED project). Results from UNPLUGGED suggest that the MLTB driving cycle is very realistic, as very similar patterns were observed in the Firenze driving cycle.

The MLTB test cycle (also known as Route 159 Drive Cycle), was specifically developed for use with buses and was derived from data logged from a bus in service within inner London. The drive cycle consists of two phases:

(1) Outer London Phase, nominal distance 6.45 km, 1,380 seconds in duration
(2) Inner London Phase, nominal distance 2.47 km, 901 seconds duration

The overall length of the test is 2281 seconds and the nominal distance covered is 8.92 km. This means, that the average speed of the bus is 14 km/h, but as can be seen in Figure 21, maximum speeds of up to 50 km/h and power peaks of up to 200 kW are reached.

As a detailed analysis of the MLTB cycle is very complex, a comparison with the SORT (Standardised On-Road Test) cycle has been carried out.

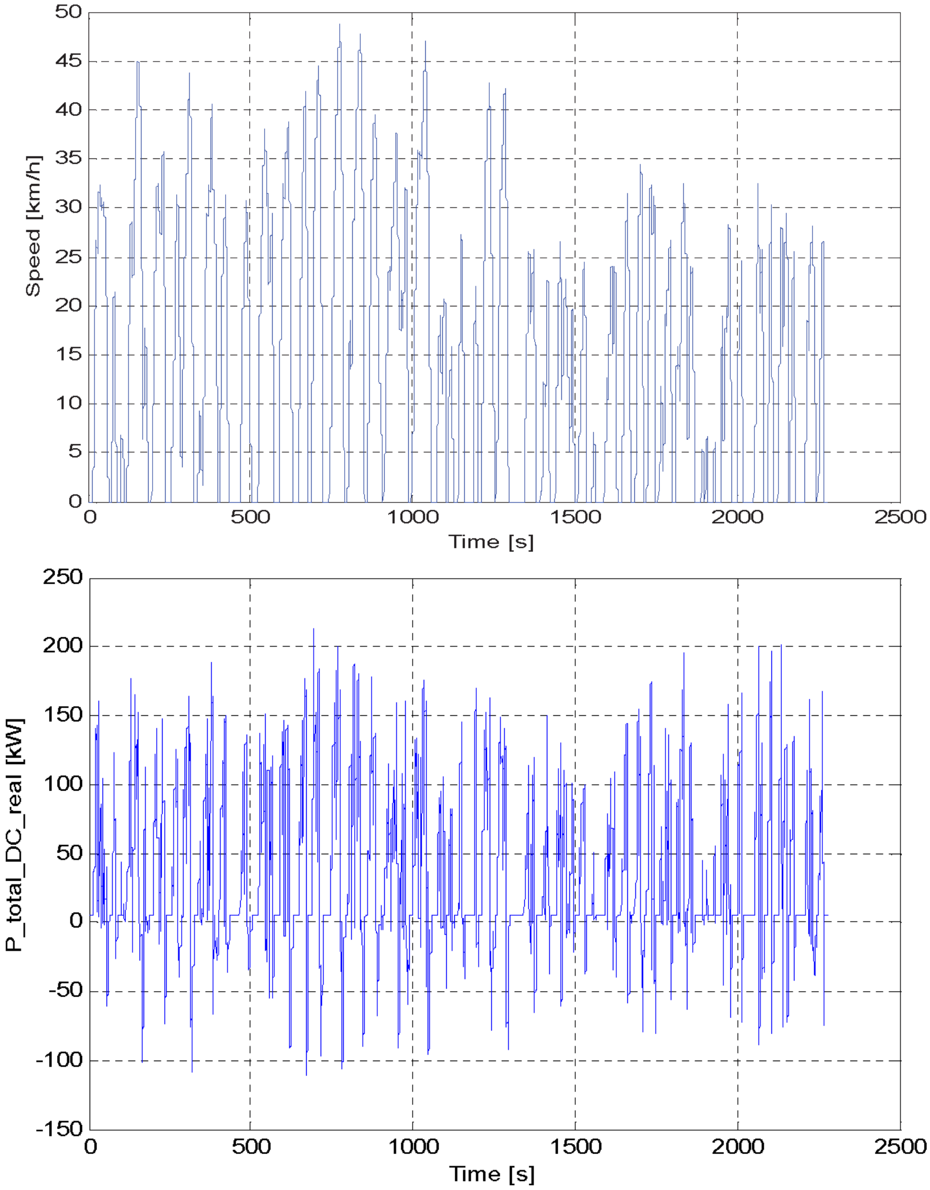

Figure 21: MLBT driving cycle (above) and corresponding DC power for 7700 Volvo Bus. Source: UNPLUGGED D3.2

SORT is a unified real-life test method developed by UITP [25]. SORT defines three different cycles:

- SORT 1 – Heavy Urban Cycle – average of 12 km/h
- SORT 2 – Easy Urban Mixed Cycle – average of 18 km/h
- SORT 3 – Easy Urban Cycle – average of 25 km/h

The 3 cycles are composed of 5 base trapezes, as shown in the table below.

	Trapeze 1	Trapeze 2	Trapeze 3	Trapeze 4	Trapeze 5
v-const. (km/h)	20	30	40	50	60
length (m)	100	200	220	600	650
Acceleration (m/s²)	1,03	0,77	0,62	0,57	0,46
Deceleration (m/s²)	0,8	0,8	0,8	0,8	0,8
SORT1	●	●	●		
SORT2	●		●	●	
SORT3		●		●	●

Table 44: The 5 basic SORT trapezes and the base-3 SORT cycles-

In the UNPLUGGED project, a cycle was considered, with the three basic cycles, one after another (see Figure 22). The most important feature of this cycle is that acceleration, deceleration and stop times can be distinguished clearly. Comparing the SORT with MLTB and Firenze cycle, it can be observed that they are very similar, regarding the number of start-stop cycles within a certain time span. For urban and mixed cycles, a stop time of 20s is considered, while in the suburban cycle, stop time is reduced, considering less passengers leaving or entering the bus.

The same chart can be translated into velocity as a function of distance (see Figure 23). Here it can be seen that the urban cycle covers approximately 500 m, the mixed cycle 1000 m and the suburban cycle 1500 m. Together the cycle considered in UNPLUGGED represents roughly 3 km, which is not a typical length for a complete urban bus line. Nevertheless, this example is maintained here in order to obtain comparable results.

Finally, the SORT cycle was translated into DC power consumption over time (using a vehicle model), at the electric motor in the bus (see Figure 24). Here it can be observed that high power demand is limited to very short periods of time. During constant speed periods, 50 kW is only surpassed for speeds beyond 50 km/h. In addition to the values from UNPLUGGED, a hypothetical 100-kW recharge on a 25-m track has been added to Figure 24.

In order to obtain a better estimate on the required length of the recharge tracks, a simulation with data from Figure 24 has been carried out, considering a recharge efficiency of the battery of 90%. The resulting state of charge of the battery is shown in Figure 25. The simplified simulation model permits variation of WPT track length, recharge power and battery efficiency. WPT efficiency is excluded here for simplicity, assuming that 100 kW are reached at the on-board DC bus.

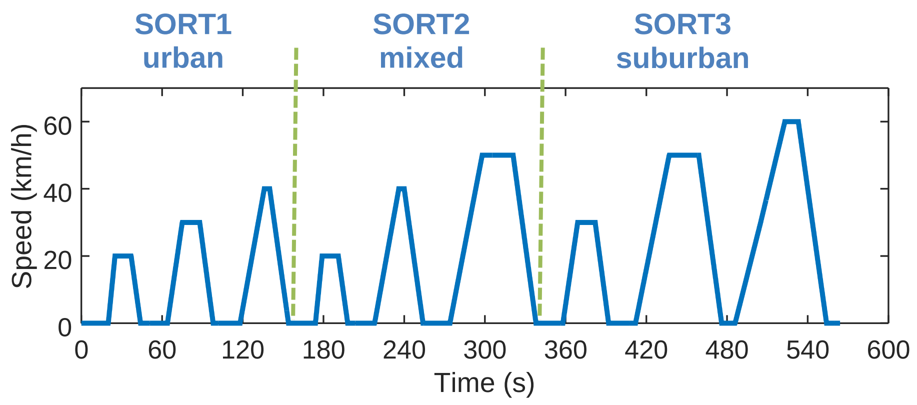

Figure 22: SORT cycle considered in UNPLUGGED project.

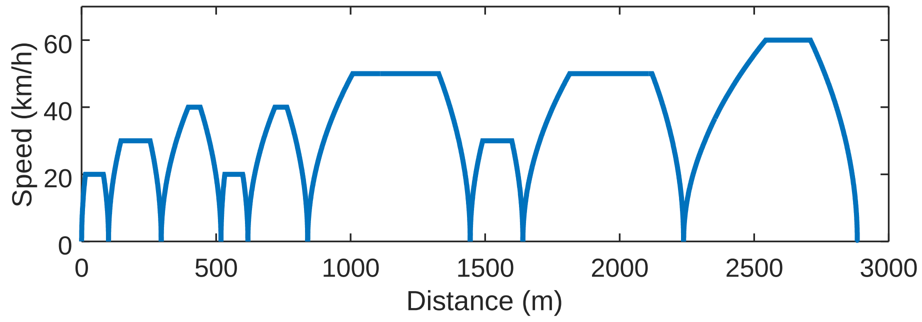

Figure 23: SORT cycle expressed in distance vs. speed.

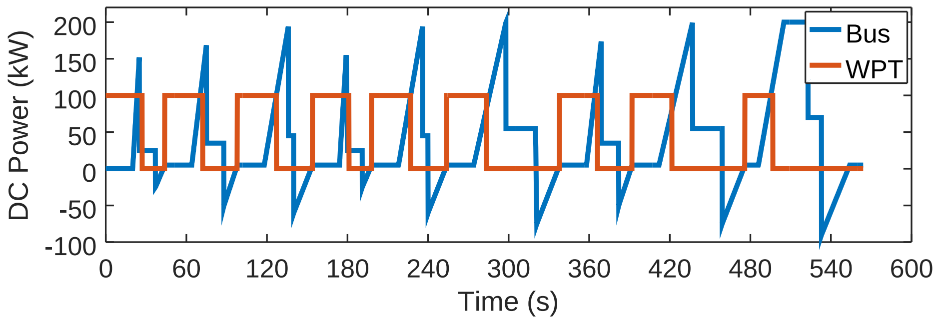

Figure 24: DC power at vehicle for 7700 Volvo Bus (Source: UNPLUGGED D3.2) and 25-m WPT tracks at each stop, recharging at 100 kW.

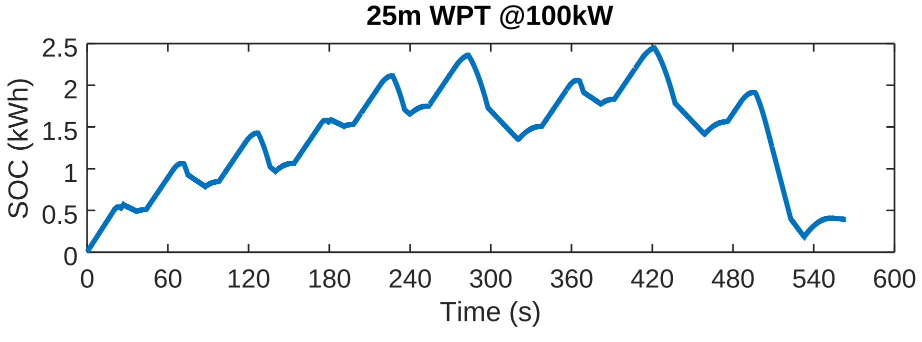

Figure 25: State of charge of vehicle battery assuming 100-kW recharge at each stop and 25 m of dynamic track and 90% battery efficiency.

By variation of the track length, an optimum of 25 m has been found. Assuming 100 kW recharge power, with this configuration, the battery is charged during the urban cycle (SORT1), state of charge is maintained during mixed cycle (SORT2) and battery is discharged during suburban cycle (SORT3). With shorter track lengths, not enough energy is recharged in order to cover also the suburban cycle, while with increased track length, recharged energy exceeds the needs. As a result, over 3 km only 9 charging tracks are needed, summing up to 225 m or 7.5% of the overall route distance.

In this case, track length has been adjusted with the objective to minimise maximum SOC, which is equivalent to required battery size. It is also considered, that at the end of the suburban cycle, there will be enough time to recharge the battery. As can be seen from Figure 25, only 2.5 kWh are needed to be recharged, which translates to 1.5 min of recharge at 100 kW. It must be highlighted here that this driving cycle only covers 3 km, while a typical line length would cover approximately 10 km. Assuming the same proportion between the three sub-cycles and multiplying the distances by 3, the battery will be recharged 3 times more during the urban cycle, reaching 7.5 kWh. Static recharging time at the end of the cycle would then be 4.5 min. In any case, the recharging track length is maintained at 25 m.

Simulations with only 50 kW power transfer capacity show that with the proposed configuration (recharging tracks of equal length at each stop), that practically the entire bus lane needs to be equipped with power transfer modules in order to be able to obtain an equilibrated energy balance over the route of 3 km (see Figure 26 below).

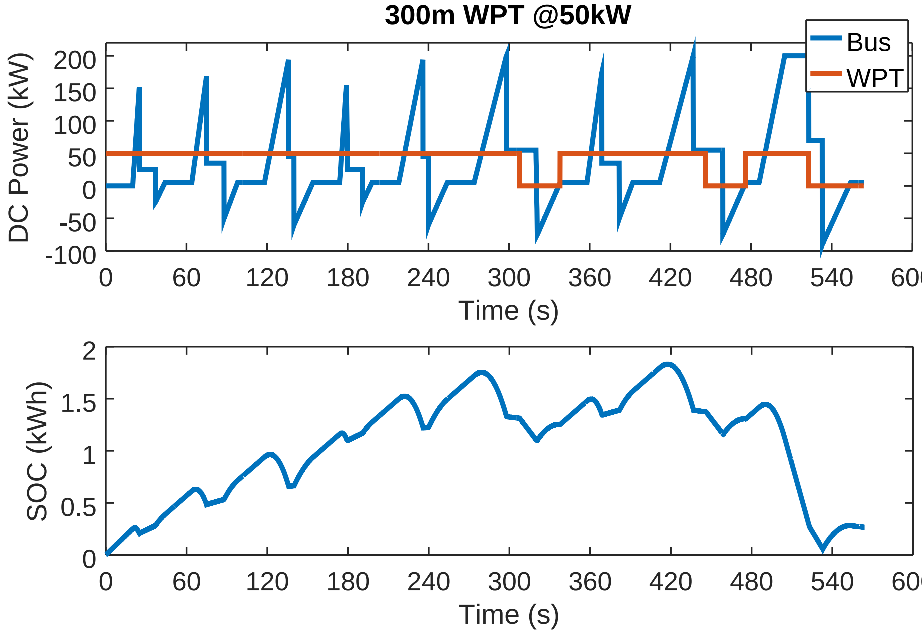

Figure 26: Power (above) and state of charge (below) for a 50-kW WPT system.

Keep in mind that a large part of energy is recharged during stop times, which add up to 30% of the overall trip duration. Therefore, just doubling charging track length is not sufficient to compensate for reduction of power transfer from 100 kW to 50 kW. In this show case, 300-m charging tracks are needed (12-fold increase), which in the urban environment exceeds the distance between two stops.

On the other hand, if 150 kW recharge power or more is considered, only stationary charging at the stops is necessary. As can be seen in the lower graph of Figure 27, a similar curve of SOC is obtained compared to the case of 100 kW recharging (see Figure 25). In this simulation, a minimum track length of 10 m is considered, due to the extension of the bus. It may be mentioned here that the stop times of the driving cycle include bus stops but also stops at traffic lights.

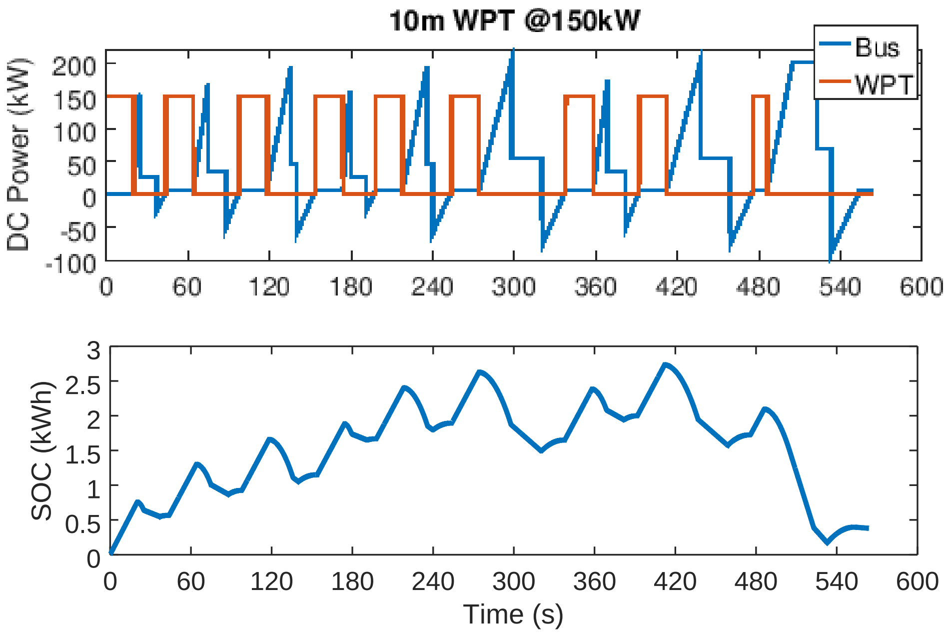

Figure 27: Power (above) and state of charge (below) for a 150-kW WPT system.

The main conclusion of this exercise is that dynamic recharging will be most effective and practicable during stop times and following acceleration phases. Stop times in the SORT model (traffic lights and bus stops) add up to approximately 30% of the total route duration. Therefore, placing WPT equipment there reduces considerably the required material to be laid down into the road. Also, increasing recharge power reduces drastically the required track length. In the example of the 7700 Volvo Bus (data from UNPLUGGED project), it was found that with 150 kW recharge power, stationary recharging would be sufficient, reducing considerably the infrastructure cost.

Another interesting conclusion is that battery size can be kept very small, even with this discontinuous WPT approach. At the same time, higher WPT power levels seem advantageous, as equipment extension is reduced. On the other hand, with 50-kW recharge power, and a continuous charging line, interoperability for recharging taxis and other vehicles is more likely to be achieved.

In any case, a battery size of 10 kWh is small compared to required recharge power levels of 50 – 150 kW. Charging rates of 5C or even 15C are not feasible with current battery technology without compromising battery life. Keep in mind that 15C means a full recharge in only 4 min (ignoring any charging curve). Also discharge peaks of up to 200 kW must be provided by the storage device in normal operation. Therefore, supercapacitors seem to be more suitable for this application.

3.2 Summary of requirements

In this section, a summary is given for the requirements of the three scenarios: Motorway (e-Corridors), Periurban (e-Launchers) and Urban buses.

3.2.1 Motorway Scenario

The first studied case is the 25-km section of e-road. In Table 45 only one example of possible traffic density scenarios is presented in order to keep the overview clear (12,000 vehicles per lane and day).

An interesting feature of the summary table is the comparison of maximum number of vehicles according to speed and 2-s safety rule and the assumed average traffic (12,000 vehicles per lane in this case). Here, a ratio between average and peak traffic of 3 is considered (see also section 3.3). It can be seen, that the assumed average traffic of 12,000 vehicles per day and lane can be considered as the limit, assuming the 2-s safety rule.

MOTORWAY SCENARIO				
Length of e-Corridor		25		km
Safety distance		2		s
Driving cycle: Constant highway speed		100		km/h
Number of vehicles per day (approx.)		12000		units
Traffic profile: max/avg ratio		3		units
Max. number of vehicles per km (safety rule)		17		veh/km
Max. number of vehicles per km (veh/day)		15		veh/km
Max. number of vehicles per 25 km		375		veh/e-corr
Time to cross 25 km		0.25		h
Max. hourly traffic		1500		veh/h
Percentage of light vehicles from total	88%	**88%**	88%	%
Dynamic Power transfer	20	**50**	100	kW
Total POWER required for 25 km (MW)	9.4	**23.4**	46.9	MW/e-corr
Energy recharged over 25 km				
One vehicle (kWh)	5.0	**12.5**	25.0	kWh/veh
Total on average day (MWh)	60	**150**	300	MWh/day
Range extension (km)				
Standard (assuming 0.15 kWh/km)	33	**83**	167	km
Highway (assuming 0.25 kWh/km)	20	**50**	100	km
Number of coils per 25 km (2m/coil)		**12500**		units
Number of LV transformers per 25 km	25	**25**	25	units
Nominal power per LV transformer (MVA)	0.4	**1.0**	2.0	MVA/trafo
Number of HV/MV transformers	1	**1**	2	units
Nominal power per MV transformer (MVA)	10	**25**	25	MVA/trafo

Table 45. Summary of e-Corridor scenario for different power levels of WPT (example of 15 vehicles/km).

Another important indicator in Table 45 is the achievable range extension when recharging over the entire 25-km e-corridor. As this feature depends on vehicle consumption, two different values are given: standard and highway range extension, referring to expected consumption of 0.15 kWh/km (standard) and 0.25 kWh/km (highway). These consumption data refer to a typical passenger EV such as the Nissan Leaf. The most important conclusion is that range extension is very low for 20 kW power transfer. Therefore, a minimum of 50 kW transfer power is considered as viable, obtaining 83 km range extension for standard and 50 km for highway consumption.

Of course, more convenient would be 100 kW power transfer, as 167 km and 100 km additional range are obtained respectively. In order to increase range extension with 50 kW power transfer, a reduction of vehicle speed while recharging can be considered. For example, if the speed is reduced to 80 km/h, 104 additional km can be recharged for standard and 63 km for highway conditions. Naturally, the reduced speed means a time loss, in this case 5 min over 25 km. It might be mentioned here, that at 80 km/h still 1650 vehicles can pass per hour, which means that

the required throughput of up to 12 thousand vehicles per day is still provided with a considerable margin.

3.2.2 Periurban Scenario

The second studied case is the 10-km section of e-road or e-Launcher. Assumptions are very similar to the motorway scenario, only changing values of some key parameters: length of infrastructure, vehicle speed, traffic density and level of power transfer (heavy vehicles instead of mainly light vehicles). As for the motorway scenario, in Table 46 only one example of traffic density is presented (3,600 vehicles per lane and day). Note that a higher ratio between average and peak traffic is applied (4 instead of 3 in the motorway scenario). As shown in section 3.1.2.1 the traffic profile tends to have more peaks with lower traffic density. The value of 4 has been the result of rounding upwards the value obtained from Figure 19.

PERIURBAN SCENARIO				
Length of e-road (e-Launcher)		10		km
Safety distance		2		s
Driving cycle: Constant highway speed		80		km/h
Number of vehicles per day (approx.)		3600		units
Traffic profile: max/avg ratio		4		units
Max. number of vehicles per km (safety rule)		17		veh/km
Max. number of vehicles per km (veh/day)		7.5		veh/km
Max. number of vehicles per 10 km		75		veh/e-corr
Time to cross 25 km		0.13		h
Max. hourly traffic		600		veh/h
Dynamic Power transfer	50	**100**	150	kW
Total POWER required for 10 km (MW)	4.7	**9.4**	14.1	MW/e-corr
Energy recharged over 10 km				
One vehicle (kWh)	6.3	**12.5**	18.8	kWh/veh
Total on average day (MWh)	23	**45**	68	MWh/day
Range extension (km)				
e-Trucks/Buses (assuming 0.75 kWh/km)	8	**17**	25	km
e-Vans (assuming 0.30 kWh/km)	21	**42**	63	km
Number of coils per 25 km (2m/coil)		**5000**		units
Number of LV transformers per 25 km	10	**10**	10	units
Nominal power per LV transformer (MVA)	0.5	**1.0**	1.5	MVA/trafo
Number of HV/MV transformers	1	**1**	1	units
Nominal power per MV transformer (MVA)	5	**10**	15	MVA/trafo

Table 46: Summary of e-Launcher scenario for different power levels of WPT (example of 7.5vehicles/km).

Main observations from this table are that range extension is very limited for e-trucks (17 km charging at 100 kW) and rather good for e-vans (42 km). Larger trucks and buses might easily charge at 150 kW if 3 50-kW receiver coils are on board. Infrastructure requirements in terms of

installed power is significantly lower with 10 MVA, compared to 25 MVA for the motorway scenario. The factor 2.5 reflects the reduced length (10 km instead of 25 km), while increased DWPT power is compensated by lower traffic density (7.5 instead of 16 vehicles per km).

3.2.3 Urban Scenario

For the Urban bus scenario, typical data extracted for medium-sized cities of 750,000 inhabitants. It is considered, that for larger cities, numbers can be extrapolated. For the presented scenario, it is assumed that there are 40 bus routes available and each one is served by 10 vehicles. Average route length is considered 9 km and according to SORT driving cycle, in each route there will be 27 stops.

URBAN SCENARIO: BUSES				
Number of buses		400		buses
Number of routes		40		routes
Driving cycle		SORT 1-1-2-2-3-3		
Average Daily route, 1 direction (half trip)		9		km
Number of stops per route		27		stops/route
Total number of stops		1,080		stops/city
Time for one route (round trip)		0.5 h (1 h)		
Service time (h) = nº of round trips		18		trips
Consumption bus on average		2		kWh/km
Energy required (one round trip)				
Per route / bus		36.0		kWh/trip
Fleet		14.4		MWh/trip
Energy required per day (18 h service)				
One bus		648		kWh/bus
Fleet		259.2		MWh/fleet
Dynamic and static Power transfer	50	**100**	150	kW
Total POWER required by fleet	25	**25**	25	MVA
Charging mode (simulation)	Conti-nuous	**25 m at stop**	10 m at stop	
Total length of e-Trenches	360	**27**	11	km
Required on-board energy storage (simulation)	12	**15**	18	kWh
Required average charging time per stop	48	**24**	16	s
Required charging time per bus and route	21.6	**10.8**	7.2	min
Number of coils per route (2.5m/coil)	3600	**270**	108	coils/route
Total number of coils	144,000	**10,800**	4,320	total coils
Number of MV/ LV transformers per route	1	**1**	1	Trafos/route
Total number of MV/LV transformers	40x 630 kVA	**40x 630 kVA**	40x 630 kVA	Total Trafos
Total number of HV/MV transformers	1x 25 MVA	**1x 25 MVA**	1x 25 MVA	Total Trafos

Table 47. Summary of urban bus scenario for different power levels of WPT.

In Table 47, three power levels for wireless power transfer for buses are shown. The most noteworthy conclusion is that with increased DWPT power levels, dynamic power transfer is rendered increasingly unnecessary. Also, at a power level of 50 kW, where a continuous DWPT track is required, still 12 kWh of on-board storage is needed, as power transfer levels are well below the driving demand peaks of up to 200 kW. In this exercise, with increased transfer power, required DWPT infrastructure has been reduced dramatically from 360 km in the case of continuous charging (50 kW) down to 27 km for mixed stationary-dynamic charging (100 kW) and 11 km in the case of stationary charging as stops (150 kW). An interesting outcome of this exercise has been that in all cases, on-board storage was reduced dramatically. Considering a daily energy consumption of an urban bus of 650 kWh (equivalent to 325 km autonomy at 2 kWh/km), required on-board storage of 12 – 18 kWh with DWPT is merely 2 – 3% of the BEV version. This requirement is probably even below the minimum required to have emergency energy on board in order to reach the garage in case of a failure of the DWPT infrastructure of black-out of the grid. A value of 10-20 km (20-40 kWh) seems a reasonable value here. Keep in mind, that all assumptions are based on consumption of 2 kWh/km (as stated in the UNPLUGGED project). Nonetheless, suppliers of modern e-buses claim that much lower consumption levels can be reached (even below 1 kWh/km). Therefore, energy requirements might be reduced significantly, if these claims turn out to be true.

Another important conclusion here is that probably supercapacitors will be needed to cope with power-to-energy ratios of up to 10, which is rather high for batteries (200 kW peak power versus 20 kWh storage capacity).

Finally, total installed power of the entire infrastructure (all over the city), has been found to be approximately 25 MVA, and independent on the DWPT level. The reason is that with higher DWPT levels, buses are charging less time and probability of charging simultaneously is reduced, which compensates increased power transfer levels. It must be mentioned here, that the value 25 MVA is by a factor 3.3 higher than the 7.5 MVA reported in UNPLUGGED project. This is due to the fact that the system has been designed to cover energy consumption of 2 kWh/km, but on top of this, a security margin of 25% was added, resulting in 2.5 kWh of consumption. On the other hand, UNPLUGGED simulations were based on data from Florence City, with bus average frequencies of 12 round-trips per day and bus, while in FABRIC 18 round-trips were assumed.

3.3 Aggregated load curves

3.3.1 25-km E-road

In order to establish an example for possible aggregated load curves of a 25-km stretch of e-road, the average of normalised daily, weekly and yearly patterns for the 4 Spanish toll highways presented in section 3.1.2.1 (Motorway – E-Corridors) has been calculated (see Figure 28).

Multiplying each day of the week with the factor of the day-of-week and after that, with the factor of month-of-year, hourly traffic data are obtained for the whole year (see Figure 29). From this figure, one can see that traffic peaks might occur which are three times the average value. This is the result of the averaging process of the 4 Spanish reference highways and represents the peaking behaviour of highways with lower traffic. Nevertheless, this scenario is maintained here as it represents a sort of worst-case scenario.

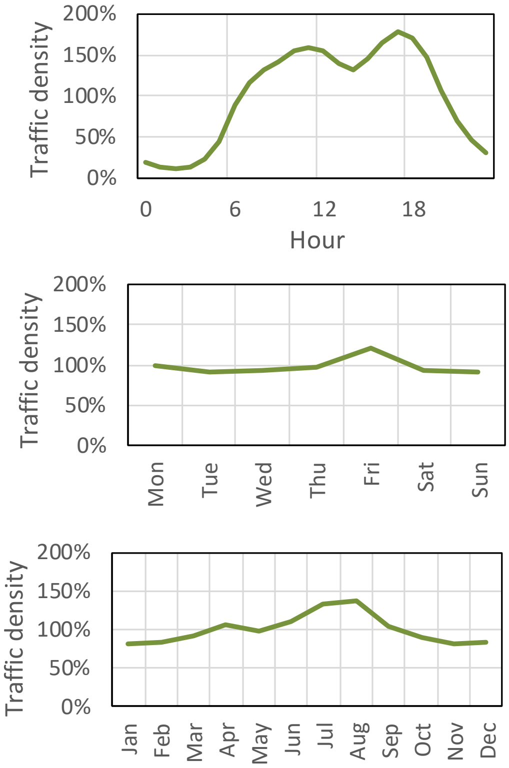

Figure 28: Average daily, weekly and yearly traffic profiles from 4 selected Spanish toll highways.

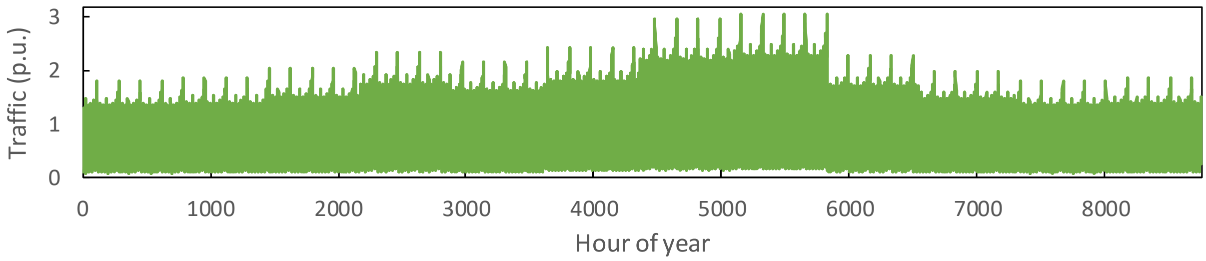

Figure 29: Hourly relative traffic data for one year.

In the following figure, a zoom is shown into one week in August, which represents the month with highest traffic in this model.

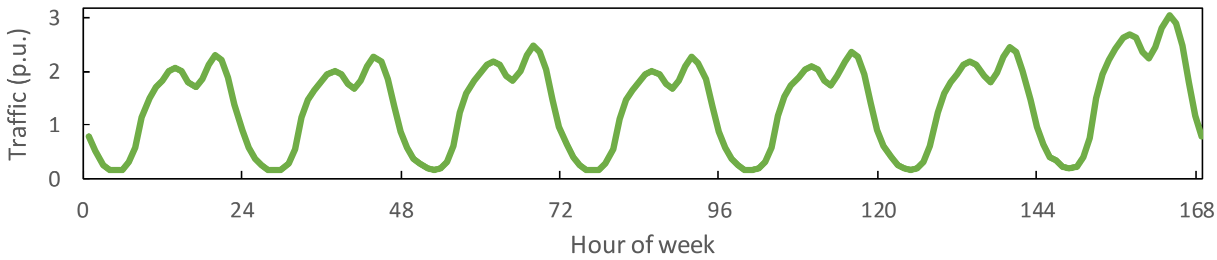

Figure 30: Hourly relative traffic for one week in august (highest traffic of the year).

In Table 45 (see section 3.2), a maximum number of vehicles per km of 15 was assumed, applying the 2-s safety rule and considering a vehicle speed of 110 km/h. In order to see if the considered peak of 15 vehicles per km is surpassed, in Figure 31 the traffic pattern is converted into vehicles per km. As can be seen, if 15 thousand vehicles per day are considered, the design limit of 15 vehicles per km is surpassed during 3 hours on Friday. So, this scenario can be considered the boundary. For more congested roads than that, saturation effects need to be taken into account. Also, these roads are not recommended for early implementations.

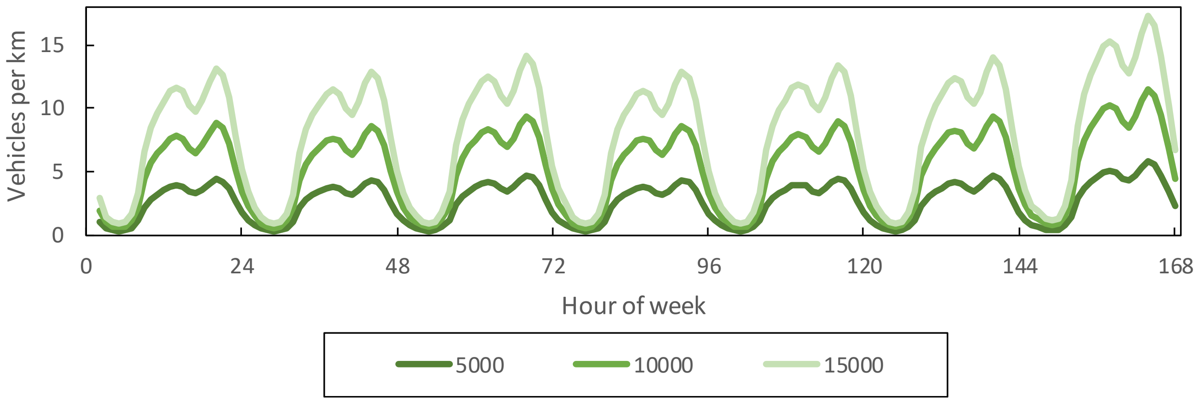

Figure 31: Number of vehicles per hour, one week in August.

Finally, these traffic profiles can be converted into aggregated load curves for a 25-km e-road, simply by defining the average number of vehicles per day/lane and transfer power. As an

example, for the week in August, demand pattern for average traffic of 5, 10 and 15 thousand vehicles per day/lane are shown in Figure 32 for a recharge power of 50 kW. As during August-Friday peaks, the design figure of 15 vehicles per km is surpassed, so does the peak demand, which was set at 23.4 MW. In this case, up to 27 MW are reached, which is 15% above the maximum. In order to obtain the same energy at reduced power, recharge speed must be reduced to 95 km/h. Anyway, according to this model, this scenario only occurs during peak hours on 9 Fridays in the summer season, and only for the scenario with 15 thousand vehicles per day/lane annual average traffic.

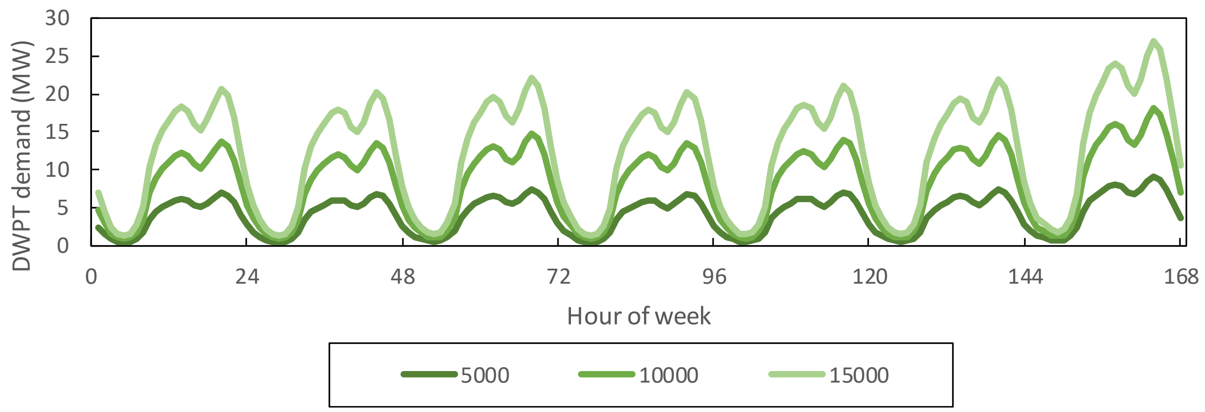

Figure 32: Hourly DWPT demand of 25 km e-road, one week in August (50 kW power transfer).

3.3.2 10-km E-road for heavy-vehicle traffic

No specific load curve has been developed for the e-Launcher. Similar traffic patterns are considered compared to the Motorway scenario. Nevertheless, it is assumed that the lower traffic density will lead to higher ratios between peak and average traffic (see section 3.1.2.1, Figure 19). As a result, peak power is obtained, which is the most important parameter for infrastructure calculations. It is assumed here that peak traffic and thus, power demand will be 4 times the average.

3.3.3 Urban bus (one city: 400 buses)

In the UNPLUGGED project, an overall power requirement of approximately 7.5 MW was found (see figure below).

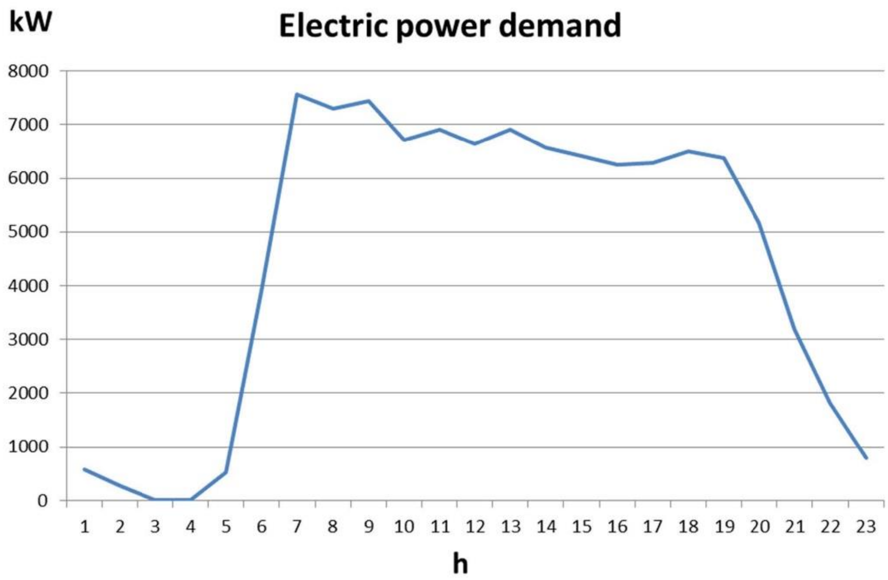

Figure 33: Daily electric power demand for whole Florence city wireless recharge infrastructure. Source: UNPLUGGED project D3.2

Assuming recharge power of 50 kW, this is equivalent to 130 buses charging simultaneously during rush hours (assuming 50 kW at bus and 80% efficiency, i.e. 62.5 kW at grid). It was concluded in the UNPLUGGED report that from the grid point of view, it is not significant to install 256 or 204 charging stations, which means that even if more than 200 charging points were available, at most, only 130 buses were charging at the same time. But even if we assume all 400 buses charging at once and at 150 kW, we would obtain 75 MW for an area of 100 km², which is a load density of 0.75 MW/km² on average (average vehicle density: 4 buses per km²). If we consider a higher bus density for the city centre of 10 buses per km² and add 80% power transfer efficiency, for 150 kW power transfer, the maximum expected power requirement reaches 1.9 MW/km², which is still a low value, compared to peak demand values of 40 MW/km² which can be found in city centres. As shown earlier in this section, findings from the FABRIC reference case suggest a system power of 25 MW, considering in the first place that all 400 buses should be able to recharge simultaneously at 50 kW (62.5 kW grid demand). Then, as first rough approach, increasing DWPT levels will reduce simultaneity and compensate for increased DWPT, so 25 MW are maintained.

3.3.4 Urban taxi (one city: 250 taxis)

Although for taxi service, no specific scenario has been developed within FABRIC, in this section an exercise is done in order to explore the option of taxis using the infrastructure of urban buses, given that taxis are often using bus lanes.

In order to give an estimate of the additional demand if the entire taxi fleet would recharge on the infrastructure, some assumptions need to be done. In Salanova 2011 [26] a Spanish review study on European taxi habits [27] has been cited which is in Catalan language. The most interesting numbers for this report are represented in the following table.

	Monthly trips*	Daily trips**	Population***	Number of taxis	Taxis per 1000 inhabitants	Daily km/Taxi	Daily km/1000 inhabitants
Amsterdam	95	3.1	850,000	1505	1.77	15.6	27.6
Athens	35	1.2	3,900,000	15249	3.91	5.8	22.5
Barcelona	70	2.3	4,390,000	11765	2.68	11.5	30.8
Berlin	106	3.5	3,390,000	6950	2.05	17.4	35.7
Brussels	100	3.3	964,000	1244	1.29	16.4	21.2
Budapest	32	1.1	1,760,000	5597	3.18	5.3	16.7
Copenhagen	179	5.9	1,810,000	2806	1.55	29.4	45.6
Dublin	148	4.9	1,120,000	1994	1.78	24.3	43.3
Lisbon	83	2.7	2,680,000	4529	1.69	13.6	23.1
London	103	3.4	7,170,000	55998	7.81	16.9	132.2
Madrid	61	2.0	5,420,000	14471	2.67	10.0	26.8
Milan	101	3.3	2,420,000	4574	1.89	16.6	31.4
Oslo	84	2.8	981,000	2148	2.19	13.8	30.2
Paris	126	4.1	11,100,000	17538	1.58	20.7	32.7
Prague	46	1.5	1,160,000	3979	3.43	7.6	25.9
Rome	120	3.9	2,810,000	5817	2.07	19.7	40.8
Stockholm	158	5.2	1,840,000	5207	2.83	26.0	73.5
Vienna	58	1.9	1,550,000	4433	2.86	9.5	27.3
Warsaw	57	1.9	1,690,000	6000	3.55	9.4	33.3
Average	93	3.0	3,000,263	9042	2.67	15.2	40.7
Median	95	3.1	1,840,000	5207	2.19	15.6	34.2

* 5 km/trip, ** 365 days per year, *** Metropolitan,

Table 48: Taxi market data from different European cities. Source: CENIT 2004.

From this data, it is most surprising how few daily km are reported per taxi. The highest value is obtained for Copenhagen with only 29 km. This is probably due to the fact that the number of taxis is the total of licences, while not all drivers are on the road. Considering 5 km per trip, only 6 daily trips are obtained on average for Copenhagen and close to 1 in Athens or Budapest.

These numbers seem very low, but for example according to data published for the City of Zaragoza [28], a fleet of 1700 taxis gives service to 600 thousand clients per year. This gives a ratio of less than 1 client per day per taxi. This means that there must be many “stand-by” licences, as with one trip per day, no taxi driver can earn money. Therefore, a value of 80 service km/day per taxi has been assumed in order to estimate a reasonable number of taxis actually on the road, simultaneously. With this number, and an average of 40 km per 1000 inhabitants, the active fleet is reduced to 0.5 taxis per 1000 inhabitants, which is 250 taxis for a city of 500 thousand people.

As can be seen, the most relevant data for this report is daily service km per 1000 inhabitants, which can be considered as indicator for **taxi service intensity**. This indicator has been depicted in Figure 34, sorted from higher to lower values. The main conclusion of this picture is that there is a wide range of taxi service intensity in European cities, ranging from 17 km in Budapest up to 132 km in London.

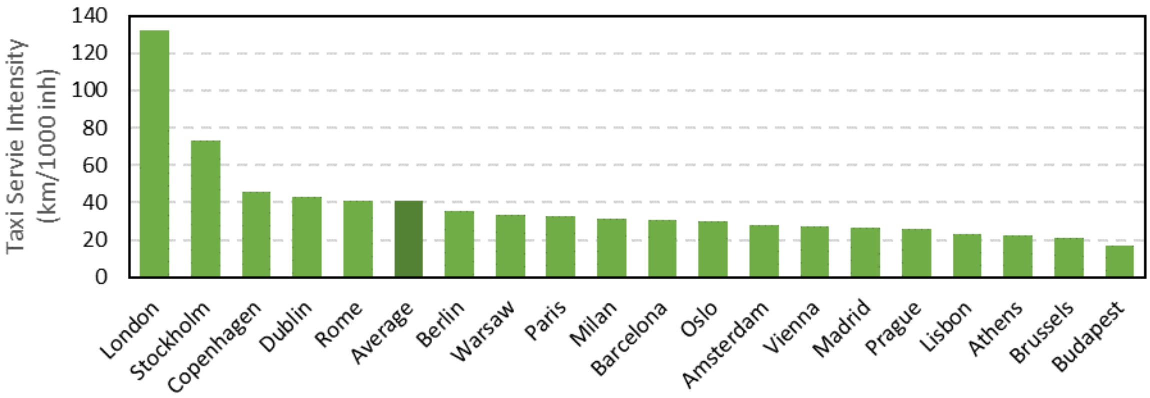

Figure 34: Taxi service intensity as daily km driven by taxis per 1000 inhabitants in European capitals.

Assuming average vehicle consumption of 0.15 kWh/km, daily average consumption from taxis can be calculated straight forward. For example, for a reference city of 500 thousand inhabitants, 40 km/1000 inh. translates to 3 MWh per day. This value needs to be increased by a factor of empty driving. Assuming empty driving factor = 2 and 80% charging efficiency, daily taxi fleet demand would be 7.5 MWh.

Apart from average daily demand, a load curve needs to be created for comparison with the example of the bus. In [29] a taxi customer demand curve has been reported for Beijing City. In absence of other sources, this curve has been considered in order to estimate a possible taxi load curve, which is shown in Figure 35. It can be observed that there is a peak demand in hour 21 of the day reaching 1.5 times the average.

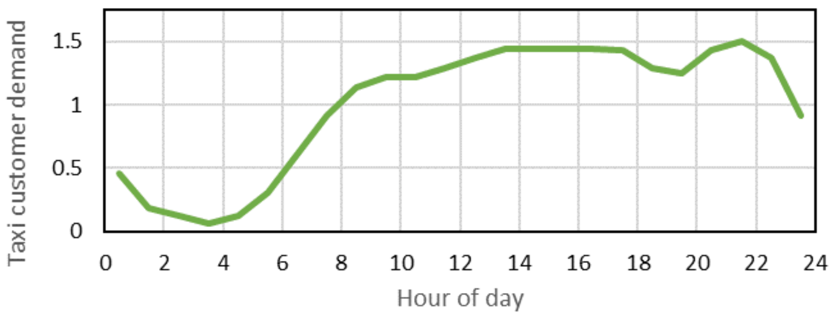

Figure 35: Normalised customer taxi demand curve derived from Li2018 [29].

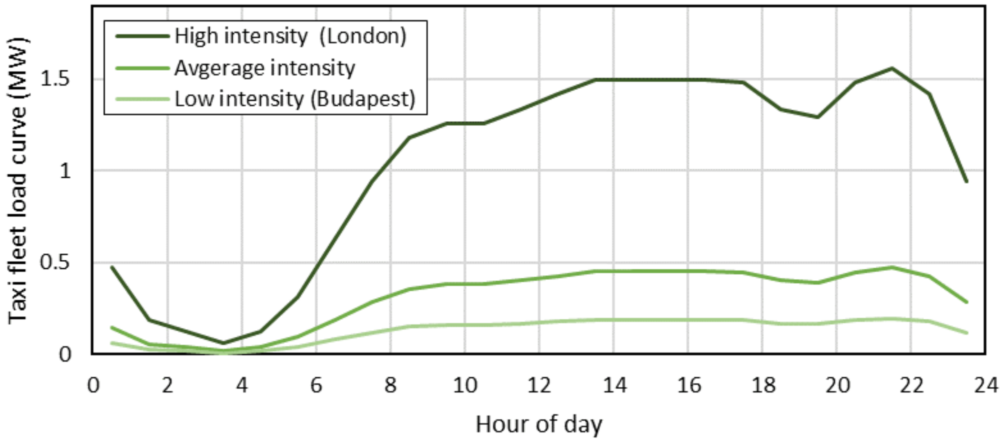

Figure 36: Load curves for taxi fleets serving 500 thousand inhabitants considering different service intensities.

With this information, and assuming similar recharging patterns from DWPT charging of the taxi fleet, the daily demand profile can be estimated. In order to account for the large variability of taxi service intensity in different European cities, in Figure 36 the average load curve is shown together with highest (London) and lowest (Budapest) service intensity. This picture illustrates that even for most intense taxi service, such as present in London, dynamic fleet recharging demand would produce a peak in the evening of approximately 1.6 MW. Assuming that this is serving an area of 100 km², a power density of only 0.016 MW/km² is obtained. For average intensities, not even 0.5 MW peak demand is expected, which is almost negligible comparted to the 7.5 MW of the expected demand peak of the urban bus fleet.

Summary of assumptions for taxi average case (assuming same city size as bus)

- Service area: 100 km²
- Inhabitants: 500,000
- 40,000 km/day (40 km/1000 inh./day, empty driving factor = 2)
- 7.5 MWh/day (0.15 kWh/km, 80% recharge efficiency)
- Average recharge power: 0.3 MW (peak: 0.47 MW)
- Taxi fleet: 1250 (2.5 Taxis / 1000 inh.)
- Individual daily service per taxi: 80 km → only 0.5 taxis per 1000 inh. needed
- Reasonable number of taxis on the street: 250
- Number of 5-km trips per day: 16

Bus infrastructure might NOT fit Taxi needs:

Given these numbers, on average, each taxi needs to recharge 30 kWh per day (24 kWh to battery). Considering 50 kW DWPT power, this requires a charging time of 29 min per day. This means slightly less than 2 min recharging after each trip.

While taxis are using bus lanes, they usually do not stop, such as buses. Therefore, the proposed infrastructure of e-trenches of 25 m at each stop (including traffic lights), might not serve the needs of taxis. It should be analysed more in detail if recharging at traffic lights would be sufficient for taxis. The energy requirement of the taxi fleet is approximately 35 times lower than the bus fleet (7.5 MWh compared to 260 MWh). This means, much less recharging occasions are needed. While for the proposed infrastructure for urban bus recharging 1080 stops are considered, 30 stops would be sufficient for the taxi fleet. In [30] static recharging with 38 charging stations was proposed for the city of Poznan considering slightly higher consumption (0.16 kWh/km) and 100 km daily service. These numbers are below the typical number of taxi stands available. For example, in Poznan 102 stands are reported and in Zaragoza there are 65. In addition, there are obligatory stands to be frequented by taxis, such as main railway stations and airports. Waiting times there are higher and thus, possible energy recharge. Recall that with 30 min recharge, the entire daily consumption of 160 km driving is recovered.

As a conclusion, stationary charging at taxi stands would be much more suitable than the proposed bus infrastructure. In addition, for 2030 it is expected that car autonomy will surpass 400 km, which is today the psychological limit for taxi drivers to switch to all-electric taxis. Considering all these conditions, it is unlikely that taxis will incur in extra costs for DWPT and thus, this business case is not further analysed in this report.

3.4 Impact on system electricity demand

3.4.1 Current demand and outlook

In the European context, demand is expected to have negative growth rates in many countries. Different scenarios will be presented, according to existing literature. A reasonable outlook scenario might be 2040 (to be aligned with overall WP5 assumptions).

In addition to this demand forecast, the uptake of electric transport will be analysed. For example, according to a very recent report from Bloomberg New Energy Finance (BNEF) [31], it is estimated that light duty vehicles will represent a share of 35% of sales in 2040 and 25% of the cars on the road by that date (see figure below). In the 2017 BNEF Summit Keynote [32] (April), a range of 35-47% was predicted, and in the BNEF Electric Vehicle Outlook [33] (July 2017) it is stated: “The EV revolution is going to hit the car market even harder and faster than BNEF

predicted a year ago. EVs are on track to accelerate to 54% of new car sales by 2040. Tumbling battery prices mean that EVs will have lower lifetime costs, and will be cheaper to buy, than internal combustion engine (ICE) cars in most countries by 2025-29."

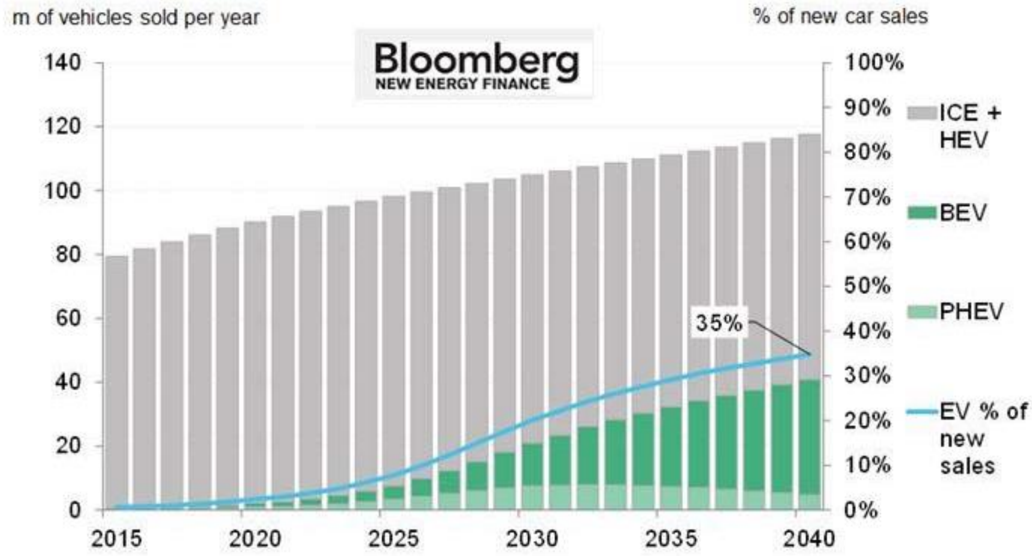

Figure 37: Expected share of electric vehicles until 2040 according to BNEF estimates.

FABRIC estimations for the stock of electric vehicles were fully explained in D5.4.2 and are summarised in the table below.

Stock EV-PHEV	´000,000	2,016	2,030	2,040	2,050	
Global Vehicles	MM	1,200	2,000	3,000	3,300	
EV-PHEV	MM	2.02	500	1,320	1,900	
By Region	**%**	**0.2%**	**25.0%**	**44.0%**	**57.6%**	%
Europe	MM	0.58	107.4	168.8	189.0	10%
North America	MM	0.58	129.8	215.7	250.7	13%
China	MM	0.56	134.6	304.2	413.8	22%
India	MM	0.24	40.1	215.7	362.1	19%
All other	MM	0.07	88.1	415.7	684.4	36%

Table 49: Expected share of electric vehicles according to FABRIC estimations.

The BNEF report states that this EV fleet would have an annual consumption of 2700 TWh or 11% of the global electricity demand from 2015. The FABRIC scenario is slightly more optimistic on EV growth, assuming a fleet of 1.32 billion cars by 2040, which leads to 2970 TWh/a or 14.7% of global electricity demand 2015. FABRIC consumption is calculated assuming average consumption of 1.5 kWh/km and 15,000 km/year.

This may seem an important extra demand, but annual growth rates are very small. The horizon is approximately 25 years, which would lead us to an average annual growth of demand of 0.4%. If we are more optimistic and just double the numbers of Bloomberg, we are with 0.8% annual

growth still below 1%. Remember that doubling the numbers is assuming 50% of all cars on the road would be EVs by 2040.

As a conclusion it can be stated that at national and European level, the additional consumption due to the uptake of electric transport is very small, compared to overall demand. If in addition a tendency of reduced demand is considered, the question would rather be if the new demand from transportation might be able to compensate demand reduction from other sectors.

Of course, this does not mean that locally, especially in crowded city centres, additional EV demand could cause grid saturation during rush hours. This only, of course, if the grid was already at its limit before.

3.4.2 Impact of dynamic power transfer demand

In this section, a global view on expected demand of DWPT systems will be given, according to assumptions for the development in Europe. For each scenario, expected installed power and energy consumption are reported in order to give an idea of the magnitude of these installations on a European scale. Finally, these values are compared to installed generation power and energy consumption, in order to give an impression of the overall impact of these installations on the European Grid.

First, some assumptions are recalled. As can be seen in Table 50, intensity of infrastructure use is expected to increase over time, as more EVs equipped with DWPT capability are circulating on European roads.

	2030	2040	2050	Comments
Motorway	880	3688	9331	Nº of EVs using each e-Corridor
Periurban	810	1768	3098	Nº of heavy EVs using each e-Launcher
Urban Bus	400	400	400	Nº of buses using e-Trenches in each city of 750,000 inh.

Table 50: Assumed number of EVs using DWPT infrastructure.

	2030	2040	2050	Comments
Motorway	10	20	32	Nº of e-Corridors (25 km length each)
Periurban	80	200	400	Nº of e-Launchers (10 km length each)
Urban Bus	40	100	200	Nº of cities with e-Trenches (27 km length each)

Table 51: Accumulated number of DWPT infrastructure in Europe.

On the other hand, the number of installed DWPT infrastructures is increasing. The assumed trend is shown in Table 51. Especially from 2040 to 2050, an important uptake is expected, with a duplication of installed infrastructure all over Europe.

Given the assumptions presented above, required power and energy can be calculated. In Table 52 unitary power requirement (expressed in MVA) is shown. As can be seen, due to expected increase in usage, unitary power requirements are increasing with time. This means, the same infrastructure will need to support higher traffic density and this, the original installations should be able to be upgraded or oversized from the beginning. In the case of Motorways, a 10-fold power increase is projected. Periurban e-Launchers are expected to see a 4-fold increase. In this case, a higher initial use is assumed, as e-Launchers will not be installed if there is not a minimum of transport fleets committed to use them. Finally, unitary increase of unitary urban bus power demand is only 33%. In this case, it is considered that the implementation of the system only makes sense if the entire bus fleet is converted to DWPT.

MVA	2030	2040	2050
Motorway	1.8	7.7	19.4
Periurban	2.2	4.8	8.5
Urban Bus	25.0	25.0	25.0

Table 52: Unitary power requirement (in MVA) of DWPT infrastructure.

Apart from power, these infrastructures will also require energy from the grid. In Table 53, assumed annual energy consumption is shown for each type of installation. For the Urban-Bus scenario, consumption of 1.5 kWh/km has been used in order to calculate the annual energy demand. This is lower than the 2 kWh/km (taken from the UNPLUGGED project) assumed for infrastructure design. This modification has been done, considering recent developments in heavy EV design and the fact that this value has been assumed for all economic simulations in WP55.

GWh	2030	2040	2050	Equivalent hours (capacity factor)
Motorway	4.0	16.8	42.6	25%
Periurban	3.7	8.1	14.1	7.5%
Urban Bus	71	71	71	32%

Table 53: Unitary annual energy requirement (in GWh) of DWPT infrastructure.

Comparing the three scenarios, it becomes apparent, that use profiles are very different in the 3 cases. A common way to express use of grid infrastructure is the ratio between energy and power (equivalent hours of nominal power operation or capacity factor if expressed as percentage of the 8760 h of one year). It can be observed, that the highest ratio is obtained by the urban bus scenario, while by far, lowest equivalent hours has the periurban e-Launcher. Buses obtain high ratios, as 18 h of operation per day has been considered. Also, traffic density on bus lanes is high during the day. Finally, this urban buses are a high-power/low-speed scenario, obtaining a good

energy-to-power ratio. On the other hand, e-Launchers have high-power / high-speed scenario with rather low traffic density. As a result, equivalent hours are low. This has direct impact on the economics of the system (see chapter 4).

If these values are multiplied with the expected number of installations all over Europe, grid requirements can be obtained and compared with existing demand on a general scale. In Table 54 power and energy requirements for DWPT infrastructure are shown. Required power can be considered as very low, considering that demand peaks of Germany alone exceed 80 GW. On the other hand, energy consumption is also very low. For comparison, according to Eurostat [34], European gross electricity generation was 3234 TWh, which means that energy consumption in 2050 of all three scenarios together represent a mere 0.8% of European electricity production from 2015.

	Power (GW)			Energy (TWh)		
	2030	**2040**	**2050**	**2030**	**2040**	**2050**
Motorway	0.02	0.15	0.62	0.04	0.34	1.4
Periurban	0.18	1.0	3.4	0.3	1.6	5.7
Urban Bus	1.00	2.5	5.0	2.8	7.1	14.2
Total	**1.19**	**3.6**	**9.0**	**4.1**	**11.4**	**25.9**

Table 54: European power and energy requirements for DWPT infrastructure upscale.

To put these numbers in another perspective, energy consumption is compared to the expected demand from the entire EV fleet for Europe. In Table 55 projected numbers are shown, as assumed in the FABRIC project (see Table 49). As can be seen from this table, by 2050 total energy consumption of the EV fleet, might sum up to approximately 13% of European gross electricity generation (data from 2015). This demand represents roughly 50% of vehicles being electric (BEV and PHEV).

	2030	2040	2050
Number of EVs in Europe (millions)	107.4	168.8	189
Expected electricity demand (TWh/a)	242	380	425
Percentage of 2015 gross generation	7.5%	11.7%	13.1%
Percentage of DWPT demand vs. EV demand	1.3%	2.4%	5.0%

Table 55: Projected electricity demand of entire EV fleet in Europe.

The final row of Table 55 shows how much of EV demand will be supplied by the expected DWPT infrastructure. Again, the share of DWPT compared to global EV demand is modest, reaching 6% by 2050. This final comparison has been done with the demand obtained from light-duty vehicles

(passenger cars and vans). According to data presented in section 3.5.2, regarding share of CO_2 emissions, this segment represents approximately 60% of all road transport. As a result, the share of DWPT consumption compared to the entire road transport will be even lower.

3.4.3 Conclusions on electricity demand

Compared to existing electricity grid infrastructure, additional requirements from DWPT installations are low. Therefore, expected power and energy demand will be easily covered by existing installations.

Anyway, it must be highlighted, that DWPT demand profiles show similar patterns as general electricity demand, with diurnal peaks. A first conclusion is that electricity system demand peaks and ramps will be increased. On the other hand, growth of solar power generation requires daylight consumption, for better grid integration. In this sense, DWPT can be considered as beneficial, as recharging is moved from night to daylight hours. Nevertheless, in the evening, there will be still a heavy demand peak, when solar generation is no more available. In California, this is known as the “Duck Curve” [35], since the Californian ISO published in 2013 a short note of “Fast Facts” titled “What the duck curve tells us about managing a green grid”. In essence, the Duck Curve shows a sharp demand ramp in the evening, when distrusted solar generation vanishes while grid demand grows. The good news about this effect is that it has a short duration of a few hours, which opens the possibility of compensating with battery storage, which is best suited for this kind of buffer operation (see also in this report section 3.6.4 Integration of storage).

3.5 CO_2 emission balance of the EU

3.5.1 Generation mix in the EU and outlook

The generation mix is relevant in order to estimate “well-to-tank” (WTT) energy losses and finally WTW energy consumption and CO_2 emissions from electric transportation.

With the numbers of electricity demand in mind, an interesting first approach is to assume that global electricity consumption at EU level will remain at the same level as today. But the generation mix will change drastically, if agreements from Paris climate summit are fulfilled. According to the roadmap of the EU binding objectives include 20% share of renewables by 2020 and 27% by 2030. The scenario is obviously very different in the member states of the EU. While countries like Denmark, Austria or Sweden already are beyond the 2030 objective, especially large countries such as Germany still need to meet EU objectives. As will be shown in the following sections, CO_2 emissions of electricity generation show huge differences between EU countries and is expected to change widely over time.

Regarding the outlook of the renewable share in the electricity generation mix, there are some important uncertainties. Especially wind and solar are on the brink to be competitive with conventional generation, which means new capacity will increasingly be installed without incentives. To give an example, a recent auction for wind projects was won in Spain by a consortium which placed a bid with zero incentives over market prices. But also solar PV is being installed increasingly without incentives, namely in self-consumption schemes. The dynamics of this situation of "grid parity" is difficult to foresee. This is true even more as fixed fees for grid-tied solar installations are discussed more and more, which reduces the benefits of these installations. Here, national regulations will play again a crucial role, but the transition from regulated to competitive market reduces the impact of regulations.

3.5.2 Current status of CO_2 emissions in Europe

CO_2 emissions of a country depend on energy consumption levels and generation mix. The CO_2 intensity of different European countries is diverse. An interesting snapshot of this situation can be seen on a website provided by the Electricitymap project [36]. Here, CO_2 emissions from electricity generation is represented on a coloured map (see Figure 38). This picture illustrates the diversity at a given moment, while in Figure 39 data from Eurostat is presented, which represents annual mean values. As can be observed, CO_2 intensity range is wide, reaching from 40g/kWh in Sweden up to 1058 g/kWh in Estonia. Average intensity over all EU-28 countries calculates to 331 g/kWh (2015 data). CO_2 emissions in the Eurostat database is given for "Fuel combustion in public electricity and heat production". Therefore, the CO_2 intensity included also heat production, but this is not significant, as heat production is much lower. Lithuania is the country with highest heat production relative to electricity with 0.2%, while EU-28 average is 0.02%.

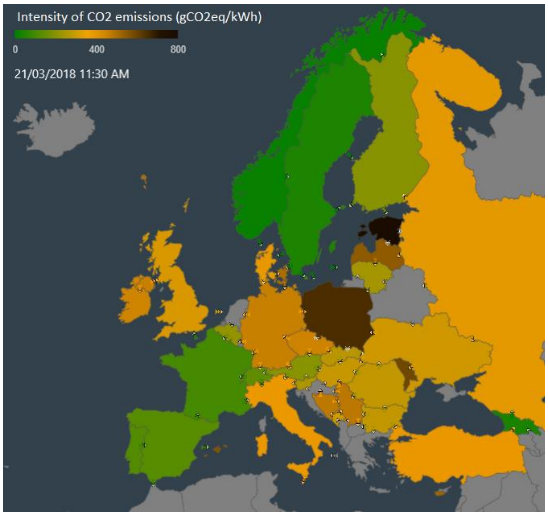

Figure 38: Snapshot of intensity of CO_2 emissions in Europe on 21/03/2018 11:30 AM (Source: www.electricitymap.org).

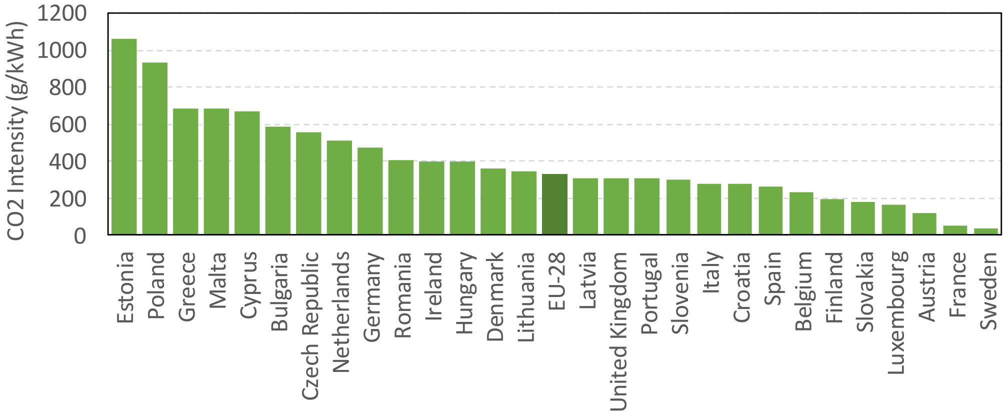

Figure 39: CO_2 intensity of EU-28 countries in 2015 according to Eurostat.

Average CO_2 intensity of EU-28 countries for the year 2015 is with 331 g/kWh sensibly lower than the value given in the JRC WTT Report 2014 [7], which gives 490 g/kWh for the EU-mix. This is in part due to the fact that the JRC report is based on data from 2009, where Eurostat reports 380 g/kWh. It is not clear to the authors of this report where the remaining gap (29%) comes from, as electricity transmission and distribution losses according to the JRC report are only responsible for a 12% increase of WTT energy consumption.

3.5.3 Outlook for 2050

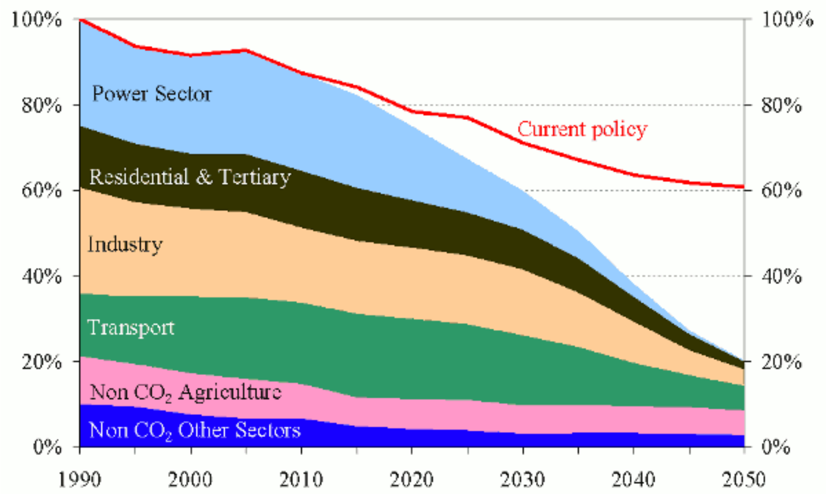

Figure 40: Estimate of EU-Commission on CO_2 emissions until 2050. Source: EC [37].

According to the European Commission, its low-carbon economy roadmap [38] suggests that:

- By 2050, the EU should cut greenhouse gas emissions to 80% below 1990 levels
- Milestones to achieve this are 40% emissions cuts by 2030 and 60% by 2040
- All sectors need to contribute
- The low-carbon transition is feasible & affordable.

The roadmap suggests that, by 2050, the EU should cut its emissions to 80% below 1990 levels through domestic reductions alone (i.e. rather than relying on international credits).

Most relevant for this consideration is the statement that "The power sector […] can almost totally eliminate CO_2 emissions by 2050."

According to Figure 40, the following CO_2-reduction targets can be assumed for FABRIC scenarios regarding the power sector, which would feed the dynamic charging system:

- 2030: 50% reduction
- 2040: 80% reduction
- 2050: 99% reduction

This means, that for the 2040-Scenario, that CO_2 emissions from power supply for dynamic power transfer can be assumed to be almost nil. If at the same time, road transport is electrified, reduction of emissions from power supply has a double effect, as it also reduces emissions in for road transport.

It should be mentioned, that there is also the EU Reference scenario [39], which states for 2050 an electricity mix of 55% renewables, 18% nuclear (73% CO_2-free), and 27% remaining from fossil origin. As a result, CO_2 emissions will not be reduced to zero by 2050 (see Figure 41).

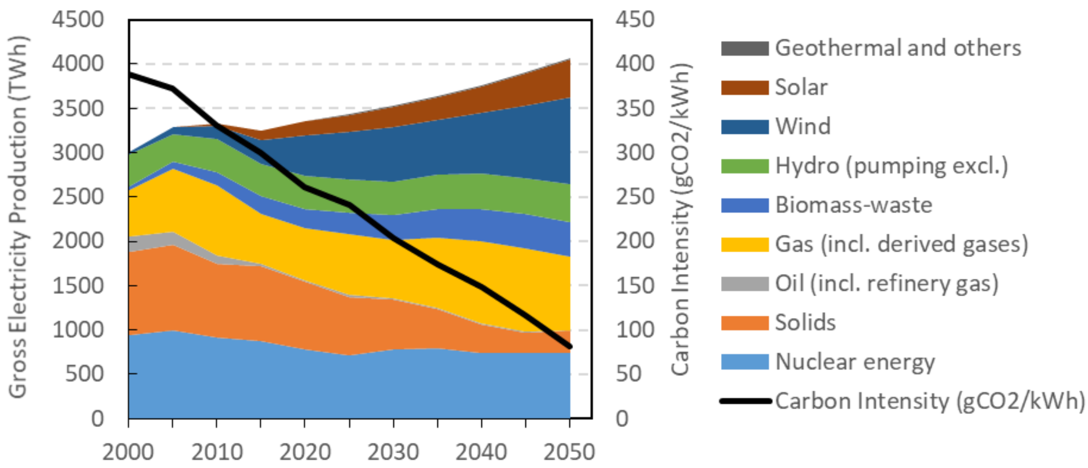

Figure 41: EU-28 electricity generation mix and carbon intensity according to the EU reference scenario 2050 [39].

In order to have an idea how much CO_2 is emitted from the European electricity supply, in Figure 42 WTW data from [7] (490 g/kWh for EU-mix and 319 g/kWh for Diesel) and the EU Reference scenario [39] have been combined with the EC-roadmap from Figure 40. This graph shows that with a 35% reduction over 2010 levels, emissions of the EU electricity mix will reach WTT emissions of Diesel fuel. Calculations in Chapter 2 have been done, considering the EU electricity mix from 2010 with emissions of 490 g/kWh. The graph also reveals major differences between

the JRC study and the EU reference scenario. At least for the year 2010 similar values should be expected. The reference scenario assumes 331 g CO_2/kWh for 2010, which is even below the reported value according to Eurostat (380 g CO_2/kWh). In any case, both projections show that CO_2 emissions from the European electricity system will be reduced dramatically, which means that derived emissions from electrified transport will be as well. Also, results from Chapter 2 are likely to over-estimate CO_2 emissions from BEV and DWPT-EV.

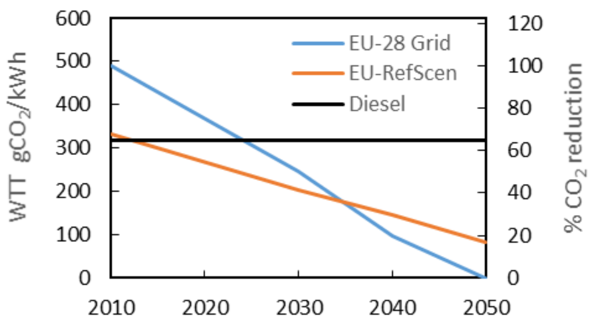

Figure 42: Comparison of CO_2 emissions between EU-28 grid, EU Reference scenario and Diesel fuel.

3.5.4 Impact of EV adoption on CO_2 balance

In this section, data from Eurostat [34] is analysed, in order to obtain the share of road transport on CO_2 emissions. The European CO_2 balance is shown starting from a wider view, until getting to road transport.

As the following data show, the great majority (more than 80%) of the GHG emissions are related with energy. In the same figure, also a reduction from the year 1990 to 2015 of 23% can be observed. Table 56 provides the numbers and percentages of Figure 43.

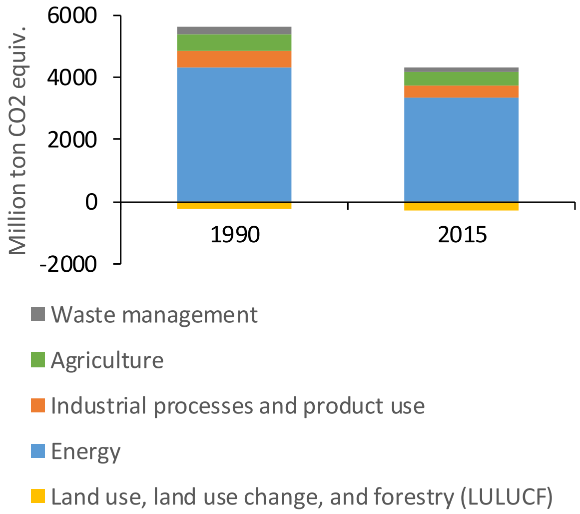

Figure 43: GHG emissions in the EU-28 countries by sector (Source: Eurostat).

	Gt CO_2 1990	Gt CO_2 2015	% 1990	% 2015
Energy	4337	3358	80.1%	83.9%
Industrial processes and product use	517	374	9.6%	9.3%
Agriculture	548	437	10.1%	10.9%
Land use, land use change, and forestry (LULUCF)	-232	-305	-4.3%	-7.6%
Waste management	241	139	4.5%	3.5%
Total	**5411**	**4003**	**100.0%**	**100.0%**

Table 56: GHG emissions in the EU-28 countries by sector (Source: Eurostat).

Given the importance of the energy use, which also includes road transport and electricity generation, this fraction is shown more in detail below in Figure 44 (numbers in Table 57). It can be seen that emissions have been reduced from 1990 levels in all categories, except in the transport sector, which increased its share from 18% to 27% within all energy uses. As a result, by 2015, transport was the second sector which most GHG emitted within the energy sector, only behind electricity and heat production.

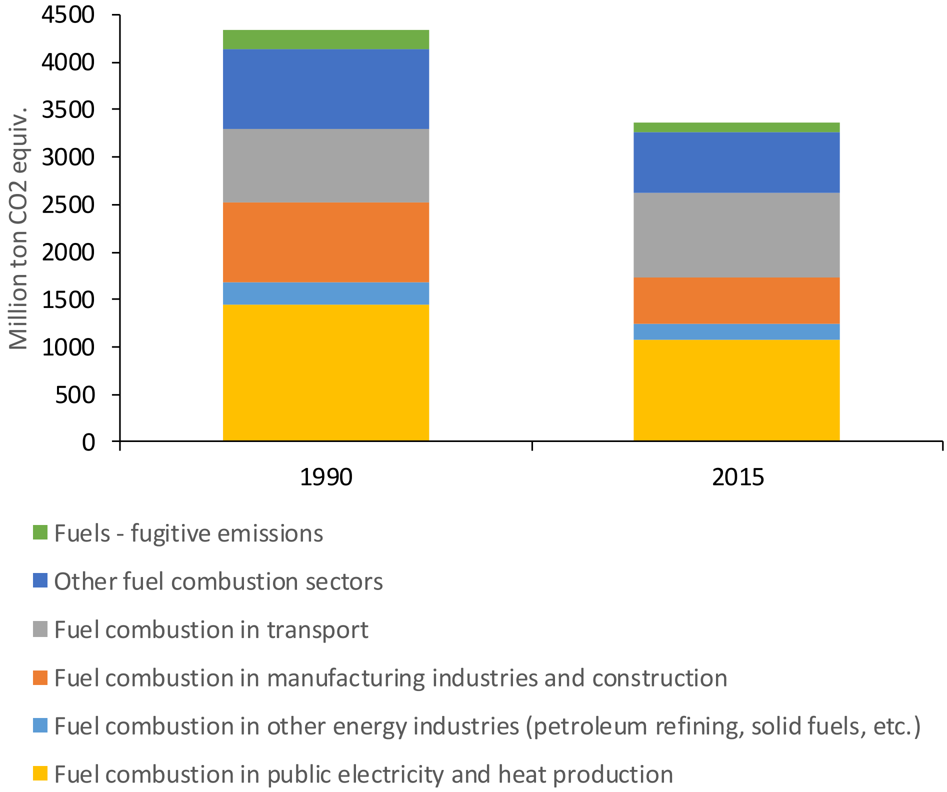

Figure 44: GHG emissions in the EU-28 by use within the Energy sector (Source: Eurostat).

	Gt CO_2 1990	Gt CO_2 2015	% 1990	% 2015
Fuel combustion in public electricity and heat production	1440	1070	33.2%	31.9%
Fuel combustion in other energy industries (petroleum refining, solid fuels, etc.)	239	172	5.5%	5.1%
Fuel combustion in manufacturing industries and construction	836	483	19.3%	14.4%
Fuel combustion in transport	782	906	18.0%	27.0%
Other fuel combustion sectors	848	637	19.5%	19.0%
Fuels - fugitive emissions	191	89	4.4%	2.7%
Total	**4337**	**3358**	**100.0%**	**100.0%**

Table 57: GHG emissions in the EU-28 by use within the Energy sector (Source: Eurostat).

Given the importance of the transport sector in general and specifically for FABRIC, below a breakdown of emissions within the transport sector is shown. As can be observed in Table 58, GHG emissions from combustion in road transport has by far the largest share, and even increased its contribution from 1990 to 2015. Note that data from Eurostat does not include international aviation and navigation.

	Gt CO_2 1990	Gt CO_2 2015	% 1990	% 2015
Fuel combustion in domestic aviation	14	15	1.8%	1.7%
Fuel combustion in road transport	723	862	92.5%	95.2%
Fuel combustion in railways	14	6	1.8%	0.7%
Fuel combustion in domestic navigation	25	16	3.2%	1.8%
Fuel combustion in other transport	5	6	0.7%	0.7%
Total	**782**	**906**	**100.0%**	**100.0%**

Table 58: GHG emissions in the EU-28 by use within the Transport sector, excluding international aviation and navigation (Source: Eurostat).

Emissions from road transport has been broken down to the different vehicle categories in Figure 45 (numbers in Table 59).

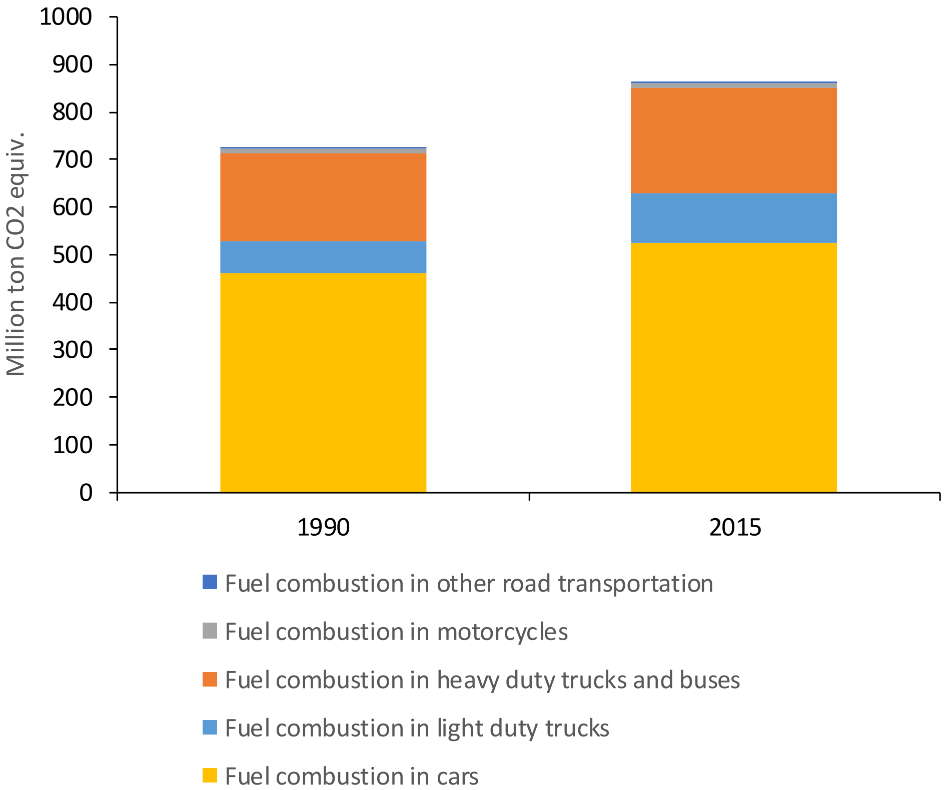

Figure 45: GHG emissions of road transport in the EU-28, by vehicle type (Source: Eurostat).

Increase in emissions from road transport is clear (14.5% since 1990) and the share from cars is remaining highest with slightly more than 60%. A slight increase in share from light duty trucks can be observed too, which can probably be attributed to increased online shopping habits and the resulting delivery to the households.

	Gt CO_2 1990	Gt CO_2 2015	% 1990	% 2015
Fuel combustion in cars	459.5	526.0	63.5%	61.0%
Fuel combustion in light duty trucks	66.9	102.0	9.3%	11.8%
Fuel combustion in heavy duty trucks and buses	187.2	222.9	25.9%	25.9%
Fuel combustion in motorcycles	9.4	10.9	1.3%	1.3%
Fuel combustion in other road transportation	0.3	0.3	0.04%	0.03%
Total	**723.3**	**862.1**	**100.0%**	**100.0%**

Table 59: GHG emissions of road transport in the EU-28, by vehicle type (Source: Eurostat).

All these numbers show the significant impact of the electrification of road transport in the EU on GHG emissions. Transport represents 27% of GHG emissions and almost 70% of this amount is emitted only by cars and light duty trucks. A transition to zero-emission electric cars will thus reduce overall emissions by 19%, while electrification of heavy trucks and buses would contribute with 7%. These numbers are of course under the assumption that the energy will be provided

from zero-emission electricity (see previous section “Outlook for 2050”). It should be mentioned here, that international aviation and navigation is excluded from this study, as it was excluded in the Eurostat Database.

As a final comment, it should be recalled, that GHG emissions from electricity generation itself accounted for 32% of total emissions in 2015. Therefore, in the final picture for 2050, reduction potential of both sectors combined add up to 58% of 2015 reference values.

3.6 Impact of DWPT adoption on Energy balance

In order to show-case the possible integration of DWPT with solar PV, wind and storage, one scenario has been chosen:

- d_{DWPT} = 25 km stretch of e-road
- P_{DWPT} = 50 kW recharge power
- η_{Syst} = 80% DWPT system efficiency (grid – to on-board DC bus)
- v_{veh} = 110 km/h vehicle speed while recharging
- N_{vpd} = 10,000 vehicles per day (intermediate scenario from section 3.3.1)
- E_a = 52 GWh annual energy consumption

Annual energy consumption is calculated from the parameters above, applying the following formula:

$$E_a[\text{GWh}] = 10^{-6} \cdot 365\, N_{vpd} \cdot \frac{P_{DWPT}[\text{kW}]}{\eta_{Syst}} \cdot \frac{d_{DWPT}[\text{km}]}{v_{veh}[\text{km/h}]}$$

The exercise of the following sections examines the size of a renewable power plant which would be needed to generate this annual energy demand, obtaining annual net energy balance. In a second step, hourly fluctuations of DWPT demand and renewable sources are examined. Assuming that the renewable resource is integrated into the DC bus of the DWPT system, hourly net energy flows between the integrated system and the grid (grid exchange) are calculated as follows:

$$P_{grid}(t) = P_{dwpt}(t) - P_{gen}(t)$$

In a final step, theoretical energy storage requirements are derived from hourly net energy flows with the grid. Although the resulting storage system is not a real one, resulting power and energy levels are an indicator for the flexibility which is required from the grid.

Below the reference demand of a 25-km stretch of e-road is shown, considering the parameters given above. This demand curve will be employed for all studies of this section. Notice that nominal grid supply is 25 MVA, but for 10,000 vehicles per hour, not even 20 MW are reached.

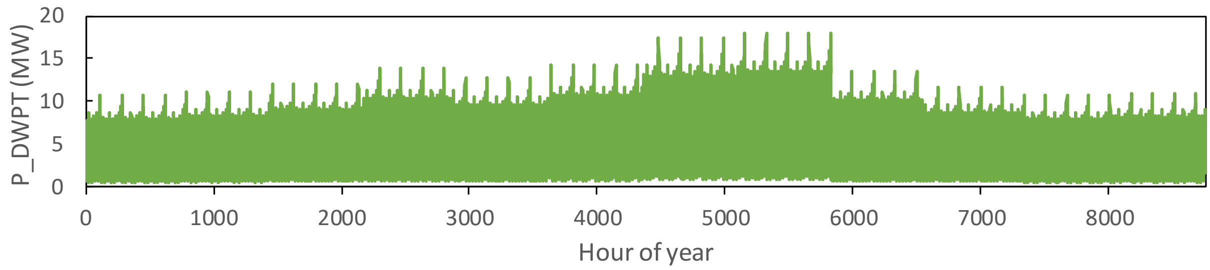

Figure 46: Hourly demand from 25-km e-road (50 kW, 10 thousand vehicles per day).

3.6.1 Integration of solar energy

Solar resources of different European locations have been obtained from PVGIS [40] and compared with annual demand from a 25-km stretch of e-road (52 GWh). In Table 60 the resulting size of a solar PV plant which would produce the same net-energy during one year is shown. The annual yield in kWh/kW is obtained directly from the PVGIS web page. Notice that Stockholm has a higher solar resource than Berlin or London. This is mainly due to the special micro-climate (low precipitations) and longer days in summer. Nevertheless, in winter, the solar resource is extremely low. In general, in northern Europe, approximately 1 MWh/kWp is obtained, while in southern Europe 50% more energy can be expected.

Location	PVGIS Annual Yield (kWh/kW)	Pinst (MWp)	(MWp/km)	Module width (m)
Berlin	962	53.9	2.16	14.4
London	1000	51.8	2.07	13.8
Stockholm	1020	50.8	2.03	13.6
Paris	1040	49.9	1.99	13.3
Rome	1450	35.8	1.43	9.5
Madrid	1550	33.4	1.34	8.9
Athens	1570	33.0	1.32	8.8

Table 60: Properties of a solar PV plant for net energy supply of a 50-kW 25-km e-road.

Installed power Pinst in Table 60 is obtained by dividing e-road consumption by solar yield, as obtained from the PVGIS website. This implies AC-integration of solar power. If DC integration is considered, part of the AC-DC conversion losses in annual production are avoided. As a result, required installed PV power is reduced. As each kWp yields different amounts of energy, this effect is higher in northern Europe, reaching up to 5% of reduction of installed power, while in Greece for example, no reduction is observed.

Finally, in order to give an impression of the extension of such an installation, additional parameters are given in this table. For example, in order to obtain installed power per km of e-road of 2 MWp/km, a solar power plant with approximately 1km x 13m module surface is needed (module efficiency: 15%). Solar power plant dimensions are given for illustration purposes. The

rather small footprint of the resulting installation shows very well the possibility of distributed solar alongside the e-road and integration into the DC distribution line. Available space alongside the road can be included into the planning process when deciding where to install the 25-km recharging stretch.

Of course, annual averages are not the whole story. Solar energy is available only during daytime, but fortunately, traffic is also most active within this timeframe, as has been shown in section 3.3.1. This effect is studied some more in detail now, considering several scenarios of solar radiation and assuming the same case of traffic density and transfer power as mentioned above. In order to have a more detailed picture, hourly values are generated for solar generation and compared with DWPT demand which has been generated from daily, weekly and yearly profiles, presented in section 3.3.1 “25-km E-road”. Hourly solar generation is obtained from standard solar system software.

In Figure 47 hourly power values are shown for grid exchange, assuming e-road demand as in Figure 46 and solar PV integration with annual net zero consumption. The upper graph shows the case of Stockholm with 49 MWp installed PV power and the lower graph Madrid with 32.5 MWp. Grid exchange is limited to 25 MW, as this is the nominal power of the e-road (see Table 31, case $P_{DWPT} = 50$ kW and $N_{vpk} = 15$), although for the case shown here (10,000 vehicles per day), expected peak demand does not surpass 20 MW. From these graphics it can be seen that in Stockholm back-feed from the solar power plant is limited to 25 MW due to the network constraint, while in Madrid, the much smaller PV plant does not reach this limit. It can also be observed that the system now operates between -25 … 20 MW, while the e-road demand itself was between 0 … 20 MW. Due to the higher installed PV power in Stockholm, summer peaks of power injected to the grid (negative grid exchange) are higher for the Swedish case than for the Spanish one. Figure 48 shows these hourly balances for one week in December and another week in August, where these back-feed peaks can be observed more in detail.

Assuming a PV system cost of 1 €/Wp, levelised cost (over 25 years) of the integrated system is 8.9 c€/kWh in Sweden and 5.6 c€/kWh in Spain (assuming grid energy purchase at 0.10 €/kWh). It should be mentioned here, that system costs are reduced for DC integration, as the grid-tied converter of the DWPT system would also be able to inject solar excess generation into the grid, if modern PWM technology is employed. On an annual basis, in the Spanish case, around 44 GWh of energy are exchanged with the grid (22 GWh purchased and another 22 GWh sold), while in the Swedish case, with 52 GWh this volume is almost 20% higher.

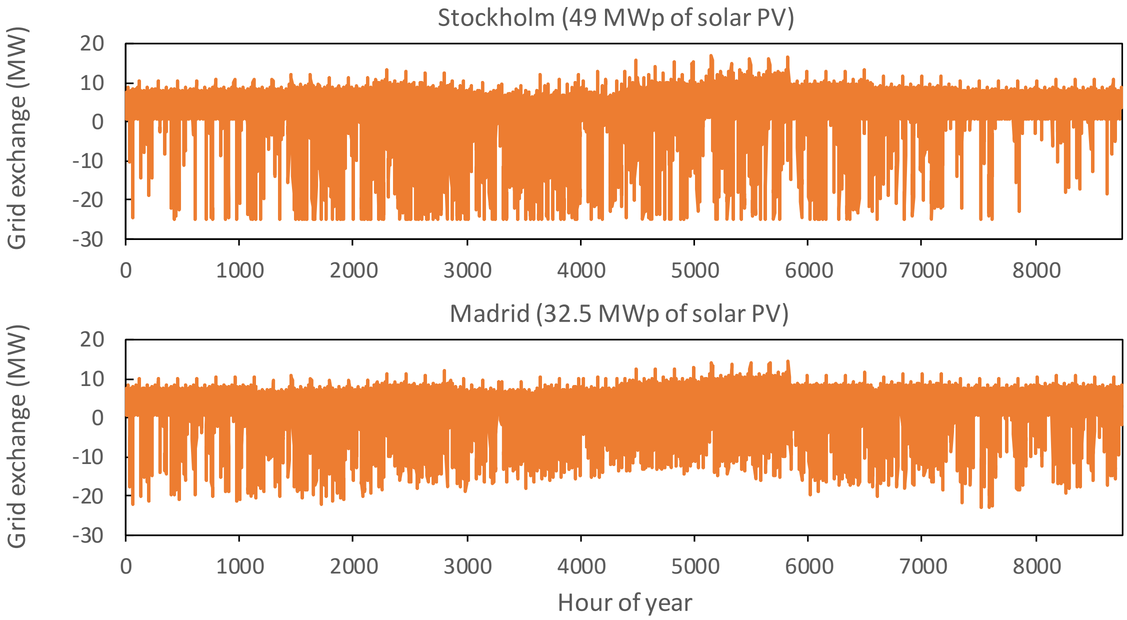

Figure 47: Hourly grid exchange power of 25-km e-road with integrated solar PV.

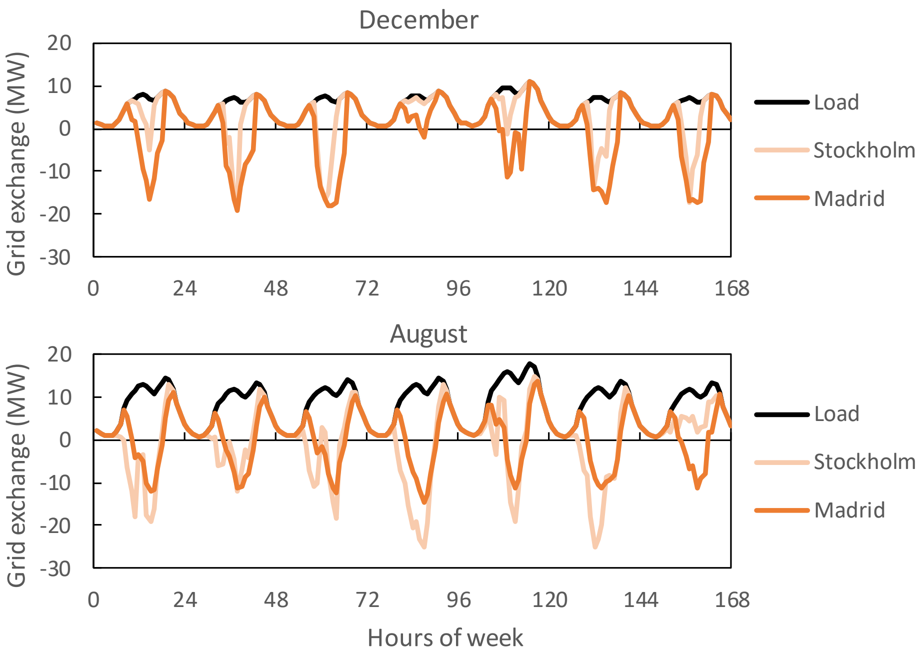

Figure 48: One week DWPT load and grid exchange with solar integration.

Although annual consumption is balanced with generation, summer demand peaks are only reduced slightly. In Stockholm, solar integration is able to reduce annual demand peaks from 18

MW to 17 MW, while in Madrid the reduction to 14.5 MW is more noticeable. On the other hand, generation (back-feed) peaks are created which are even higher in magnitude than demand peaks. Notice, that for this simulation, a limit of 25 MW was imposed for back-feeding to the grid, as this was assumed to be the rated power of the 25-km e-road grid connection anyway. Due to the fact that maximum solar generation always occurs while e-road demand is also high, this 25-MW limit actually does not imply any significant curtailment for PV generation. In fact, even for the system of the Swedish case (49 MW with DC integration) only 0.9% of the annual production is lost due to this limit. In the Spanish case, maximum back-feed peak is with 23 MW still below the limit.

In Figure 49 monthly energy balance is shown for the two show cases. Notice that the sum of monthly purchased energy ("Purchased") and self-consumed PV generation ("PV-self") is equal in both cases, as this is the monthly demand of the DWPT system itself. While the two different solar PV systems generate the same energy in one year, the different seasonal distribution causes significant differences in the monthly energy balances.

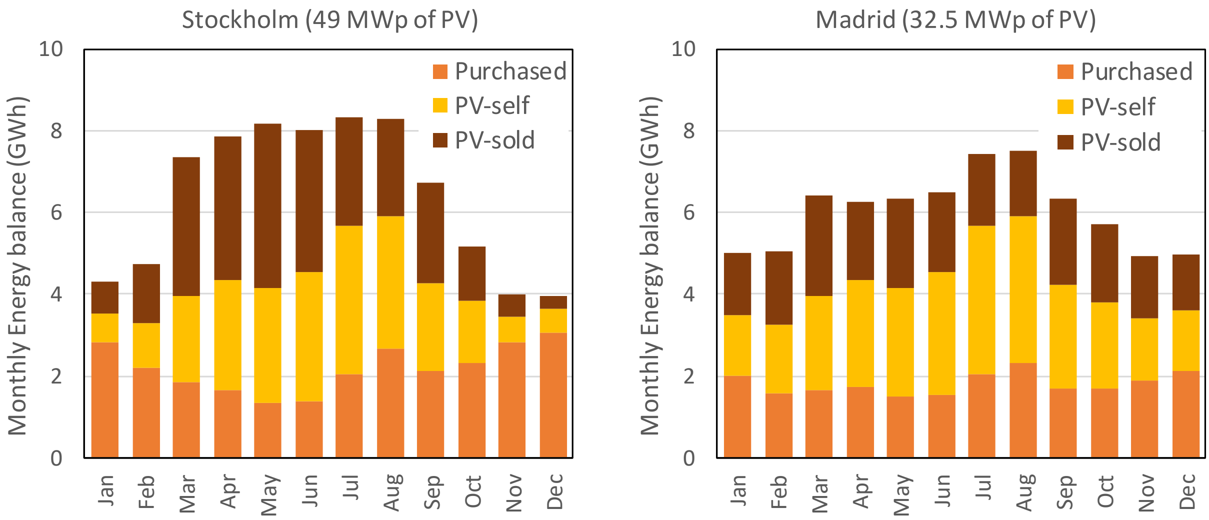

Figure 49: Monthly energy balance of the integrated system with solar (left: Stockholm, right: Madrid).

As mentioned before, exchange with the grid ("Purchased" and "PV-sold") is much higher for Stockholm. The illustration in Figure 49 shows the reason for this. In northern latitudes, low solar generation in winter is compensated with higher generation in summer, which causes a larger mismatch between generation and demand in comparison with more southern locations. As a result, comparing out two show cases, the ratio of direct self-consumption is significantly higher for Madrid. While in Stockholm 46% of solar PV generation is instantly self-consumed by the DWPT system, in Madrid this ratio is 55%. As "instant" self consumption hourly mean values are considered here, as this is the simulation time step.

As a conclusion, it can be stated that solar integration with e-roads is more beneficial in southern Europe, although 46% of self-consumption for Stockholm is a surprisingly high ratio. In general, relatively high ratios of self-consumption can be expected thanks to the similarity between traffic patterns and solar resource.

Storage requirements for increasing self-consumption and to make the whole system more grid-friendly will be analysed in section 3.6.4 (Integration of storage).

3.6.2 Integration of wind energy

Wind resources depend much more on local climate than solar. Therefore, it is hard to find "typical" wind data for similar locations as provided for solar integration in the previous section. Therefore, only ONE case will be presented here with real data of a very good wind resource from the Ebro valley in Spain which presents in a capacity factor of 26.4% (Yield: 2310 kWh/kW). This showcase demonstrates what kind of variability must be expected from wind integration, which is most important the storage assessment. The idea behind this procedure is that wind will only be integrated if there is a good resource.

With such a resource available, the following list shows the properties of a wind park which would produce the required 52 GWh over one year:

- Pinst: 22.5 MW
- Pinst/km: 0.9 MW/km (one 2.5-MW wind turbine each 2.8 km)
- Annual grid-exchange (feed-in + purchase): 58 GWh

In Figure 50 hourly power values are shown for grid exchange, assuming e-road demand as in Figure 46 and wind power integration with annual net zero consumption. The graph shows the case of 22.5 MW installed power.

Equal to the solar case, grid exchange is limited to 25 MW, which is not a limitation in this case, as installed wind power is below this limit. Here, the clear limitation of back-feed to the grid is given by the installed wind power of 22.5 MW. In this case, as wind power is uncorrelated with traffic patterns, nominal power generation can occur during night, when traffic load is almost zero. Therefore, back-feed of nominal power can be observed all over the year, but in this case especially in Winter. Compared to solar, highest back-feed power is slightly lower for wind integration. Figure 48 shows these hourly balances for one week in December and another week in August, where these back-feed peaks can be observed more in detail.

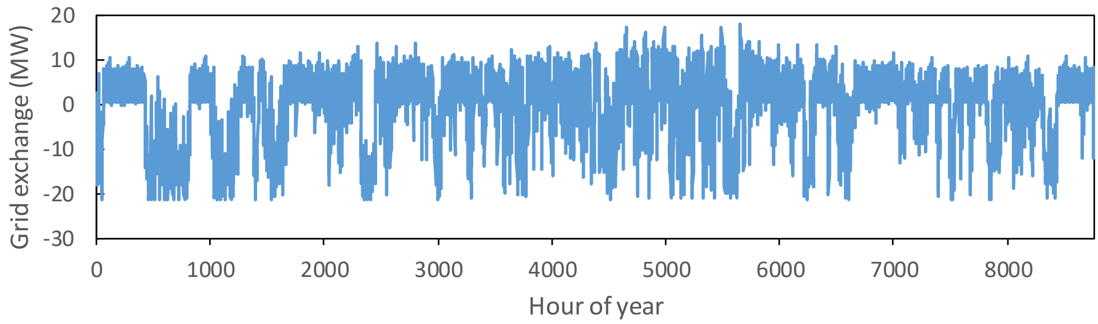

Figure 50: Hourly grid exchange power of 25-km e-road with integrated 22.5-MW wind park.

Assuming a wind power system cost of 1.25 €/Wp, levelised cost (over 25 years) of the integrated system would be 6.7 c€/kWh (assuming grid energy purchase at 0.10 €/kWh), which is slightly higher than solar case in southern Europe. The higher installation and maintenance cost for wind compensates most of the much higher energy yield per installed kW. In this case, no DC integration was considered, although full-converter turbines are gaining terrain, so also for wind power, DC integration is definitely an option.

Compared to solar integration, grid exchange is with 58 GWh even higher than in the case of Stockholm. The reason for this is that wind is not correlated with traffic patterns. As a consequence, also the self-consumption ratio is lower, reaching still an interesting 44%.

Summer demand peaks are not reduced, as highest e-road demand comes together with low wind resources, while with solar integration, higher demand in summer is correlated with higher resource.

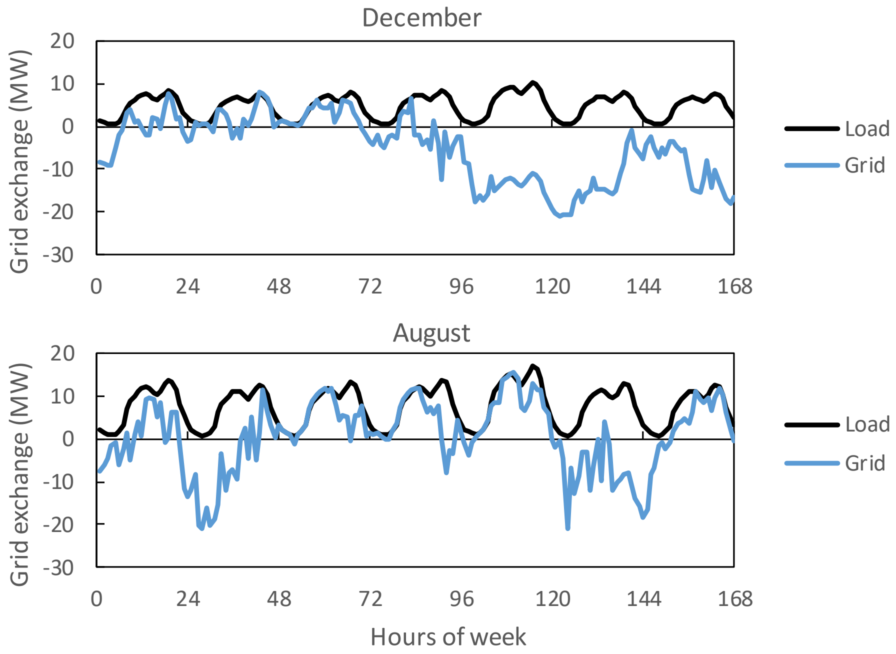

Figure 51: One week DWPT load and grid exchange with solar integration.

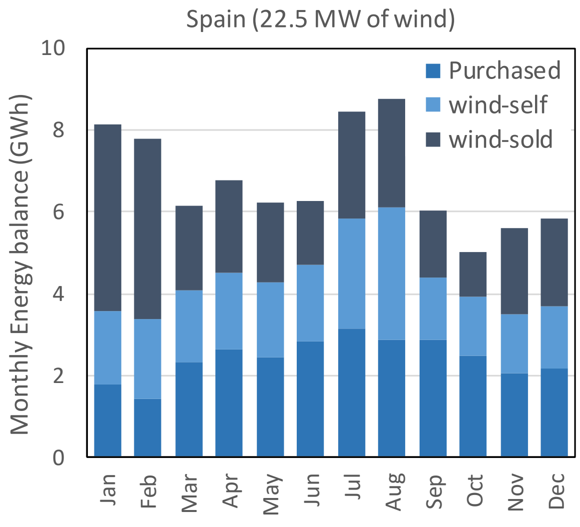

Figure 52: Monthly energy balance of the integrated system with wind.

In Figure 52 monthly energy balance is shown for the case of wind integration. Again, the sum of monthly purchased energy ("Purchased") and self-consumed PV generation ("PV-self") represents monthly demand of the DWPT system. Compared to solar integration, self-consumption is more constant over the year with considerable levels also in winter. Similar to solar, highest values are observed in August, when demand is highest.

As a conclusion, it can be stated that with 44% wind integration attains respectable levels of self-consumption. This value is significantly lower than the 55% obtained for solar integration in southern Europe and similar to the 46% in Stockholm. Generation costs are similar to solar in southern Europe, which might make it an interesting solution for northern countries. Annual energy exchange with the grid is higher compared to solar, because wind power is not correlated to e-road demand.

Storage requirements for increasing self-consumption and to make the whole system more grid-friendly will be analysed in section 3.6.4 (Integration of storage).

3.6.3 Integration of wind and solar PV

In order to provide also some insight into the effect of combined integration of solar PV and wind energy, solar showcases of Stockholm and Madrid have been combined with the presented wind resource. The interpretation of this combination is that if a good wind resource exists at a given site along an e-road, how would a hybrid solar-wind system look like, which would provide a zero net energy balance over one year at least cost. Results of this exercise are presented below.

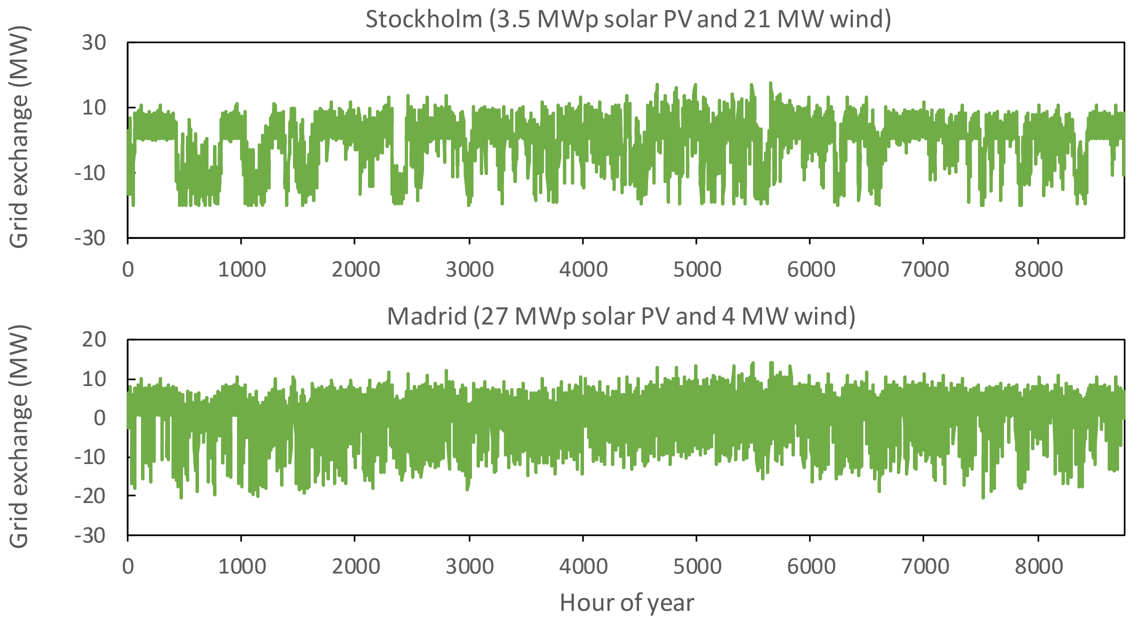

Figure 53: Hourly grid exchange power of 25-km e-road with integrated solar PV and wind.

As for solar and wind integration, Figure 53 shows hourly power values are for grid exchange for the case of hybrid solar-wind integration (always assuming e-road demand as in Figure 46 and renewable energy (RE) sized for annual net zero consumption).

The upper graph shows the case of Stockholm with a combined RE installed power of 32 MW (18 MW solar and 14 MW wind) and the lower graph Madrid with 31 MW (27 MW solar and 4 MW wind). The first observation is that in this hybrid case, back-feed to the grid does not reach the grid connection limit of 25 MW. This is because combined solar and wind power is with 31-32 MW only slightly above the 25-MW limit. Also, solar peak power always occurs during high e-road demand and wind power, which can reach nominal values during low demand times (at night), is well below this limit. Comparing the charts, in Stockholm, variability is mainly characterised by wind, while in Madrid solar is predominant. Figure 54 shows hourly balances for one week in December and August. In this zoom-view, reduced back-feed levels can also be observed.

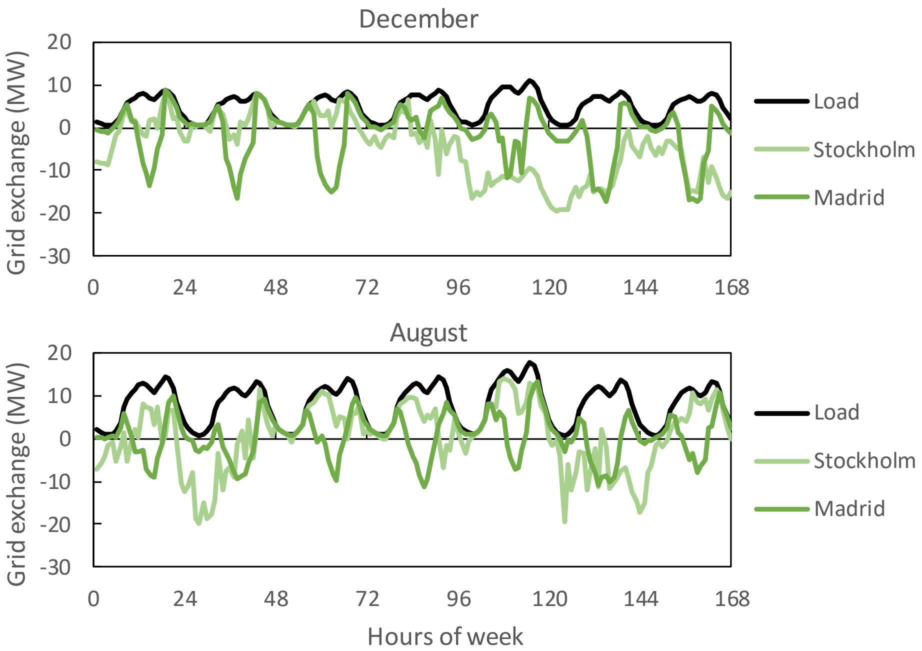

Figure 54: One week DWPT load and grid exchange with solar and wind integration.

Assuming a system cost of 1 €/Wp for solar and 1.25 €/W for wind, levelised cost (over 25 years) of renewable energy would be 6.6 c€/kWh in Sweden and 5.5 c€/kWh in Spain (assuming grid energy purchase at 0.10 €/kWh).

On an annual basis, in the Spanish case, around 36 GWh of energy are exchanged with the grid (18 GWh purchased and another 18 GWh sold), while in the Swedish case, with 53 GWh this volume is significantly higher. In the Spanish case, the addition of only 4 MW of wind reduces grid exchange volume from 44 GWh in the solar-only scenario to 36 GWh with the hybrid system (18% reduction). In the Swedish case, the addition of just 3.5 MW solar PV yields a reduction of grid exchange volume from 58 GWh in the only-wind scenario to 53 GWh in the hybrid system (8.6% reduction). These numbers should not be interpreted as absolute values, but rather a tendency is shown here. The important conclusion is that if there is good wind resource available along the e-road, a hybrid system with solar will be beneficial, as self-consumption ratios are increased. The benefit regarding system LCOE is marginal in the examples shown here, even if the self-consumption ratio was increased in the Spanish case from 55% in the solar-only scenario to 61% in the solar-wind hybrid scenario.

The behaviour regarding annual peak demand and back-feed is very similar to the solar-only case in the Spanish case and the wind-only case in the Swedish case, but in any case, values are slightly reduced.

In Figure 55 monthly energy balance is shown for the two show cases. Due to the dominance of each resource, the balance for Stockholm resembles very much the wind-only case, while the balance for Madrid is very similar to de solar-only scenario. Nevertheless, self-consumption in winter is higher in Madrid thanks to wind and higher in Summer in Stockholm thanks to solar.

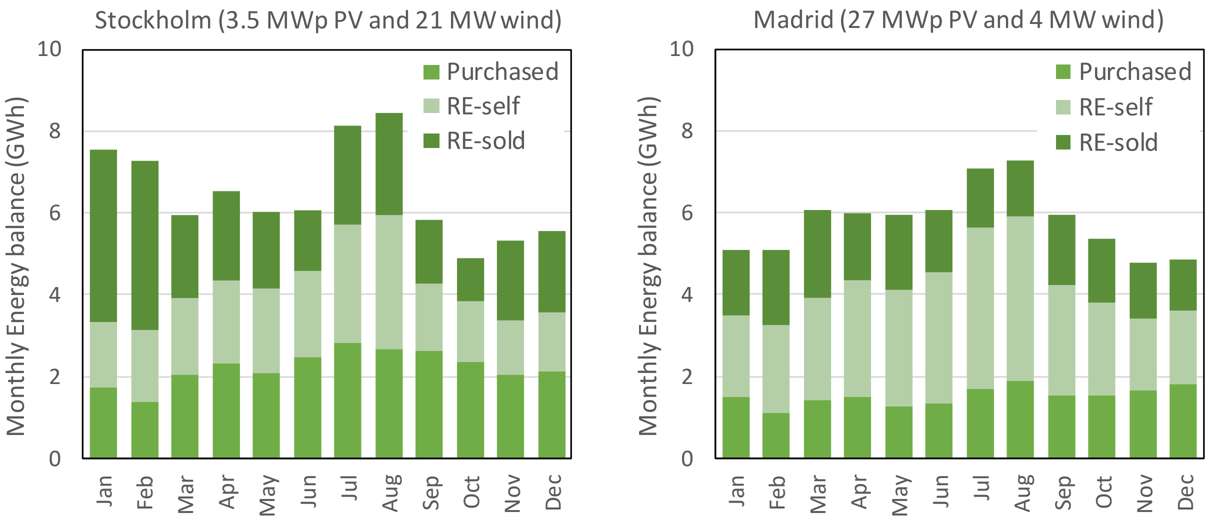

Figure 55: Monthly energy balance of the integrated system with solar and wind (left: Stockholm, right: Madrid).

3.6.4 Integration of storage

Storage is considered as the missing link in order to balance variable generation (solar and wind) and demand. In this case, it will be studied how much storage would be needed in order to allocate additional demand from DWPT. For this purpose, 4 basic scenarios have been evaluated: Only DWPT, DWPT+solar, DWPT+wind, DWPT+solar+wind. In addition, the impact of different locations with different solar radiation was studied, taking solar conditions of Stockholm for northern Europe and Madrid representing southern Europe (see preceding sections on integration on solar and wind energy). As a result, 6 energetic scenarios have been created and analysed:

- Solar Stockholm
- Solar Madrid
- Wind generic
- Hybrid Stockholm
- Hybrid Madrid
- DWPT only

All studies were carried out on an annual basis, considering hourly time steps for renewable resource and DWPT demand. For energy storage system (ESS) sizing, two different scenarios have been considered:

- Self-sufficient micro-grid
- 24-h smoothing

The self-sufficient micro-grid scenario is intended to show the large amount of seasonal mismatch between renewable generation and DWPT demand. It is not proposed to install such a system, but to show how much balancing energy and power will be needed to integrate everything into the grid.

The DWPT-only scenario is not relevant for the first study, which analyses self-sufficient systems. Nevertheless, for the second analysis (24-h smoothing) it is included. As a result, a total of 11 different cases have been elaborated.

Self-sufficient micro-grid

In this first approach, ESS size has been calculated which would be needed to obtain 100% self-sufficient DWPT micro grids. The evolution of the state of charge (SoC) over one year is shown in Figure 56. In the simulation, SoC is assumed to be zero at the beginning and can be negative. The difference between minimum and maximum SoC is at the end the required energy capacity of a given ESS. Nominal power is obtained from the difference between demand and generation. Again, the highest value (positive or negative) in one year is taken to define the power requirement. Numerical results are summarised in Annex B: Tables for Storage Integration.

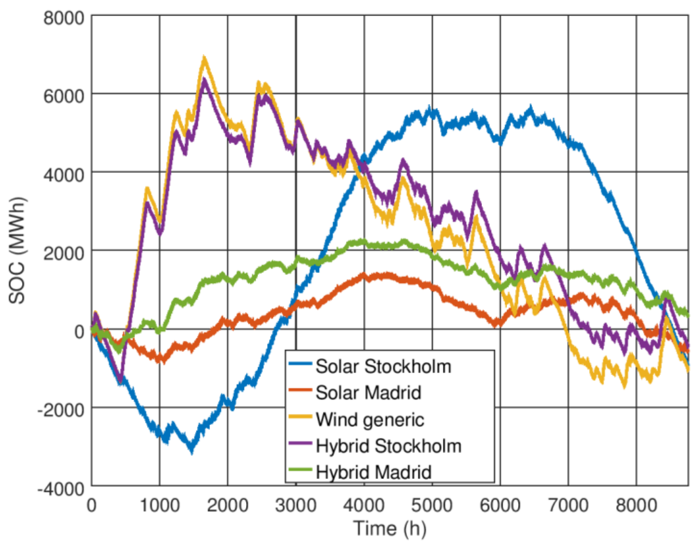

Figure 56: Evolution of ESS charge for 100% self-consumption.

In Figure 56, large differences can be observed between the 5 scenarios which are caused by the fundamental differences of availability of renewable resources over the year.

E-road RE show case	RE P_{inst} (MW)	P_{ESS} (MW)	E_{ESS} (MWh)	Storage percentage of annual demand	ESS throughput (GWh)	Equiv. annual full cycles	System demand peak (MW)
Only e-road	0	0	0	0	0	0	18
Solar Stockholm	49.0	25.0	9404	18%	52.7	2.8	0
Solar Madrid	32.5	23.1	2573	5%	43.9	8.5	0
Wind generic	22.5	21.5	8393	16%	58.2	3.5	0
Solar-Wind Stockholm	24.5	20.0	7826	15%	54.0	3.4	0
Solar-Wind Madrid	31.0	20.5	3184	6%	37.5	5.9	0

Table 61: Storage requirements for 100% compensation of RE variability.

"Solar Stockholm" requires largest storage, as the northern winter does not provide any solar resource and several months of balancing energy are needed. Seasonal storage requires approximately 2 months of average demand (18% percent of annual demand).

Second largest requirement is obtained by "Wind generic". In this case, the situation is opposite: large amounts of energy need to be stored in winter, in order to provide energy in weak summer months. The scenario "Hybrid Stockholm" is very similar to "Wind generic" due to the fact that the optimisation process assigned a large portion of wind power to Stockholm location, in order to obtain an optimised hybrid system. The most favourable situation can be found in southern Europe ("Solar Spain"), where the storage capacity reaches 5% of annual DWPT demand or 18 days of average demand for a pure solar system. Similar pattern is obtained for "Hybrid Madrid", as it includes only a minor portion of wind.

Looking at the energy throughput of the storage system (adding up all energy charged and discharged), it can be concluded that energy throughput is in the range of total annual DWPT demand. This means that half of all energy is cycled through the storage system (percentages are complementary to self-consumption in Table 66). The number of equivalent full cycles is a measure for intensity of use of the storage. Here it can be seen that values between 2.8 and 8.5 cycles are extremely low.

24-h smoothing

As 100% self-sufficiency requires prohibitive amounts of storage capacity, a relaxed condition has been applied. For 24-h smoothing, the mission of the hypothetical ESS is to achieve that the DWPT micro-grid exchanges with the grid only the moving average of the last 24 hours. As a result, daily fluctuations due to typical pattern of DWPT demand and especially solar generation are compensated entirely. Grid exchange is only used to compensate remaining longer-term trend

of the balance between generation and DWPT demand. As a result, much smaller ESS sizes are obtained, as can be observed in Figure 57. Numerical results are shown in Table 62.

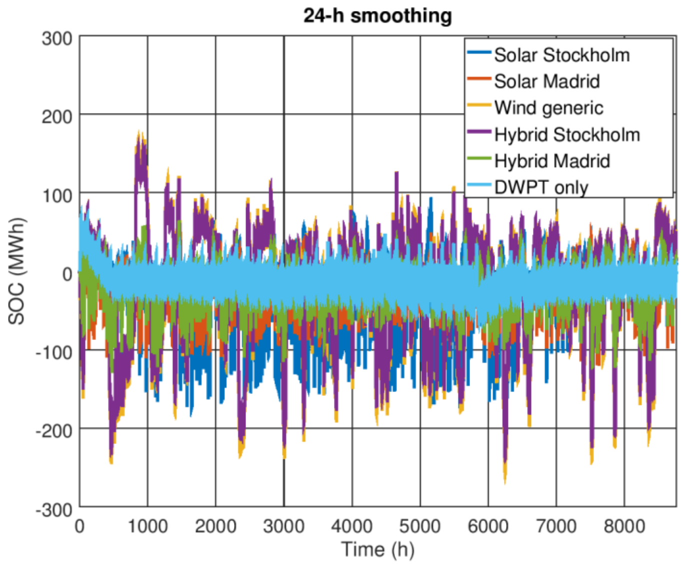

Figure 57: Evolution of ESS charge with 24-h smoothing.

E-road RE show case	RE P_{inst} (MW)	P_{ESS} (MW)	E_{ESS} (MWh)	Storage percentage of annual demand	ESS throughput (GWh)	Equiv. annual full cycles	System demand peak (MW)
Only e-road	0.0	9.5	136	0.26%	27.9	103	10.1
Solar PV Stockholm	49.0	27.8	266	0.51%	52.1	98	8.1
Solar PV Madrid	32.5	24.0	183	0.35%	44.7	122	5.2
Wind generic	22.5	27.9	425	0.82%	39.4	46	16.8
Solar-Wind Stockholm	24.5	26.1	397	0.76%	36.4	46	16.1
Solar-Wind Madrid	31.0	18.4	196	0.38%	37.5	96	5.7

Table 62: Storage requirements for 24-h smoothing.

The first observation is that 24-h smoothing, requires much smaller storage capacities in terms of energy, but slightly higher power. This power requirement results from the applied smoothing algorithm (moving average of 24 h window width) and might be reduced, if the algorithm is refined (this was not main focus of the study). While throughput is only reduced slightly, equivalent annual full cycles are increased to 46 – 122, which represents a much better utilization factor of the storage.

Interestingly, the smallest system is obtained for “DWPT only”. Actually, this case can be considered as “base case” for grid integration, as daily fluctuations are completely absorbed and grid connection power requirements might be reduced.

Remember that a factor 2-3 can be expected between average and peak demand of the e-road. As a result, the ESS can be used to reduce grid infrastructure. In any case, a trade-off must be found between the extra costs of ESS and savings of a reduced grid infrastructure. This analysis is not part of this study, but it can be expected that additional revenue streams need to be exploited in order to make the installation of such an ESS profitable. Grid infrastructure is normally less expensive on unitary energy and power costs than the ESS. Nevertheless, grid balancing services might be very interesting.

For the other scenarios, a similar ranking compared to the 100% self-sufficient micro-grid is obtained regarding required ESS energy capacity. Again, Solar Madrid and Hybrid Madrid require lowest storage capacity. One exception is “Solar Stockholm”, which outscores wind-scenarios and ranks fourth behind Solar Madrid and Hybrid Madrid. The largest smoothing capacity is required for the wind-only scenario. This can be explained by the more irregular generation pattering of wind, compared to very periodical pattern of solar generation.

But to see the actual benefit from the smoothing, grid connection indicators have to be analysed. Therefore, the remaining pattern exchanged with the grid is evaluated, which is shown in Figure 58. Numerical values of simulation results regarding grid connection indicators for 24-h smoothing can be seen in Table 63.

An intrinsic consequence of the smoothing method, power peaks are reduced in both directions: demand and back-feed. Most noteworthy is the case of DWPT only, which obtains the smoothest grid exchange pattern, without any back-feed and only small fluctuations around the average, which are representing weekly cycles with highest traffic on Fridays and lowest on Sundays.

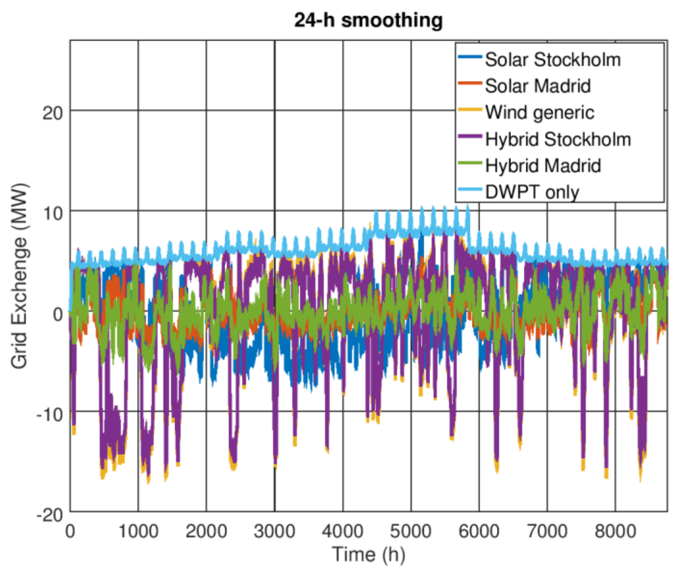

Figure 58: Grid exchange with 24-h smoothing.

E-road RE show case	RE P_{inst} (MW)	P_{ESS} (MW)	E_{ESS} (MWh)	Annual grid exchange (GWh)	System demand peak (MW)	System back-feed peak (MW)	RE Self-consumption ratio (%)
Only e-road	0	9.5	136	52.3	10.1	0.0	0%
Solar PV Stockholm	49.0	27.8	266	27.7	8.1	7.4	73%
Solar PV Madrid	32.5	24.0	183	13.4	5.2	3.5	87%
Wind Spain	22.5	27.9	425	46.1	9.8	16.8	56%
Solar-Wind Stockholm	24.5	26.1	397	42.8	9.2	16.1	59%
Solar-Wind Madrid	31.0	18.4	196	13.8	5.2	5.7	87%

Table 63: Grid connection indicators for 24-h smoothing.

Also, the mostly solar systems ("Solar Madrid" and "Hybrid Madrid") show relatively small fluctuations around the average (which in this case is zero). Although back-feeding occurs frequently, grid requests are symmetrical around zero, which means a better usage factor of system infrastructure. Finally, wind scenarios show large back-feed peaks, as windy weather conditions can be sustained more than 24 h and the storage system cannot compensate them.

For a 18 MW e-road, system demand is reduced below 10 MW and even close to 5 MW in the best case. Back-feed power is also reduced, while wind power is less favourable. Solar systems obtain similar values of demand and back-feed power.

Another important feature is an important increase in self-consumption ratios. For Spain, impressive 87% self-consumption is obtained with a storage system which only stores 0.35% of annual DWPT demand or 1.3 days of average demand. Even the solar system in Stockholm reaches 73% self-consumption, with a slightly larger storage system (0.5% of annual DWPT demand). As self-consumption is increased, the volume of energy exchanged with the grid is reduced.

European upscale

If the numbers of assumptions presented in section 3.4.2 of this report (Table 50 and Table 51) are taken into account, storage capacity can be expressed in kWh/vehicle served. In order to keep this example simple, only solar PV integration with 24-h smoothing is presented here. Estimated storage capacity was calculated to be 183 MWh for a 25-km e-Corridor, serving daily 9330 clients, which is 3.4 million in one year. But in order to obtain a reasonable value of kWh/vehicle, the number of physical clients is needed, so the additional storage can be added to each individual car. To know, how many individual clients are actually using the e-corridor, again, assumptions of this exercise are used. For the year 2050, the following figures are considered:

- 189 million EV in Europe (more than 50% of the vehicle stock)
- 56.7 million are using DWPT infrastructure (30% of all EVs)
- 32 e-Corridors installed in Europe (25 km each)
- Annual traffic on all e-corridors: 109 million (9331 vehicles/year in 32 e-Corridors)
- Ratio between number of DWPT-EVs/Annual traffic: 1.92

As a conclusion of these numbers, it is considered, that each EV equipped with DWPT is using the e-Corridor twice a year. This may seem very low, but this is consistent with statistics regarding vehicles travelling more than 100 km in a day. On average, only a few trips per year are longer than 100 km and even less are longer than 400 km, which would be the use case of the DWPT infrastructure. With this ratio of 2, annual traffic can be converted in individual clients of the infrastructure, and unitary storage capacity can be assigned. An annual traffic of 3.4 vehicles converts to 1.7 million clients. Dividing storage capacities obtained for the different scenarios, unitary kWh/client are obtained, as shown in Table 64.

Scenario	24-smoothing	Autonomous microgrid
Only e-road	0.08	0.0
Solar Stockholm	0.16	5.5
Solar Madrid	0.11	1.5
Wind generic	0.25	4.9
Solar-Wind Stockholm	0.23	4.6
Solar-Wind Madrid	0.12	1.9

Table 64: Unitary storage requirement (kWh/client) for integration of e-Corridors

The installed ESS capacity of 183 MWh required for the scenario Solar Madrid converts to a mere 0.11 kWh/client of additional storage capacity per vehicle. In Stockholm the number increases to 0.16 kWh/client. At the light of these small numbers, even the ESS capacity of the autonomous DWPT micro-grid seems not too large, with 1.5 kWh per vehicle for solar Madrid and 5.5 kWh for solar Stockholm. Values of storage per vehicle for the autonomous system give an impression of equivalent system flexibility, needed to integrate the system. This can be some sort of seasonal energy storage (in Scandinavia, hydro storage might be an option), or just alternative energy sources and flexible demand. Again, 5.5 kWh in for the worst-case scenario of solar PV in Stockholm seems a surprisingly low value.

Regarding the use cases of periurban and urban bus, daily pattern is similar (diurnal maximum and nocturnal minimum), which suggests similar results in the order of magnitude for required energy storage. Nevertheless, capacity factors of the daily pattern are very different (25% for motorway scenario, 7.5% for periurban scenario and 68% for urban bus.

For each scenario, total required installed capacity of renewable generation for annual zero net balance can be calculated, considering the assumptions mentioned above. Results are shown in Table 65. The different scenarios of renewable energy integration are considering that all DWPT infrastructures are located at the same place, which results in a range of 7 – 10 GW of installed RE power. In a rough first approach, the average of all was assumed to be the estimate for Europe. This is not an exact method, but sufficient for the purpose of this study. The result is that approximately 10 GW of additional renewable energy (RE) generation capacity needs to be installed all over Europe until 2050, in order to cover the annual energy demand of all deployment scenarios together. It is worth noticing that urban buses and periurban e-Launchers account for the vast majority of the expected energy consumption, while e-Corridors only account for 10% of the total.

Scenario	Motorway	Periurban	Urban Bus	Total
Solar Stockholm	1.57	6.49	7.20	15.3
Solar Madrid	1.04	4.30	4.78	10.1
Wind generic	0.72	2.98	3.31	7.0
Solar-Wind Stockholm	0.78	3.24	3.60	7.6
Solar-Wind Madrid	0.99	4.10	4.56	9.7
Average	**1.02**	**4.22**	**4.69**	**9.9**

Table 65: Renewable installed power (GW) for annual zero net energy, requirement for 2050.

In Figure 59, this average requirement has been taken as a reference in order to sketch a roadmap from 2030 to 2050 for accumulated installed RE capacity. Until 2030, a mere 2 GW is needed, while by 2040 this value more than duplicated to 5 GW and duplicated again to reach 10 GW by 2050. In any case, these values are small, compared to the European goals for the expansion of renewable generation.

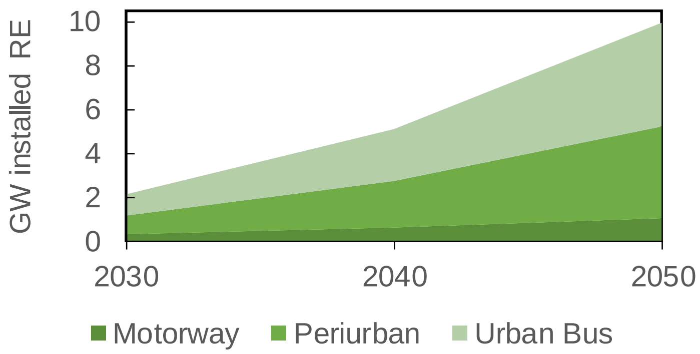

Figure 59: Roadmap for installed renewable energy (RE) installed power (GW) to cover energy consumption from DWPT infrastructures all over Europe until 2050.

3.6.5 Summary and conclusions

Zero annual net energy – No storage

In order to study possible options of integration of renewable energy sources with DWPT infrastructure, in a first step an annual zero net energy balance of an integrated microgrid was assumed. In Table 66 grid connection indicators are summarised. Most important conclusion is that results depend heavily on the location and energy source, but in any case, energy costs in terms of LCOE are reduced. Interestingly, wind energy requires lowest installed power, but annual volume of grid exchange is highest. The most favourable case is a solar-wind hybrid system (mainly solar) in Spain which obtains lowest LCOE and highest self-consumption ratio of 61%. For all solutions, back-feed peak power to the grid exceeds DWPT nominal power of 18 MW. Here, the solar system installed in Stockholm produces highest back-feed power, as installed solar peak power is with 49 MW highest of all. Lowest back-feed power is obtained with 20 MW by a hybrid wind-solar system (mostly wind) in Stockholm solar conditions, which represents a northern location with good wind conditions. In general, self-consumption ratios are surprisingly high, being lowest for pure wind energy and highest for solar-wind hybrid systems. The reason for this is a coincidence of daily solar and traffic patterns and the fact that traffic tends to be higher in summer than in winter.

E-road RE show case	RE P_{inst} (MW)	Annual grid exchange (GWh)	System LCOE (€/kWh)	System demand peak (MW)	System back-feed peak (MW)	RE Self-consumption ratio (%)
Only e-road	0	52.0	0.100	18.0	0	0
Solar Stockholm	49.0	52.7	0.089	16.9	25.0	46%
Solar Madrid	32.5	43.9	0.056	14.5	23.1	55%
Wind generic	22.5	58.2	0.067	17.9	21.5	44%
Solar-Wind Stockholm	24.5	54.0	0.066	17.6	20.0	45%
Solar-Wind Madrid	31.0	37.5	0.055	14.3	20.5	61%

Table 66: Grid connection indicators for annual zero net energy balance without storage.

Self-sufficient micro-grid

The second question was, how much energy storage system (ESS) capacity would be needed to obtain a self-sufficient system, compensating all fluctuations. As could be expected, resulting storage capacities are huge. Depending again heavily on the location and energy sources, storage capacities between 2.6 and 9.4 GWh are required. The smallest ESS system is obtained for a hybrid solar-wind system (mostly solar) located in southern Europe in a place with good wind conditions. The largest ESS is required for a solar system in northern Europe (Solar Stockholm), due to the large imbalance of solar resource between winter and summer months.

24-h smoothing

As the required storage capacity for 100% compensation is far too high, usefulness of a reduced storage system has been explored. The result was that a 24-h smoothing capability turns out to be a good compromise between storage size and benefits. Apart from a dramatic reduction (more than 10-fold) of storage capacity, smoothing improves several parameters of grid demand pattern, such as demand peaks, back-feed peaks and ramp rates. As an interesting application of smoothing, the case “only e-road” is included, showing the capability of reducing system demand peaks. On the other hand, self-consumption ratios are improved considerably, most notably for solar systems, reaching above 70% self-consumption with a relatively small storage capacity of less than 2 days of average annual demand.

As a conclusion is can be noticed that solar systems require less storage. Thanks to their stable daily pattern, the 24-h smoothing is especially well-suited in order to compensate daily pattern from both, traffic and solar power.

European upscale

Just multiplying the required energy capacity by the number of 32 expected e-Corridors in Europe, would give a large number of GWh, which is not easy to interpret. Therefore, storage per vehicle has been calculated. It has been found that each individual client will cross the e-Corridor approximately twice a year, which means, estimated traffic is divided by 2 in order to obtain the reference number of clients for calculation of EES capacity-per client. Results for 24-h smoothing show that a very small energy capacity of storage is required per DWPT-client, ranging from 0.11 kWh/client for the best case (solar Madrid) to 0.25 kWh/client for the worst case (wind generic). For compensation of all fluctuations (autonomous microgrid), values between 1.5 kWh/client (solar Madrid) and 5.5 kWh/client (Solar Stockholm) are obtained. All values are very small, which suggests good feasibility of the proposed system. It is highlighted, that seasonal storage capacity for the autonomous microgrid can be interpreted also as required system flexibility, rather than actual storage capacity.

In terms of annual energy, results for required renewable generation capacity of the Motorway scenario can be extrapolated linearly to the other two scenarios. By 2050 additional 10 GW of renewable generation capacity (mix of solar and wind) is needed to compensate the energy consumption of the projected European DWPT infrastructure. It is noteworthy to mention that only 10% of this demand will come from e-Corridors where direct integration of renewable sources has been shown. The remaining 90% is drawn from e-Launchers and Urban bus fleets, which need support from the surrounding grid (self-sufficient microgrids not feasible for reasons of space).

4 ECONOMIC CONSEQUENCES OF MORE ELECTRICITY INFRASTRUCTURE AND GENERATION PLANTS

4.1 Introduction

This chapter will introduce the economic consequences of the e-Road deployment in Europe with in the decades 2020-2030, 2030-2040 and 2040-2050. Results are based on estimates and assumptions from previous FABRIC deliverables and from within this report.

This chapter describes cost models to estimate economic effects of e-road deployment on EU energy strategy (Europe's dependence on energy imports), considering the impact of e-Road massive deployment on the following key indicators:

- European energy generation costs.
- Infrastructure costs.
- Levelized cost of energy.

The strategy for the calculations is mainly explained in D5.5.2 but some information is taken from D5.3.4. Demand estimation for EVs deployment and the e-Corridors was obtained from D5.4.2.

4.2 Strategy for cost calculations

The strategy for the calculations is depicted below (D5.5.2), organised in four main stages: demand side analysis, unitary costs, global analysis and other impacts.

DEMAND SIDE ANALYSIS		UNITARY COSTS		GLOBAL ANALYSIS		OTHER IMPACTS	
D521	1. Reference Scenarios for e-Roads penetration (Motorway, Periurban, Urban,)	D534	4. Identification of infrastructure costs (POLITO, SAET for each business case)	D552	7. Deployment of European E-Roads in three scenarios in years 2030, 2040 and 2050	D541	10. Impact on renewables
D542	2. EVs Roadmaps (light and heavy BEV-PHEV)	D552	5. Identification of Unitary Costs for the DWPT Equipment on board	D541	8. Grid impact (Total energy requirements in e-Roads charging, years 2030, 2040 and 2050)	D541	11. Impact on LCOE
D542	3. Demand Estimation of DWPT-EVs crossing through e-Roads	D552	6. Business Models (Cost-benefit analysis in each reference case) from investors and DWPT-EVs users viewpoint	D552/ D541	9. Global Cost calculation for e-Roads uptake in years 2030, 2040 and 2050	D552	12. Other Social Impacts
						D554	13. Sensibility Analysis

Previous or parallel deliverable
Current deliverable
Post deliverable

Table 67. Strategy for the global cost calculations.

The overall strategy is described in the following sections according to Table 67. Four main stages are exposed:

- Demand side analysis

- Unitary costs
- Global analysis
- Other impacts

Within each stage, steps are numbered in a consecutive manner, as the process can be understood as a sequence of 13 steps. The overall process is distributed in 8 different FABRIC deliverables (including this report and one future report to be provided after this one), which are mentioned in brackets.

4.2.1 Demand side analysis

1. Main reference scenarios (D5.2.1)

It was concluded that only three scenarios might be feasible. At that moment, no cost references were available, but experts agreed on them based on their experience. The description of these three main scenarios (Motorway, Periurban and Urban) are described in section 1.4 of this report.

2. EV penetration roadmap (D5.4.2)

Most likely roadmap scenarios for progressive penetration of EVs (PHEV and BEV) were developed, based on recent literature (Avere, Frost & Sullivan, Roland Berger, Navigant, EU Roadmap, Bloomberg, Mc Kinsey, NTL and others). Updates were added according to the last roadmaps from 2017 and 2018.

3. Demand Estimation (D5.4.2)

Penetration of DWPT-EVs on e-roads for the years 2030, 2040 and 2050 are provided, aligning them with the EV penetration roadmap. These deployment forecasts are gathered in Table 2 (Motorway), Table 3 (Periurban) and Table 4 (Urban) of the present report.

4.2.2 Unitary Costs

4. Infrastructure costs (D5.3.4)

Unitary cost (€/km) of new e-road infrastructure built using different constructive technologies from partners POLITO and SAET was analysed. These costs for the dynamic charging infrastructure are summarized in Table 68. Details for the calculation can be found in D5.3.4.

5. On-board equipment costs (D5.5.2)

A deep analysis was done to calculate the total cost of ownership (TCO) for DWPT-EVs owners. This information was used to implement the Cost-Benefit analysis (the balance made by the EVs owners in front of the decision to pay for a vehicle equipped with the DWPT technology). This information was key to determine the DWPT-EVs expected demand which was also the base for the business models.

FABRIC PROJECT LCCA Summary	MOTORWAY SCENARIO				PERIURBAN	URBAN
	POLITO		SAET		POLITO	POLITO
	2030-25 km	2050-25 km	2030-25 km	2050-25 km	2030-10 km	2030-27 km
PRESENT VALUES	e-Corridor	e-Road	e-Corridor	e-Road	e-Launcher	e-Trenches
R+D (E-Roads)	1,111,111	292,398	1,111,111	220,588	444,444	1,200,000
Project Planning and Engineering	4,240,525	1,989,153	4,206,505	1,993,236	1,839,072	4,579,767
Construction	48,943,361	31,402,003	49,083,694	31,458,095	23,521,175	52,858,830
Electric infrastructure and others	15,115,025	13,514,818	16,813,682	16,783,949	13,652,988	24,016,142
Operating Costs	6,872,547	6,872,547	6,369,498	6,369,498	4,426,533	6,590,737
Maintenance Costs	1,117,550	1,117,550	1,131,900	1,131,900	710,274	1,206,954
Renewal Costs	26,275	26,275	26,275	26,275	15,765	28,377
Disposal Costs	-9,217	2,514,124	2,452	2,525,793	-3,687	-9,955
User costs	0	10,796,797	0	10,818,966	0	11,660,541
TOTAL PRESENT VALUES	**77,417,177**	**68,525,665**	**78,745,118**	**71,328,301**	**44,606,564**	**102,131,394**
Real Value (per each of the 20 years)	4,719,335	4,251,670	4,808,334	4,416,207	2,752,954	6,004,187
Present Value (per each of the 20 years)	**3,870,859**	**3,426,283**	**3,937,256**	**3,566,415**	**2,230,328**	**5,106,570**
Present Value per km	**3,096,687**	**2,741,027**	**3,149,805**	**2,853,132**	**4,460,656**	**3,782,644**
Type of vehicles	88% e-DWPT light Vehicles and 12% e-Heavy vehicles				100% HV/Vans	100% Buses

Table 68. Summary cost table for the dynamic charging infrastructure in the three scenarios.

6. Business Models (D5.5.2)

Each selected reference scenario was analysed and three business models were prepared from the perspective of the e-Road infrastructure investor, to determine if the foreseen deployment scenarios for DWPT-EVs could justify the investments. The business models are fully described in D5.5.2. The main conclusion was that the urban scenario for buses is the most positive and likely the entry point for the technology in 2030 due to the special conditions of the bus lanes and frequent stops. The Periurban scenario is also interesting and could be profitable if some pre-agreements are signed between transport companies (owner of large fleets of heavy EVs) and the infrastructure investors. The battery-shrink strategy – a reduction of the battery size due to available DWPT infrastructure – might give some room for the technology uptake in trucks and intercity buses. Lastly, the motorway business model requires a critical mass of light EVs and some additional conditions that move the opportunity beyond 2050.

4.2.3 Global Analysis

7. Deployment in 3 scenarios (D5.5.2)

D5.5.2 included also a summary of the deployment scenarios (number of e-Roads and DWPT-EVs) in Europe for each scenario (Motorway, Periurban and Urban) for the years 2030, 2040 and 2050. Obtained numbers are summarised in Table 69.

E-Roads in Europe	2,030	2,040	2,050
Motorway	10	20	32
Periurban	80	200	400
Urban Bus	40	100	200
Total	**130**	**320**	**632**

Table 69. Cumulative e-Road deployment in Europe by type of scenario.

8. Grid Impact (D5.4.1)

D5.4.1 gathers also the grid impact at European level considering the deployed scenarios in terms of nominal power required and expected e-Road energy consumption. Some reference scenarios were considered with a number of daily DWPT-EVs per lane as a base for the calculation of energy and power requirements according to dynamic daily charging. Results are included in the three tables below (see Global cost calculations). This calculation assumes 12,000 EVs (88% light and 12% heavy) per day and charging lane in the motorway scenario, 3,600 EV (e-heavy) in the periurban scenario and 400 e-buses with 1,080 stops and 40 routes in the urban scenario for the reference case and then, there has been a extrapolation considering the number of vehicles crossing the e-roads predicted in the forecast DWPT penetration ratios (tables 70).

Motorway Scenario		2030	2040	2050	Reference
Nº of E-Corridors	units	10	10	12	
Nominal Power /E-Corridor	MVA	1.83	7.68	19.44	**25.00**
Unitary cost Grid section	€	342,255 €	1,390,843 €	3,446,904 €	**4,666,050 €**
Total cost Grid-all e-Corridors	Million €	3.42	13.91	41.36	**58.69**

Periurban Scenario		2030	2040	2050	Reference
Nº of E-Launchers	units	80	120	200	
Nominal Power /E-Launcher	MVA	2.21	4.83	8.47	9.84
Unitary cost Grid section	€	413,383 €	875,102 €	1,501,989 €	**1,866,420 €**
Total Cost Grid all e-Launchers	Million €	33.07	105.01	300.40	**438.48**

Urban Scenario		2030	2040	2050	Reference
Nº of Cities (e-Trenches)	units	40	60	100	
Nominal Power /E-City	MVA	25.00	25.00	25.00	25.00
Unitary cost Grid section/City	€	4,666,050 €	4,266,438 €	4,130,730 €	**4,855,172 €**
Total Cost Grid all cities	Million €	186.64	106.66	103.27	**396.57**

TOTAL DEPLOYMENT	Million €	223.14	225.58	445.03	893.75

Figure 60: Estimate of grid costs for the three scenarios.

9. Global cost calculation (D5.5.2, D5.4.1)

D5.5.2 presents the overall costs for the expected e-Roads to be deployed in Europe in the decades of 2030, 2040 and 2050.

Many of the data calculated in previous tables are now added to this final table to estimate the cost of the deployment process of e-Roads in Europe in the decades 2030, 2040 and 2050 considering that the assumptions listed in D5.5.2 are fulfilled.

In Table 70 energy and power requirements and global costs of expected e-Corridors (Motorway scenario – the less promising) are shown. In the last line, cumulated cost of the 32 e-Roads can be seen. The reference column represents the base scenario that was used to calculate the grid

needs (12,000 vehicles, 25 MVA). Notice that each column represents costs for installed e-roads within the given decade (2020-30, 2030-40 and 2040-50). These costs do not include cost of the grid infrastructure.

Motorway Scenario		**2,030**	**2,040**	**2,050**	**Reference**
Nº of DWPT Light Vehicles	units	832	3,345	8,211	10,560
Nº of DWPT Heavy Vehicles	units	49	342	1,120	1,440
Total Nº DWPT Vehicles	**units**	**880**	**3,688**	**9,331**	**12,000**
Nominal Power /E-Corridor	MVA	1.8	7.7	19.4	25
Consumption / E-Corridor year	MWh	4,016	16,824	42,574	54,750
Nº of E-Corridors (each decade)	units	10	10	12	
Costs per e-Corridor	M€	78.1	74.0	69.9	**Total**
Total Costs all e-Corridors Europe	**M€**	780.8	740.0	839.1	**2,360**

Table 70. Costs of expected e-Corridors in Europe in decades 2030, 2040 and 2050.

The Periurban scenario requires pre-agreement of the main stakeholders for ramp-up (owners of fleets of heavy EVs and infrastructure investors). A critical mass of heavy EVs (trucks and buses) need to charge daily on e-Launchers (close to logistic centres, ports, periurban roads, etc.), in order to obtain a positive business result.

Periurban Scenario		**2,030**	**2,040**	**2,050**	**Reference**
Nº of DWPT Heavy Vehicles	units	**810**	**1,768**	**3,098**	**3,600**
Nominal Power	MVA	2.2	4.8	8.5	10
Consumption	MWh	3,696	8,065	14,134	16,425
Nº of E-Launchers (each decade)	units	80	120	200	
Costs per e-Launcher	M€	44.4	42.1	39.8	**Total**
Total Costs all e-Launcher	**M€**	3,555.4	5,054.7	7,960.3	**16,570**

Table 71. Costs of expected e-Launchers in Europe in decades 2030, 2040 and 2050.

The urban scenario will be the first entry point. The business model (D5.5.2) reflects that in case the whole fleet of buses is switched to stationary-dynamic charging and all of them follow the battery-shrink strategy (reduction of battery size and consequently the cost of the e-bus), the model could be sustainable from the very beginning, resulting also in a great environmental advantage for the citizens. Dedicated bus lanes are very appropriate to set up the stationary-dynamic charging infrastructure specially if there is a tramway already in place in the city, due to synergies in the power distribution infrastructure, which is very similar to DWPT requirements.

Urban Scenario		**2,030**	**2,040**	**2,050**	**Reference**
Nº of DWPT Buses	units	**400**	**400**	**400**	**400**
Nominal Power	MVA	25.0	25.0	25.0	25
Consumption	MWh	70,956	70,956	70,956	70,956
Nº of cities with e-Trenches (each decade)	units	40	60	100	
Costs per e-cities (e-Trenches)	M€	102.1	96.8	91.5	**Total**
Total Costs all e-Cities (e-Trenches)	**M€**	4,085.3	5,807.9	9,146.6	**19,040**

Table 72. Cost of expected e-Trenches in Europe in decades 2030, 2040 and 2050.

As can be seen in Table 73, required investment to reach the target of 632 e-Roads (considering the three scenarios) reaches **EUR 37,970 million** over three decades.

TOTAL COSTS E-ROADS IN EUROPE		2,030	2,040	2,050	TOTAL
Nº of e-Roads (each decade)	units	130	190	312	632
Total Costs e-Roads Europe	**M€**	8,421.5	11,602.6	17,946.0	**37,970**

Table 73. Total Cost of e-Roads in Europe in decades 2030, 2040 and 2050.

10. Impact on Renewables (D5.4.1)

From the previous information, an analysis has been done in this report to show how energy requirements of e-roads can be covered by renewables sources.

The motorway scenario with at least two e-Corridors (one per direction) connected to the same microgrid, represent around 40 MVA in the most demanding scenario and around 85.000 MWh/year to be covered by renewables. It could be shown that in this case annual zero net energy can be obtained from renewable sources (PV or wind depending on location) without major problems. Self-consumption without additional storage is above 50% for solar PV in southern Europe, as demand pattern match availability of solar energy. With a storage for 24-h smoothing (remove intra-daily fluctuations), self consumption is drastically increased above 80% for solar in southern Europe. For wind power, self consumption is also increase by storage, but much less, not reaching 60% in any studied case.

The periurban infrastructure due to the lack of physical space for near-by renewable installations will be mostly covered by the current electricity mix from the grid (increasingly renewable though). In the most demanding scenario in 2050 and considering just four e-Launchers per city (a minimum number is required to encourage fleet owners to invest in on-board DWPT equipment), supposes around 34 MVA and 57 GWh/year. Compared to a typical energy consumption of a large city (750,000 inhabitants) of approximately 4.5 TWh/year (assuming 6 MWh/capita), this is less than 1.5%. The percentage may vary significantly by country. According to data from the World Bank [41], in northern European countries electricity consumption is above 10 MWh/capita (highest is 53 MWh/capita for Iceland), while lowest values of below 4 MWh/capita can be found in south-eastern Europe (lowest: Albania with 2.1 MWh/capita).

For the urban scenario, similar to the periurban case, energy is obtained from the grid, as no space for dedicated local generation is available. In the most demanding case (2050), with 25 additional MVA required, the extra consumption will reach 71 GWh/year, which is approximately 2% of the demand of a city with 750,000 inhabitants.

11. Impact on LCOE (D5.4.1)

Calculation of the impact on average LCOE (levelized cost of energy) for the European energy mix is included to reflect the economic impact considering the number of DWPT-EVs and the number of e-Roads.

The analysis of LCOE starts from the comparison of this value for different technologies. A recent report from Lazard [42] reflects the unsubsidised comparison between alternative and conventional generation technologies.

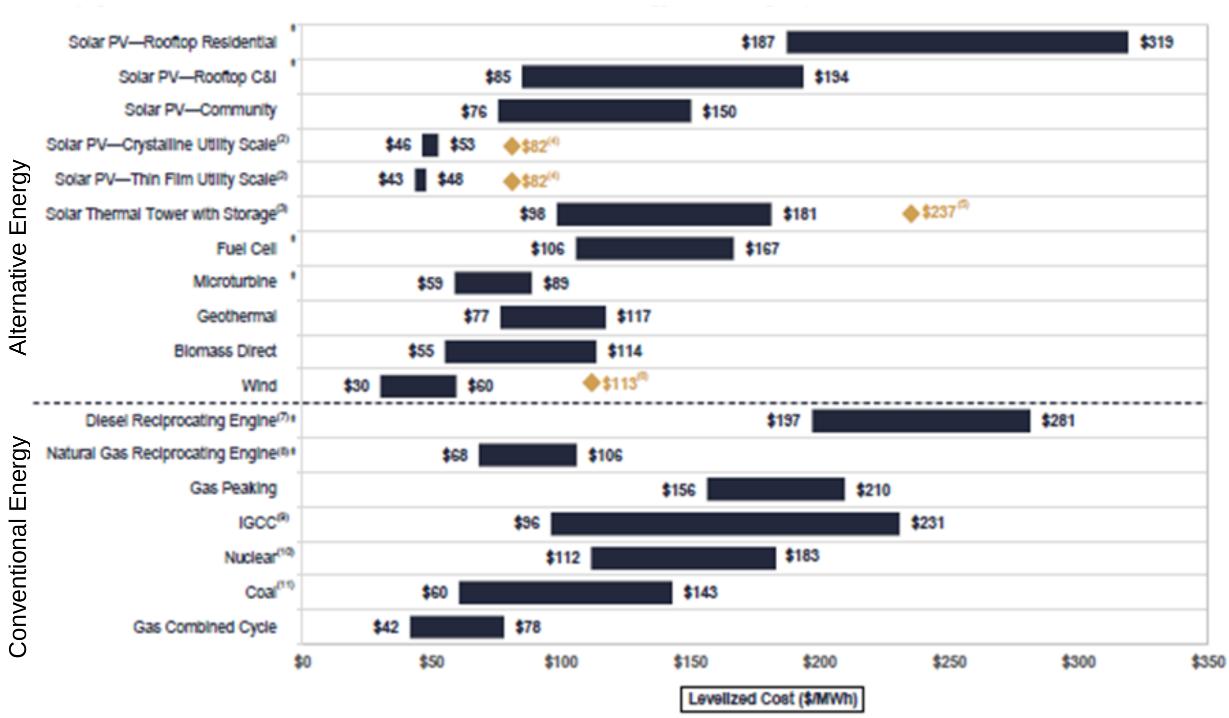

Figure 61: LCOE for different technologies before subsidies, according to [42].

Certain alternative energy generation technologies are cost-competitive with conventional generation technologies under some scenarios. This observation does not consider potential social and environmental externalities (e.g. social costs/benefits of distributed generation or environmental consequences of conventional generation), reliability or intermittency-related considerations (e.g. transmission and back-up generation costs associated with certain alternative energy technologies).

From the 9 GW new installed capacity only 0.6 GW could be assigned directly to on-site renewable installations (motorway scenario), representing between 6 to 10 Wind Farms or large PV arrays in 40 years. As a result, the energy mix will not suffer substantial variations in relation with the targets already in place for the increase of renewable generation capacity until 2030, reflected in Figure 62. In any case, no matter if the demand of the e-roads is fed by an integrated micro grid or from the main grid, expected demand pattern with a daily peak are favouring solar power integration, which will contribute to reduce system costs, as less daily balancing capacity is needed.

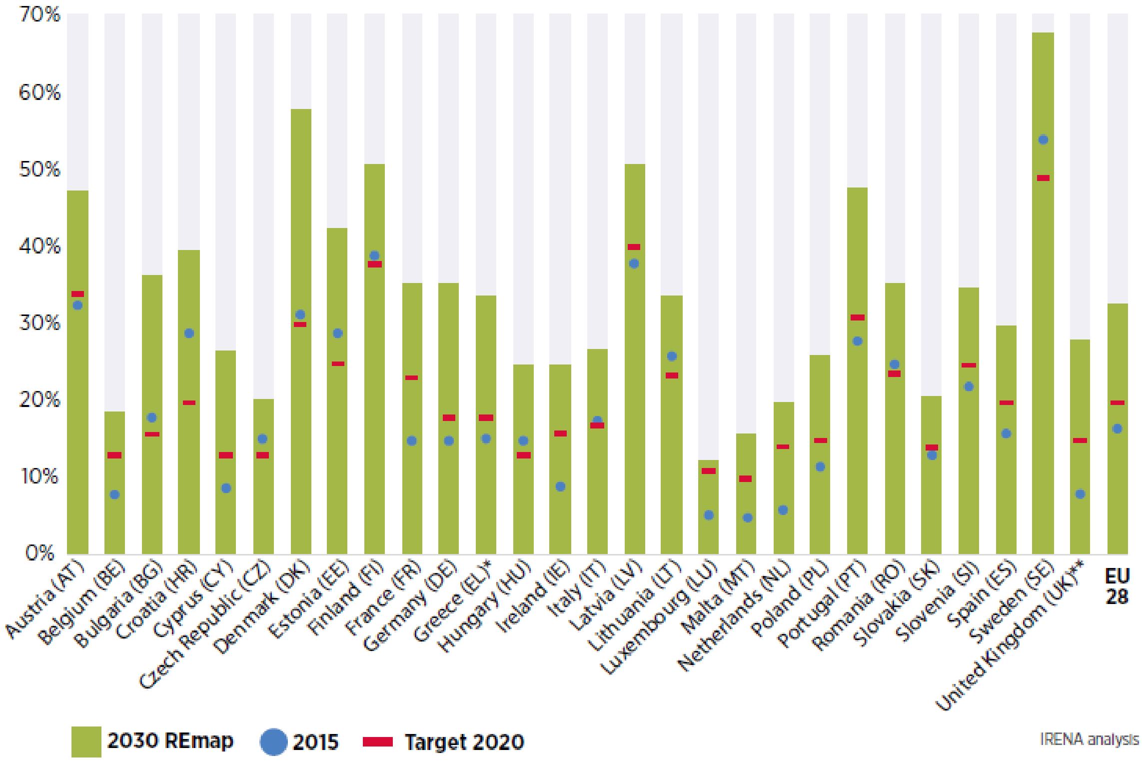

Figure 62: Renewable energy share in gross final energy consumption – 2015, 2020 target and 2030 potential with accelerated uptake of renewables (REmap) [43].

5 CONCLUSIONS

5.1 Vehicle level consequences of DWPT requirements

5.1.1 Vehicle performance model

In order to evaluate the vehicle level consequences of DWPT regarding WTW energy consumption and CO_2 emissions, a vehicle performance model has been developed. This model allows the comparison of conventional vehicles (equipped with ICE only), BEV and DWPT-EV. Reference values for conventional and BEV have been calculated for different driving scenarios and vehicle classes. Two basic DWPT scenarios have been implemented: “Battery-shrinking” and “Range-extension”. Global results revealed that reducing the battery size has more environmental benefits, as it reduces vehicle weight and thus, WTW energy consumption and CO_2 emissions. Nevertheless, range-extension (maintaining battery size) seems to be the more attractive business case.

In general, battery shrink DWPT-EV has shown to give better results than range-extend DWPT-EV for all considered vehicle class and driving scenarios. However, a sensitivity study carried out by reducing the battery price, shows that range extend DWPT-EV can be very promising in terms of TCO if battery price is going to be significantly reduced in the future. In addition, we should keep in mind that vehicle TCO figures reported in this section do not include the investment costs for infrastructure (e-road). Reduction of the battery size (according to battery shrink option) might imply more investment in e-roads and, especially at early stage of deployment, there could not be sufficient critical mass of DWPT-EV to justify such an extra investment. This means that range-extension DWPT-EV results should not be disregarded and should be further considered.

5.1.2 Specific results for reference scenarios motorway, periurban and urban bus

The vehicle performance model has been applied to the three identified business cases: motorway, periurban and urban bus. Both, battery-shrinking and range-extension scenarios have been analysed. Nevertheless, as viable business cases, range-extension has been identified for motorway and periurban (e-Corridors and e-Launchers) and battery-shrinking for urban bus.

For the motorway scenario, passenger cars show slightly increased CO_2 emissions compared to the BEV reference, while DWPT heavy duty trucks show slightly reduced energy consumption and CO_2 emissions. In all cases, TCO is higher, due to additional costs for DWPT. For passenger cars, an important potential for reduction of battery size has been identified, but it is considered unlikely, that private car owners would like to buy cars with smaller batteries.

The same conclusions apply for the periurban scenario, as only heavy vehicles are considered.

For urban buses, DWPT is found to be key for important reductions in battery size. In this case, range-extension is not justified. As a result, costs and environmental impacts of e-buses can be reduced which gives positive results for both, environmental and economic criteria.

5.1.3 Considerations regarding present and future WTW energy consumption and CO_2 emissions

For the estimation of WTW energy consumption of electric vehicles, it is important to consider the expected future electricity mix. Traditional thermal processes have low efficiencies between 30-50% which increase energy expended for each electric MJ (MJe) to the end consumer. For data from 2009, JRC calculated a coefficient of 1.95 MJ/MJe to be applied for electricity. Nevertheless, renewable energies have extremely low coefficients, typically 0.12, which is electricity transmission and distribution, assuming overall system efficiency of 89%. Main conclusion from these considerations is, that with a 40% reduction in energy expended per MJe (reduction from 1.95 to 1.17), all electric scenarios will show lower energy consumption on a WTW basis than the Diesel reference, including heavy vehicles, which turned out to consume up to 50% more energy in the case of range-extending DWPT.

5.2 Assessment of up-scaling on electricity grid

5.2.1 Energy and power requirements for DWPT

The impact on the electricity grid has two dimensions: energy and power. On the one hand, additional energy consumption needs to be supplied by the grid. On the other hand, specific load profiles might cause temporal grid congestions, if DWPT peak load is correlated with existing peak load. Therefore, in a first step, power and energy requirements have been assessed for the 3 scenarios: motorway, periurban and urban bus. Especially power requirements are important for sizing of transformer stations. Energy requirements in this stage, are related to the balance between energy consumption of the vehicle and energy supply form the DWPT infrastructure. Here, range extension and reduces battery sizes can be derived.

5.2.2 System-wide impact on electricity demand

In a second step, the system-wide impact on electricity demand is analysed. Main conclusion is, that, compared to existing electricity grid infrastructure, additional requirements from DWPT installations are low. Therefore, expected power and energy demand will be easily covered by existing installations. It is also observed, that DWPT demand profiles show similar patterns as general electricity demand, with diurnal peaks. A first conclusion is that electricity system demand peaks and ramps will be increased.

5.2.3 Impact on CO_2 emissions

A study on CO_2 emissions of EV adoption in general reveals that CO_2 intensity is expected to be reduced drastically until 2050, which means that additional electricity demand due to electrification of transport will have very positive impact on reduction of CO_2 emissions. Compared to the CO_2 intensity of 319 g/kWh for combustion engines (Diesel as reference), the electricity grid is currently slightly worse (2010: 380 g/kWh according to Eurostat). According to the EU roadmap for reduction of CO_2 emissions in the electricity sector, at latest by 2025, EU average emissions from electricity generation will be below the reference of Diesel fuel. It should also be mentioned, that EV fore-runners like Norway have especially low CO_2 intensity.

5.2.4 Integration of renewable sources and storage

Finally, a study has been carried out on the possibility of integration of renewable energy generation and storage, together with a DWPT system. The study case of motorways was chosen, as here, an integration within a mircogrid is considered feasible, as enough space is available. Here, the most important conclusion is the correlation between solar generation and DWPT consumption pattern. DWPT can be considered as beneficial for renewable energy integration, as recharging is moved from night to daylight hours. In order to cover the entire demand for DWPT infrastructure, as projected for 2050 (all 3 scenarios together), 10 GW of renewable generation will be needed, in order to obtain annual zero net energy balance on European level. This requirement can be considered as very low, compared to foreseen additions of renewable generation.

The analysis of energy storage for improving grid integration, revealed again the positive effect of daily pattern. With a 24-smoothing approach, fast demand ramps are avoided and the sharp evening peak, after sunset (so-called “Californian Duck Curve”), is mitigated completely. This solution would require storage capacity in the range of 150-400 MWh for each motorway (25 km), according to the location. In general, southern countries with high solar resources need less storage, as wind power requires more (less cyclic behaviour). This stationary storage capacity has been put into relation with DWPT clients. As a result, it was found, that not more than 0.25 kWh of additional storage is added to the system per DWPT client. In the most favourable case, only 0.11 kWh are needed in order to obtain 24-smoothing. Seasonal fluctuation need to be covered otherwise. Here, battery storage might not be the best solution. Calculations show that up to 5.5 additional kWh/client are needed in order to obtain an autonomous microgrid, compensation also seasonal fluctuations. This exercise has only been done for the motorway scenario. Similar results are expected for the periurban scenario. Patterns of urban bus demand are different and probably more storage would be needed. Nevertheless, expected reduction of

battery size for urban buses (20 kWh instead of 650 kWh), will more than compensate the difference.

5.3 Economic consequences of more electricity infrastructure and generation plants

The cost for additional grid requirements in terms of LV/MV and MV/LW transformer stations has been estimated to be approximately 900 million € for Europe in a period of 30 years. This is 0.006 % of 2017 EU GDP which was 15.3 billion €. In addition to the grid infrastructure it has been estimated how much RES capacity would be needed to compensate energy demand of 25 TWh in terms of annual zero net balance. It has been found that 10 GW of solar and wind power would be needed (assuming 25% capacity factor for RES). For better grid integration, storage of 150 – 400 MWh would be sufficient. Considering 2017 costs of 1.5 Million €/MW for onshore wind and 1.1 Million €/MW for photovoltaics, average of 1.3 Million €/MW is assumed. Installing 10 GW would then require investments of 13,000 Million € EU-wide in 20 years, something perfectly assumable. In the light of the European policy against climate change, 10 GW is a very small number anyway.

REFERENCES

[1] Ecologistas en Acción, “Los tranvías, una oportunidad para hacer nuestras ciudades más habitables,” 2010. [Online]. Available: https://www.ecologistasenaccion.org/article17546.html. [Accessed April 2018].

[2] S. J. Pachernegg, «A Closer Look at the Willans-Line,» SAE International, 1969.

[3] R. Finesso, E. Spessa y M. Venditti, «An Unsupervised Machine-Learning Technique for the Definition of a Rule-Based Control Strategy in a Complex HEV,» *SAE International Journal of Alternative Powertrains,* vol. 5, nº 2, pp. 308-327, 2016.

[4] R. Finesso, E. Spessa y M. Venditti, «Layout design and energetic analysis of a complex diesel parallel hybrid electric vehicle,» *Applied Energy,* vol. 134, pp. 573-588, 2014.

[5] J. B. Heywood, Internal combustion engine fundamentals, vol. 930, New York: Mcgrawhill, 1988.

[6] S. d’Ambrosio, R. Finesso y E. Spessa, «Calculation of mass emissions, oxygen mass fraction and thermal capacity of the inducted charge in SI and diesel engines from exhaust and intake gas analysis,» *Fuel,* vol. 90, nº 1, p. 152–166, 2011.

[7] R. Edwards, J.-F. Larivé, D. Rickered and W. Weindorf, “WELL-TO-TANK Appendix 2 - Version 4a, Summary of energy and GHG balance of individual pathways,” JRC Technical Reports, 2014.

[8] R. Graham, «Comparing the benefits and impacts of hybrid electric vehicle options,» EPRI, 2001.

[9] M. Delucchi, A. Burke, T. Lipman y M. Miller, «Electric and gasoline vehicle lifecycle cost and energy-use model,» Institute of Transportation Studies, 2000.

[10] T. Markel y A. Simpson, «Cost-benefit analysis of plug-in hybrid electric vehicle technology,» de *Proceedings of 22nd International electric vehicle symposium*, Yokohama, 2006.

[11] A. Moawad, P. Sharer y A. Rousseau, «Light-duty vehicle fuel consumption displacement potential up to 2045,» Argonne National Laboratory, 2013.

[12] L. Serrao, S. Onori, A. Sciarretta, Y. Guezennec y G. Rizzoni, «Optimal energy management of hybrid electric vehicles including battery aging,» de *IEEE American Control Conference*, San Francisco, 2011.

[13] Greenpeace, “100% Renewable Energy for All: Energy [r]evolution – A sustainable world energy outlook 2015, 5th Edition 2015 World Energy Scenario,” 2015.

[14] FABRIC, «D3.5.1 Architecture definition,» 2017.

[15] FABRIC, «D5.4.2 Report on Maturity, reliability, efficiency and stability of the supply chain» 2017.

[16] FABRIC, «D5.2.1 Feasibility study on societal perspectives towards on road charging and set of current data regarding societal dimension,» 2015.

[17] Ultra-E, “Ultra Charging Study Europe,” 2018. [Online]. Available: https://www.ultra-e.eu/. [Accessed April 2018].

[18] FABRIC, “D3.2.1 Technical and user requirements,” 2014.

[19] C. F. Daganzo, Fundamentals of Transportation and Traffic Operations, Emerald Group Publishing Limited, 1997.

[20] J. Green, R. Steinbach, A. Jones, P. Edwards, C. Kelly, J. Nellthorp, A. Goodman, H. Roberts, M. Petticrew and P. Wilkinson, “On the buses: a mixed-method evaluation of the impact of free bus travel for young people on the public health,” *Public Health Research,* vol. 2, no. 1, pp. 1-206, 2014.

[21] J. Setreus y L. Bertling, «Introduction to HVDC Technology for Reliable Electrical Power Systems,» de *Proceedings of the 10th International Conference on Probablistic Methods Applied to Power Systems*, Rincon, 2008.

[22] UNPLUGGED, “D3.2 Power grid power request and grid management strategies technical report,” 2014.

[23] M. Hyvärinen, Electrical networks and economies of load density, Helsinki: Helsinki University of Technology, 2008.

[24] Ministerio de Fomento de España, «The traffic on toll highways 2012 (El tráfico en las autopistas de peaje 2012),» 2013.

[25] UITP, “The international association of public transport operators,” [Online]. Available: www.uitp.org. [Accessed April 2018].

[26] J. M. Salanova, M. Estrada, G. Aifadopoulou y E. Mitsakis, «A review of the modeling of taxi services,» *Procedia - Social and Behavioral Sciences,* vol. 20, pp. 150-161, 2011.

[27] CENIT, «Metodologia per a l'establiment de les tarifes del taxi a l'AMB i la seva revisió, 2004. Informe final per a l'Institut Metropolità del Taxi,» 2004.

[28] City of Zaragoza, «Zaragoza City Information: Taxi Service,» 2018. [En línea]. Available: https://www.soydezaragoza.es/taxis-de-zaragoza/.

[29] Y. Li, H. Chen, Y. Yang, Z. Guo y F. He, «Electrifying the Urban Taxi Fleet: A Data-driven Approach,» *Submitted to Transportation Research Part D: Transport and Environment (Dec. 2017),* 2017.

[30] A. Merkisz-Guranowska y M. Maciejewski, «The Implementation Of The Electric Taxi Fleet In The City Of Poznan, Poland,» *WIT Transactions on The Built Environment,* vol. 146, pp. 243-254, 2015.

[31] BNEF, “Electric vehicles to be 35% of global new car sales by 2040,” Press Release, 2016.

[32] M. Liebreich, «BNEF Summit Keynote,» April 2017. [En línea]. Available: https://data.bloomberglp.com/bnef/sites/14/2017/04/2017-04-25-Michael-Liebreich-BNEFSummit-Keynote.pdf. [Último acceso: April 2018].

[33] BNEF, «BNEF Electric Vehicle Outlook (EVO 2017 Report),» 2017.

[34] Eurostat, «Eurostat,» [En línea]. Available: http://ec.europa.eu/eurostat/web/main/home. [Último acceso: April 2018].

[35] California ISO, «What the duck curve tells us about,» 2013. [En línea]. Available: https://www.caiso.com/Documents/FlexibleResourcesHelpRenewables_FastFacts.pdf. [Último acceso: May 2018].

[36] Tomorrow, «Electricity Map,» Tomorrow, 2018. [En línea]. Available: https://www.electricitymap.org. [Último acceso: April 2018].

[37] European Commission, «A Roadmap for moving to a competitive low carbon economy in 2050,» 2011.

[38] European Commission, “2050 low-carbon economy,” [Online]. Available: https://ec.europa.eu/clima/policies/strategies/2050_en. [Accessed April 2018].

[39] European Commission, «EU Reference Scenario 2016, Energy, transport and GHG emissions Trends to 2050,» 2016.

[40] JRC, «PVGIS,» JRC, [En línea]. Available: http://re.jrc.ec.europa.eu/pvgis/. [Último acceso: April 2018].

[41] Wold Bank, «Electric power consumption (kWh per capita),» [En línea]. Available: https://data.worldbank.org/indicator/EG.USE.ELEC.KH.PC?name_desc=false. [Último acceso: April 2018].

[42] Lazard, «Lazard's Levelized Cost of Energy Analysis — Version 11.0,» November 2017. [En línea]. Available:

https://data.worldbank.org/indicator/EG.USE.ELEC.KH.PC?name_desc=false. [Último acceso: April 2018].

[43] IRENA, «Renewable Energy Prospects for the European Union,» February 2018. [En línea]. Available: http://www.irena.org/publications/2018/Feb/Renewable-energy-prospects-for-the-EU. [Último acceso: April 2018].

[44] CEER, «5th Benchmarking report on the quality of electricity supply,» CEER, 2011.

[45] CEER, «4th benchmarking report on quality of electricity supply,» CEER, Bruxelles, 2008.

[46] M. Moschakis, E. Karfopoulos, E. Zountouridou y S. Papathanasiou, «On adaptation of electric vehicle and microgrid issues to emc, power quality standards,» IEEE, Athens, 2012.

[47] UNECE, «Proposal for an Electric Vehicle regulatory reference guide,» United Nations, Geneva, 2014.

[48] A. Ruddle y R. Armstrong, «Current EMC standards and gaps detected regarding FEVs,» HEMIS consortium, Heslington, 2013.

[49] bdew, «Generating plants connected to the medium voltage network,» bdew, Berlin, 2008.

[50] R. Electrica, «Draft Technical Guidelines for Wind and Photovoltaic Power Plants Connected Directly to the Distribution and Transmission Network: Minimum Requirements of Design, Equipment, Operation, Setting in Service and Security,,» Red Electica, 2009.

[51] «Royal Decree 1565/2010 Means of Which Certain Aspects of the Production of Energy under the Special Regime are Modified,» 2010.

[52] National Grid Electricity Transmission, «Great Britain National Grid Code (Issue 4 Revision 5),» 2011.

[53] «Technical Prescriptions for Conception and Performance of the Connection to a Public Electricity Distribution Network of an Electric Energy Production Installation,» 2010.

[54] C. Nolle, E. Rodriguez, D. Dragomir y I. Papaioannou, «D3.2 Standardization analysis,» STARGRID, 2014.

[55] A. Amditis y E. Portouli, «PowerUp Final V2G Architecture,» Athens, 2012.

[56] A. Klajn y M. Batkkewicz, «Application Note: Standard EN 50160 voltage characteristics of Electricity supplied by public electricity networks,» European Copper Institute, 2013.

[57] CEN-CENELEC-ETSI, «Functional reference architecture for communications in smart metering systems,» CEN-CENELEC-ETSI, 2011.

[58] Smart Energy Demand Coalition, «Maping Demand Response in Europe Today,» Smart Energy Demand Coalition, 2014.

[59] J. Lopes, F. Soares y P. Almeida, «Integration of Electric Vehicles in the Electric Power System,» de *Proceedings of the IEEE*, 2011.

[60] S. Hadley, «Impact of plug-in hybrid vehicles on the electric grid,» Oak Ridge National Laboratory, 2006.

[61] J. Carrasco, L. Franquelo, J. Bialasiewicz, E. Galvan, R. Guisado, M. Prats, J. Leon y N. Moreno-Alfonso, «Power-Electronic Systems for the Grid Integration of Renewable Energy Sources: A Survey,» *Industrial Electronics, IEEE Transactions on,* vol. 53, nº 4, pp. 1002-1016, 2006.

[62] S. Bai, D. Yu y S. Lukic, «Optimum design of an EV/PHEV charging station with DC bus and storage system,» de *IEEE Energy Conversion Congress and Exposition (ECCE)*, 2010.

[63] S. Wang, R. Crosier y Y. Chu, «Investigating the power architectures and circuit topologies for megawatt superfast electric vehicle charging stations with enhanced grid support functionality,» de *IEEE International Electric Vehicle Conference (IEVC)*, 2012.

[64] G. Reed, B. Grainger, A. Sparacino, R. Kerestes y M. Korytowski, «Advancements in medium voltage DC architecture development with applications for powering electric vehicle charging stations,» de *IEEE Energytech*, 2012.

[65] C. Jin, X. Sheng y P. Ghosh, «Optimized Electric Vehicle Charging With Intermittent Renewable Energy Sources,» *IEEE Journal of Selected Topics in Signal Processing,* vol. 8, nº 6, pp. 1063-1072, 2014.

[66] C. Jin, X. Sheng y P. Ghosh, «Energy efficient algorithms for Electric Vehicle charging with intermittent renewable energy sources,» de *IEEE Power and Energy Society General Meeting (PES)*, 2013.

[67] H. Guillou, D. L. Ha, V.-D. Cung y M. Jacomino, «Power allocation problem in charging electric vehicles with photovoltaic production,» de *8th International Conference on Supply Chain Management and Information Systems (SCMIS)*, 2010.

[68] Nesscap, «Nesscap Ultracapacitors,» [En línea]. Available: http://www.nesscap.com/ultracapacitor/EDLC/Supercapacitor/high_voltage_supercapacitor_module.jsp. [Último acceso: 15 01 2015].

[69] Eurelectric, «Power distribution in Europe,» Eurelectric, [En línea]. Available: http://www.eurelectric.org/powerdistributionineurope/. [Último acceso: 15 01 2015].

[70] FABRIC, «D5.3.4 Detailed LCA/LCC assessment of environment and cost impact of E-roads» 2018.

[71] FABRIC, «D5.5.2 Cost-benefit analysis and business models of large-scale deployment of on-road charging» 2018.

ANNEX A: TABLES FOR VEHICLE PERFORMANCE MODEL

	vclsNm	cyc	EC wtt [Wh/km]	EC ttw [Wh/km]	EC wtw [Wh/km]	CO2wtt [g/km]	CO2ttw [g/km]	CO2wtw [g/km]	TCO [k€]	batMass [kg]	BES [kWh]
Conventional	suv	amdc	115	576	691	32	144	175	49	-	-
SUV	suv	audc	160	798	958	44	199	243	55	-	-
Diesel	suv	clust7	87	433	520	24	108	132	45	-	-
	suv	clust8	105	524	629	29	131	160	47	-	-
	suv	j1015m	112	558	670	31	139	170	48	-	-
	suv	nedc	99	494	592	27	123	150	47	-	-
	suv	wltp3	102	508	609	28	127	155	47	-	-
Conventional	suv	amdc	108	601	710	30	146	176	51	-	-
SUV	suv	audc	150	831	981	41	202	243	59	-	-
Gasoline	suv	clust7	79	441	520	22	107	129	46	-	-
	suv	clust8	99	548	647	27	133	160	49	-	-
	suv	j1015m	103	571	674	28	139	167	50	-	-
	suv	nedc	91	504	594	25	122	147	48	-	-
	suv	wltp3	94	522	615	26	127	153	48	-	-
BEV SUV	suv	amdc	486	249	735	122	0	122	55	373	89
AER 400 km	suv	audc	412	211	623	103	0	103	53	373	89
	suv	clust7	286	146	432	72	0	72	49	373	89
	suv	clust8	427	219	646	107	0	107	53	373	89
	suv	j1015m	293	150	443	73	0	73	49	373	89
	suv	nedc	307	157	464	77	0	77	50	373	89
	suv	wltp3	359	184	542	90	0	90	51	373	89
Conventional	hdv	cbd	587	2935	3522	163	732	895	536	-	-
HDV	hdv	csc	555	2773	3327	154	691	845	522	-	-
Diesel	hdv	etc	553	2764	3317	153	689	842	521	-	-
	hdv	hdudds	636	3179	3815	176	793	969	558	-	-
	hdv	hwm	667	3334	4001	185	831	1016	571	-	-
	hdv	whvc	542	2709	3250	150	675	826	516	-	-
		average	599	2996	3596	166	747	913	542	-	-
BEV HDV	hdv	cbd	2081	1067	3149	522	0	522	428	1749	417
AER 250 km	hdv	csc	2174	1115	3289	545	0	545	452	1749	417
	hdv	etc	2843	1458	4301	713	0	713	511	1749	417
	hdv	hdudds	2921	1498	4419	732	0	732	519	1749	417
	hdv	hwm	3630	1861	5491	910	0	910	604	2156	514
	hdv	whvc	2567	1316	3884	644	0	644	488	1749	417
		average	2990	1533	4524	750	0	750	531	1850	441
Conventional	bus	etc	444	2220	2664	123	554	677	351	-	-
BUS	bus	mbc	763	3817	4580	212	952	1163	490	-	-
Diesel	bus	sort3	597	2987	3584	166	745	910	418		
	bus	nybus	1025	5127	6152	284	1278	1563	605	-	-
BEV BUS	bus	etc	2194	1125	3319	550	0	550	374	1399	334
AER 250 km	bus	mbc	2518	1291	3809	631	0	631	402	1399	334
(325 km for	bus	sort3	2257	1157	3415	566	0	566	401	1818	434
sort3)	bus	nybus	3193	1638	4831	801	0	801	460	1399	334

Table 74: Reference cases – absolute values.

Simulation results Motorway

	vclsNm	cyc	EC wtt [Wh/km]	EC ttw [Wh/km]	EC wtw [Wh/km]	CO2wtt [g/km]	CO2ttw [g/km]	CO2wtw [g/km]	TCO [k€]	batMass [kg]	BES [kWh]
P 50 [kW]	suv	amdc	527	270	797	132	0	132	56.979	373	89.0
V charge 60 [km/h]	suv	audc	492	252	744	123	0	123	55.831	373	89.0
L 25 [km]	suv	clust7	373	191	565	94	0	94	52.353	373	89.0
delta 6.25 [%]	suv	clust8	481	247	728	121	0	121	55.550	373	89.0
	suv	j1015m	367	188	556	92	0	92	52.179	373	89.0
	suv	nedc	354	182	536	89	0	89	51.796	373	89.0
Range extender	suv	wltp3	391	200	591	98	0	98	52.959	373	89.0
P 50 [kW]	suv	amdc	527	270	797	132	0	132	56.979	373	89.0
V charge 80 [km/h]	suv	audc	492	252	744	123	0	123	55.831	373	89.0
L 25 [km]	suv	clust7	373	191	565	94	0	94	52.353	373	89.0
delta 6.25 [%]	suv	clust8	481	247	728	121	0	121	55.550	373	89.0
	suv	j1015m	367	188	556	92	0	92	52.179	373	89.0
	suv	nedc	354	182	536	89	0	89	51.796	373	89.0
Range extender	suv	wltp3	391	200	591	98	0	98	52.959	373	89.0
P 50 [kW]	suv	amdc	527	270	797	132	0	132	56.979	373	89.0
V charge 100 [km/h]	suv	audc	492	252	744	123	0	123	55.831	373	89.0
L 25 [km]	suv	clust7	373	191	565	94	0	94	52.353	373	89.0
delta 6.25 [%]	suv	clust8	481	247	728	121	0	121	55.550	373	89.0
	suv	j1015m	367	188	556	92	0	92	52.179	373	89.0
	suv	nedc	354	182	536	89	0	89	51.796	373	89.0
Range extender	suv	wltp3	391	200	591	98	0	98	52.959	373	89.0

Table 75: Motorway SUV – Range extender.

	vclsNm	cyc	EC wtt [Wh/km]	EC ttw [Wh/km]	EC wtw [Wh/km]	CO2wtt [g/km]	CO2ttw [g/km]	CO2wtw [g/km]	TCO [k€]	batMass [kg]	BES [kWh]
P 50 [kW]	suv	amdc	497	255	753	125	0	125	52.200	283	67.4
V charge 60 [km/h]	suv	audc	446	229	675	112	0	112	50.370	283	67.4
L 0.125[km]	suv	clust7	310	159	468	78	0	78	46.310	283	67.4
delta 6.25 [%]	suv	clust8	441	226	666	110	0	110	50.569	283	67.4
	suv	j1015m	380	195	575	95	0	95	48.383	283	67.4
	suv	nedc	330	169	499	83	0	83	46.991	283	67.4
Battery shrinking	suv	wltp3	377	193	571	95	0	95	48.544	283	67.4
P 50 [kW]	suv	amdc	500	256	756	125	0	125	53.287	306	72.9
V charge 80 [km/h]	suv	audc	450	231	681	113	0	113	51.537	306	72.9
L 0.125 [km]	suv	clust7	312	160	472	78	0	78	47.439	306	72.9
delta 6.25 [%]	suv	clust8	443	227	670	111	0	111	51.633	306	72.9
	suv	j1015m	383	197	580	96	0	96	49.536	306	72.9
	suv	nedc	332	170	502	83	0	83	48.081	306	72.9
Battery shrinking	suv	wltp3	380	195	575	95	0	95	49.615	306	72.9
P 50 [kW]	suv	amdc	501	257	758	126	0	126	53.940	320	76.2
V charge 100 [km/h]	suv	audc	453	232	685	114	0	114	52.230	320	76.2
L 0.125 [km]	suv	clust7	313	161	474	79	0	79	48.112	320	76.2
delta 6.25 [%]	suv	clust8	444	228	672	111	0	111	52.280	320	76.2
	suv	j1015m	385	197	582	97	0	97	50.222	320	76.2
	suv	nedc	333	171	504	84	0	84	48.719	320	76.2
Battery shrinking	suv	wltp3	381	196	577	96	0	96	50.265	320	76.2

Table 76: Motorway SUV – Battery shrinking.

	vclsNm	cyc	EC wtt [Wh/km]	EC ttw [Wh/km]	EC wtw [Wh/km]	CO2wtt [g/km]	CO2ttw [g/km]	CO2wtw [g/km]	TCO [k€]	batMass [kg]	BES [kWh]
P 100 [kW]	hdv	cbd	2177	1117	3294	546	0	546	440.54	1749	417
V charge 60 [km/h]	hdv	csc	2315	1187	3503	581	0	581	469.46	1749	417
L 25 [km]	hdv	etc	2830	1451	4282	710	0	710	514.60	1749	417
delta 6.25 [%]	hdv	hdudds	3120	1600	4721	783	0	783	541.09	1749	417
	hdv	hwm	3600	1846	5446	903	0	903	605.70	2157	514
	hdv	whvc	2579	1323	3902	647	0	647	493.22	1749	417
Range extender		average	3184	1633	4816	798	0	798	553.79	1885	449
P 100 [kW]	hdv	cbd	2177	1117	3294	546	0	546	440.54	1749	417
V charge 80 [km/h]	hdv	csc	2315	1187	3503	581	0	581	469.46	1749	417
L 25 [km]	hdv	etc	2830	1451	4282	710	0	710	514.60	1749	417
delta 6.25 [%]	hdv	hdudds	3120	1600	4721	783	0	783	541.09	1749	417
	hdv	hwm	3600	1846	5446	903	0	903	605.70	2157	514
Range extender	hdv	whvc	2579	1323	3902	647	0	647	493.22	1749	417

Table 77: Motorway HDV – Range extender.

	vclsNm	cyc	EC wtt [Wh/km]	EC ttw [Wh/km]	EC wtw [Wh/km]	CO2wtt [g/km]	CO2ttw [g/km]	CO2wtw [g/km]	TCO [k€]	batMass [kg]	BES [kWh]
P 100 [kW]	hdv	cbd	2164	1110	3274	543	0	543	450.55	1647	393
V charge 60 [km/h]	hdv	csc	2204	1130	3334	553	0	553	454.64	1647	393
L 0.125 [km]	hdv	etc	2831	1452	4284	710	0	710	510.10	1647	393
delta 6.25 [%]	hdv	hdudds	2894	1484	4379	726	0	726	516.02	1647	393
	hdv	hwm	3578	1835	5412	897	0	897	599.19	2058	491
Battery shrinking	hdv	whvc	2569	1317	3886	644	0	644	487.61	1647	393
P 100 [kW]	hdv	cbd	2168	1112	3280	544	0	544	452.19	1676	400
V charge 80 [km/h]	hdv	csc	2207	1132	3339	553	0	553	456.23	1676	400
L 0.125 [km]	hdv	etc	2834	1453	4287	711	0	711	511.59	1676	400
delta 6.25 [%]	hdv	hdudds	2897	1486	4383	727	0	727	517.59	1676	400
	hdv	hwm	3579	1836	5415	898	0	898	600.65	2086	497
Battery shrinking	hdv	whvc	2571	1318	3890	645	0	645	489.13	1676	400

Table 78: Motorway HDV – Battery shrinking.

vclsType	Reference vehicle	cyc	EC wtt [Wh/km]	EC ttw [Wh/km]	EC wtw [Wh/km]	CO2wtt [g/km]	CO2ttw [g/km]	CO2wtw [g/km]	TCO [k€]	batMass [kg]	BES [kWh]
Passenger Car	BEV400	amdc	486	249	735	122	0	122	54.955	373	89.0
	Gasoline	amdc	108	601	710	30	146	176	50.970	-	-
	Diesel	amdc	115	576	691	32	144	175	49.007	-	-
	RE400	amdc	527	270	797	132	0	132	56.979	373	89.0
Heavy duty trucks	BEV250	hwm	3630	1861	5491	910	0	910	604.230	2156	514.2
	Diesel	hwm	667	3334	4001	185	831	1016	571.105	-	-
	RE250	hwm	3600	1846	5446	903	0	903	605.696	2157	514.2

Table 79: Summary Motorway, range extender – Reference Vehicles.

vclsType	P_er [kW]	V_er [km/h]	ΔEC wtt [Wh/km]	ΔEC ttw [Wh/km]	ΔEC wtw [Wh/km]	ΔCO2wtt [g/km]	ΔCO2ttw [g/km]	ΔCO2wtw [g/km]	ΔTCO [k€]	ΔbatMass [kg]	ΔBES [kWh]
Passenger car	50	60	11.8	6.1	17.9	3.0	0.0	3.0	-2.755	-90.5	-21.6
		80	14.3	7.3	21.6	3.6	0.0	3.6	-1.668	-67.4	-16.1
		100	15.7	8.1	23.8	3.9	0.0	3.9	-1.015	-53.6	-12.8
Heavy duty trucks	100	60	-52.3	-26.8	-79.2	-13.1	0.0	-13.1	-5.045	-98.7	-23.5
		80	-50.5	-25.9	-76.4	-12.7	0.0	-12.7	-3.584	-69.9	-16.7

Table 80: Summary Motorway, range extender – DWPT Results.

Simulation results Periurban

	vclsNm	cyc	EC wtt [Wh/km]	EC ttw [Wh/km]	EC wtw [Wh/km]	CO2wtt [g/km]	CO2ttw [g/km]	CO2wtw [g/km]	TCO [k€]	batMass [kg]	BES [kWh]
P 100 [kW]	hdv	cbd	2149	1102	3251	539	0	539	438.06	1749	417
V charge 60 [km/h]	hdv	csc	2297	1178	3475	576	0	576	467.82	1749	417
L 10 [km]	hdv	etc	2823	1448	4271	708	0	708	513.95	1749	417
delta 4 [%]	hdv	hdudds	3094	1587	4681	776	0	776	538.75	1749	417
	hdv	hwm	3593	1843	5436	901	0	901	605.13	2157	514
Range extender	hdv	whvc	2571	1319	3890	645	0	645	492.52	1749	417
			3020	1549	4569	757	0	757	537.59	1851	441
P 100 [kW]	hdv	cbd	2149	1102	3251	539	0	539	438.06	1749	417
V charge 80 [km/h]	hdv	csc	2297	1178	3475	576	0	576	467.82	1749	417
L 10 [km]	hdv	etc	2823	1448	4271	708	0	708	513.95	1749	417
delta 4 [%]	hdv	hdudds	3094	1587	4681	776	0	776	538.75	1749	417
	hdv	hwm	3593	1843	5436	901	0	901	605.13	2157	514
Range extender	hdv	whvc	2571	1319	3890	645	0	645	492.52	1749	417

Table 81: Periurban HDV – Range extender.

	vclsNm	cyc	EC wtt [Wh/km]	EC ttw [Wh/km]	EC wtw [Wh/km]	CO2wtt [g/km]	CO2ttw [g/km]	CO2wtw [g/km]	TCO [k€]	batMass [kg]	BES [kWh]
P 100 [kW]	hdv	cbd	2150	1103	3253	539	0	539	450.92	1684	401
V charge 60 [km/h]	hdv	csc	2181	1119	3300	547	0	547	454.25	1684	401
L 0.05 [km]	hdv	etc	2817	1445	4262	707	0	707	510.50	1684	401
delta 4 [%]	hdv	hdudds	2884	1479	4363	723	0	723	516.77	1684	401
	hdv	hwm	3574	1833	5406	896	0	896	600.47	2093	499
Battery shrinking	hdv	whvc	2560	1313	3872	642	0	642	488.48	1684	401
		average	2959	1517	4476	742	0	742	529.05	1786	426
P 100 [kW]	hdv	cbd	2152	1104	3256	540	0	540	436.20	1702	406
V charge 80 [km/h]	hdv	csc	2183	1120	3303	548	0	548	455.27	1702	406
L 0.05 [km]	hdv	etc	2819	1446	4264	707	0	707	511.45	1702	406
delta 4 [%]	hdv	hdudds	2886	1480	4366	724	0	724	517.78	1702	406
	hdv	hwm	3575	1833	5408	896	0	896	601.40	2112	504
Battery shrinking	hdv	whvc	2561	1313	3875	642	0	642	489.45	1702	406
		average	2960	1518	4478	742	0	742	530	1804	430

Table 82: Periurban HDV – Battery shrinking.

vclsType	Reference vehicle	cyc	EC wtt [Wh/km]	EC ttw [Wh/km]	EC wtw [Wh/km]	CO2wtt [g/km]	CO2ttw [g/km]	CO2wtw [g/km]	TCO [k€]	batMass [kg]	BES [kWh]
Heavy duty trucks	BEV250	hwm	2990	1533	4524	750	0	750	530.605	1850	441.2
	Diesel	hwm	599	2996	3596	166	747	913	541.557	-	-
	RE250	hwm	3020	1549	4569	757	0	757	537.589	1851	441.3

Table 83: Summary Periurban, range extender – Reference Vehicles.

vclsType	P_er [kW]	V_er [km/h]	ΔEC wtt [Wh/km]	ΔEC ttw [Wh/km]	ΔEC wtw [Wh/km]	ΔCO2wtt [g/km]	ΔCO2ttw [g/km]	ΔCO2wtw [g/km]	ΔTCO [k€]	ΔbatMass [kg]	ΔBES [kWh]
Heavy duty trucks	100	60	-31	-16	-48	-8	0	-7.9	-1.550	-64.5	-15
		80	-30	-15	-45	-8	0	-7.5	-0.582	-46.1	-11

Table 84: Summary Periurban, range extender – DWPT Results.

Simulation results Urban Bus

	vcls Nm	cyc	EC wtt [Wh/km]	EC ttw [Wh/km]	EC wtw [Wh/km]	CO2wtt [g/km]	CO2ttw [g/km]	CO2wtw [g/km]	TCO [k€]	batMass [kg]	BES [kWh]
P 50 [kW]	bus	etc	2190	1123	3313	549	0	549	383.68	1819	434
V charge 18 [km/h]	bus	mbc	2537	1301	3839	636	0	636	433.48	1819	434
L 0.3 [km], delta 100 [%]	bus	nybus	3277	1681	4958	822	0	822	498.04	1819	434
Range extender	bus	sort3	2216	1136	3352	556	0	556	385.98	1819	434
P 50 [kW]	bus	etc	2087	1070	3157	523	0	523	331.70	188	45
V charge 18 [km/h]	bus	mbc	2287	1173	3460	574	0	574	351.78	188	45
L 0.3 [km], delta 100 [%]	bus	nybus	2948	1512	4460	739	0	739	417.34	188	45
Battery shrinking	bus	sort3	2924	1499	4423	733	0	733	411.68	188	45

Table 85: Urban Bus – 50 kW, continuous DWPT.

	vcls Nm	cyc	EC wtt [Wh/km]	EC ttw [Wh/km]	EC wtw [Wh/km]	CO2wtt [g/km]	CO2ttw [g/km]	CO2wtw [g/km]	TCO [k€]	batMass [kg]	BES [kWh]
P 100 [kW]	bus	etc	2230	1143	3373	559	0	559	387.20	1819	434
V charge 3 [km/h]	bus	mbc	2854	1464	4318	716	0	716	459.91	1819	434
L 0.025 [km], delta 7.5 [%]	bus	nybus	4005	2054	6058	1004	0	1004	560.97	1819	434
Range extender	bus	sort3	2342	1201	3544	587	0	587	414.13	1819	434
P 100 [kW]	bus	etc	2121	1088	3209	532	0	532	334.68	188	45
V charge 3 [km/h]	bus	mbc	2674	1371	4045	671	0	671	388.42	188	45
L 0.025 [km], delta 7.5 [%]	bus	nybus	3665	1880	5545	919	0	919	484.49	188	45
Battery shrinking	bus	sort3	2364	1213	3577	593	0	593	356.48	188	45

Table 86: Urban Bus – 100 kW, 25m e-Trench at bus stops (dynamic/stationary).

	vcls Nm	cyc	EC wtt [Wh/km]	EC ttw [Wh/km]	EC wtw [Wh/km]	CO2wtt [g/km]	CO2ttw [g/km]	CO2wtw [g/km]	TCO [k€]	batMass [kg]	BES [kWh]
P 150 [kW]	bus	etc	2208	1132	3340	554	0	554	385.28	1819	434
V charge 2.26 [km/h]	bus	mbc	2561	1313	3875	642	0	642	435.48	1819	434
L 0.011 [km], delta 3.3 [%]	bus	nybus	3209	1646	4855	805	0	805	491.93	1819	434
Range extender	bus	sort3	2380	1221	3600	597	0	597	417.42	1819	434
P 150 [kW]	bus	etc	2103	1079	3182	527	0	527	333.11	188	45
V charge 2.26 [km/h]	bus	mbc	2307	1183	3491	579	0	579	353.32	188	45
L 0.011 [km], delta 3.3 [%]	bus	nybus	2880	1477	4357	722	0	722	411.00	188	45
Battery shrinking	bus	sort3	2469	1266	3735	619	0	619	366.49	188	45

Table 87: Urban Bus – 150 kW, 10m e-Trench at bus stops (stationary).

vclsType	Reference vehicle	cyc	EC wtt [Wh/km]	EC ttw [Wh/km]	EC wtw [Wh/km]	CO2wtt [g/km]	CO2ttw [g/km]	CO2wtw [g/km]	TCO [k€]	batMass [kg]	BES [kWh]
	BEV325	sort3	2257	1157	3415	566	0	566	400.801	1818	433.6
Bus	Diesel	sort3	597	2987	3584	166	745	910	417.662	-	-
	RE325	sort3	2216	1136	3352	556	0	556	414.128	1819	433.7

Table 88: Summary Urban Bus, Battery shrinking – Reference Vehicles.

vclsType	P_er [kW]	V_er [km/h]	ΔEC wtt [Wh/km]	ΔEC ttw [Wh/km]	ΔEC wtw [Wh/km]	ΔCO2wtt [g/km]	ΔCO2ttw [g/km]	ΔCO2wtw [g/km]	ΔTCO [k€]	ΔbatMass [kg]	ΔBES [kWh]
	50	18	667	342	1008	167	0	167	10.884	-1630	-389
Bus	100	3	107	55	162	27	0	27	-44.325	-1630	-389
	150	2.26	212	109	321	53	0	53	-34.307	-1630	-389

Table 89: Summary Urban Bus, Battery shrinking – DWPT Results.

ANNEX B: TABLES FOR STORAGE INTEGRATION

This Annex is related to results presented in section 3.6.4 Integration of storage. Several smoothing intervals were considered, considering the use of storage (ESS) as a low-pass filter (applying a moving average) with the aim of reducing variability and increasing predictability of grid exchange. Results are assuming storage round-trip efficiency of 96%.

All tables contain the following results:

- ww (h): Smoothing window width
- Pss (MW): nominal installed power of the ESS
- Ess (MWh): nominal energy capacity of the ESS
- Tss (h): Discharge time of the ESS at nominal power
- Thrpt (GWh): Energy throughput of the ESS
- Egrid (GWh): Remaining energy exchange with the grid
- Pmax (MW): Peak power of grid exchange
- Equiv. Cycles: Annual equivalent full cycles of the ESS

ww(h)	Pss(MW)	Ess(MWh)	Tss(h)	Thrpt(GWh)	Egrid(GWh)	Pmax(MW)	Equiv. Cycles
3	3.9	22	5.6	8.0	52.0	17.3	184
6	7.6	51	6.7	17.4	52.2	15.8	171
12	10.3	98	9.5	30.0	52.4	15.3	154
24	9.5	136	14.3	27.9	52.3	10.1	103
48	9.1	213	23.5	28.0	52.2	9.1	66
72	9.4	281	29.8	28.0	52.1	8.7	50
168	9.9	525	53.1	28.0	51.6	8.3	27

Table 90: DWPT only.

ww(h)	Pss(MW)	Ess(MWh)	Tss(h)	Thrpt(GWh)	Egrid(GWh)	Pmax(MW)	Equiv. Cycles
3	16.9	46	2.7	19.3	50.0	25.0	208
6	24.4	107	4.4	37.1	45.7	24.8	174
12	25.6	189	7.4	52.1	37.9	17.6	138
24	27.8	266	9.6	52.1	27.7	8.1	98
48	29.1	404	13.9	52.2	23.3	6.9	65
72	29.6	534	18.0	52.2	21.3	6.1	49
168	29.5	885	29.9	52.3	18.3	4.9	30

Table 91: Solar integration, Stockholm.

ww(h)	Pss(MW)	Ess(MWh)	Tss(h)	Thrpt(GWh)	Egrid(GWh)	Pmax(MW)	Equiv. Cycles
3	11.9	40	3.4	18.3	41.1	21.7	226
6	18.7	88	4.7	35.3	35.4	18.0	201
12	19.0	142	7.5	44.1	25.6	9.7	156
24	24.0	183	7.6	44.7	13.4	5.2	122
48	25.9	279	10.8	44.5	10.5	4.5	80
72	26.3	319	12.1	44.5	8.9	3.7	70
168	24.9	488	19.6	44.4	6.1	2.2	46

Table 92: Solar integration, Madrid.

ww(h)	Pss(MW)	Ess(MWh)	Tss(h)	Thrpt(GWh)	Egrid(GWh)	Pmax(MW)	Equiv. Cycles
3	16.1	46	2.8	15.4	55.8	21.4	168
6	19.8	108	5.5	25.4	53.7	20.9	118
12	24.7	228	9.3	36.1	50.4	19.3	79
24	27.9	425	15.2	39.4	46.1	16.8	46
48	26.9	786	29.2	45.3	40.4	15.4	29
72	27.5	1113	40.5	48.5	35.7	14.8	22
168	29.2	2256	77.3	55.3	25.5	14.1	12

Table 93: Wind integration, generic.

ww(h)	Pss(MW)	Ess(MWh)	Tss(h)	Thrpt(GWh)	Egrid(GWh)	Pmax(MW)	Equiv. Cycles
3	14.9	43	2.9	14.7	51.8	19.9	171
6	18.7	102	5.4	24.1	49.7	19.5	119
12	23.3	214	9.2	33.4	46.7	17.8	78
24	26.1	397	15.2	36.4	42.8	16.1	46
48	24.8	736	29.7	41.9	37.6	14.8	28
72	25.5	1043	40.8	44.9	33.1	14.0	22
168	27.0	2110	78.2	51.5	23.5	13.3	12

Table 94: Hybrid solar-wind integration, Stockholm.

ww(h)	Pss(MW)	Ess(MWh)	Tss(h)	Thrpt(GWh)	Egrid(GWh)	Pmax(MW)	Equiv. Cycles
3	10.2	36	3.5	16.4	34.8	19.3	227
6	15.8	80	5.0	31.2	29.4	17.4	196
12	15.5	132	8.5	37.2	21.6	10.7	140
24	18.4	196	10.6	37.5	13.8	5.7	96
48	21.3	307	14.4	37.6	11.3	4.9	61
72	22.4	393	17.6	37.7	9.7	4.6	48
168	21.6	612	28.4	38.0	6.7	3.8	31

Table 95: Hybrid solar-wind integration, Madrid.

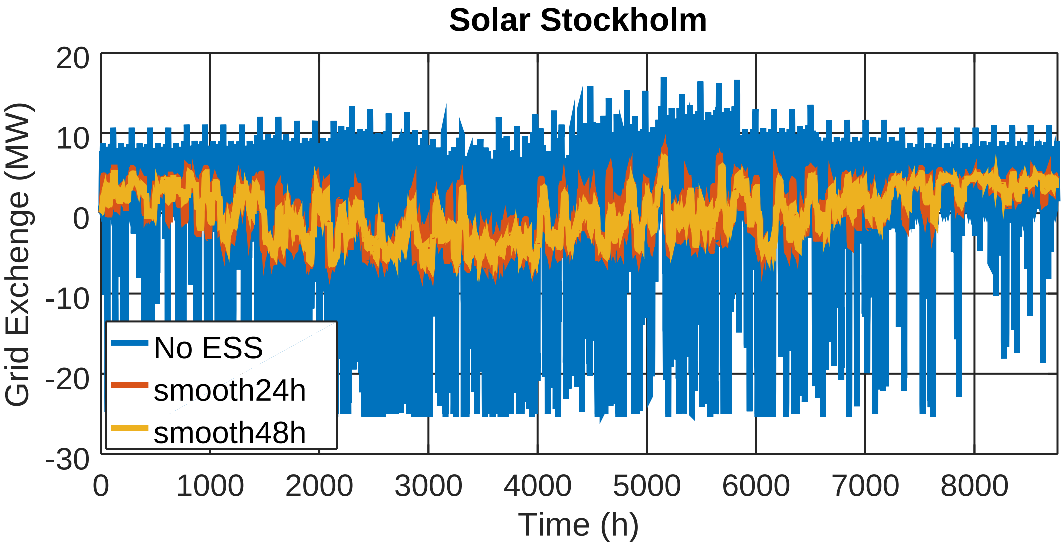
Solar Stockholm
Grid Exchenge (MW)
Time (h)
No ESS
smooth24h
smooth48h
20
10
0
-10
-20
-30
0
1000
2000
3000
4000
5000
6000
7000
8000

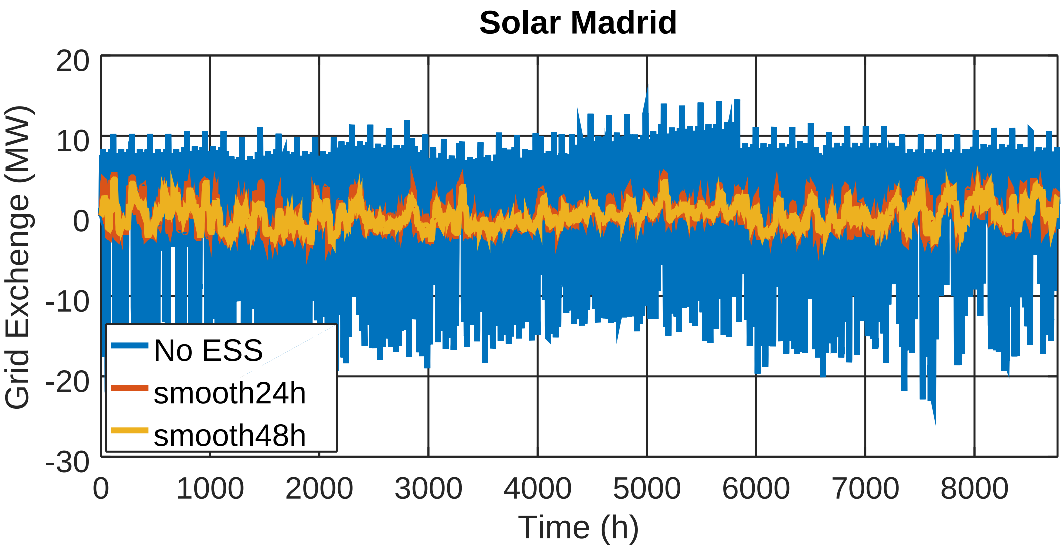
Solar Madrid
Grid Exchenge (MW)
Time (h)
No ESS
smooth24h
smooth48h
20
10
0
-10
-20
-30
0
1000
2000
3000
4000
5000
6000
7000
8000

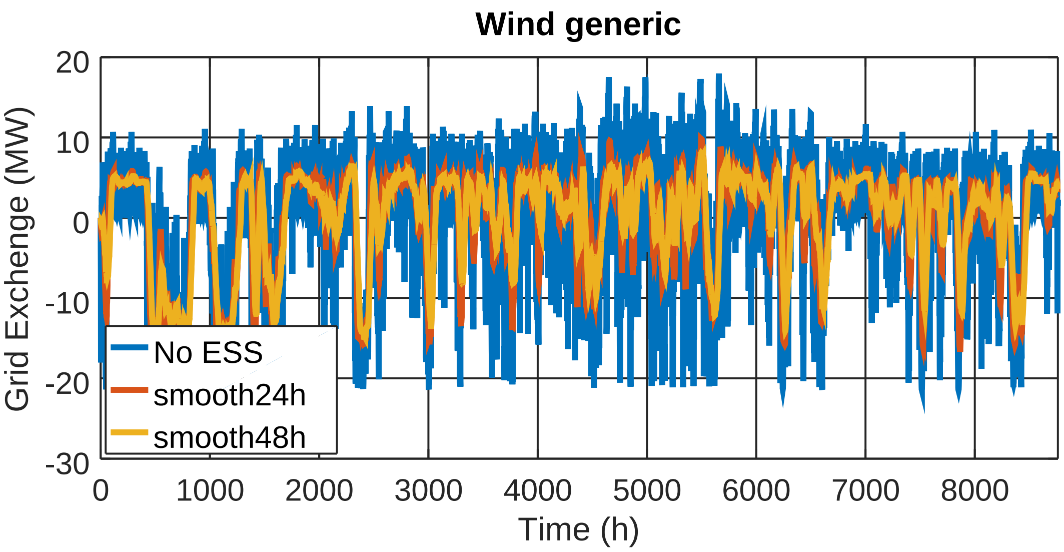
Wind generic
Grid Exchenge (MW)
Time (h)
No ESS
smooth24h
smooth48h
20
10
0
-10
-20
-30
0
1000
2000
3000
4000
5000
6000
7000
8000

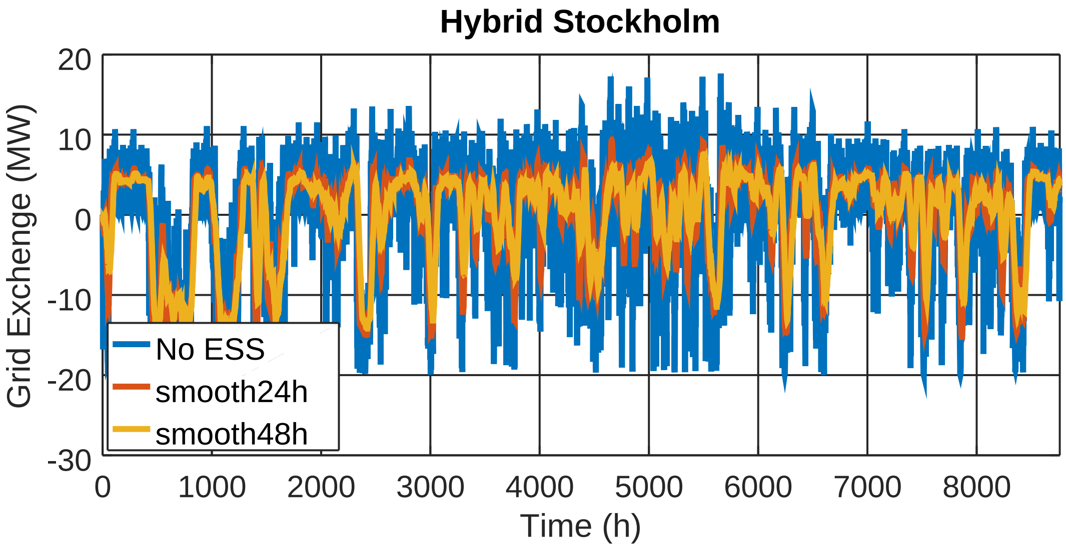
Hybrid Stockholm
Grid Exchenge (MW)
20
10
0
-10
-20
-30
0
1000
2000
3000
4000
5000
6000
7000
8000
Time (h)
No ESS
smooth24h
smooth48h

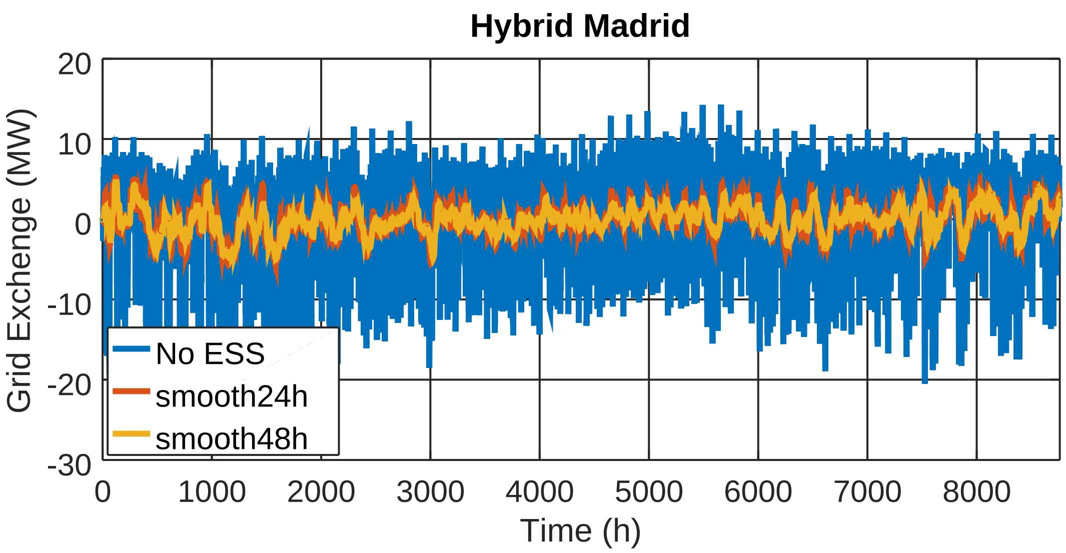
Hybrid Madrid
Grid Exchenge (MW)
20
10
0
-10
-20
-30
0
1000
2000
3000
4000
5000
6000
7000
8000
Time (h)
No ESS
smooth24h
smooth48h

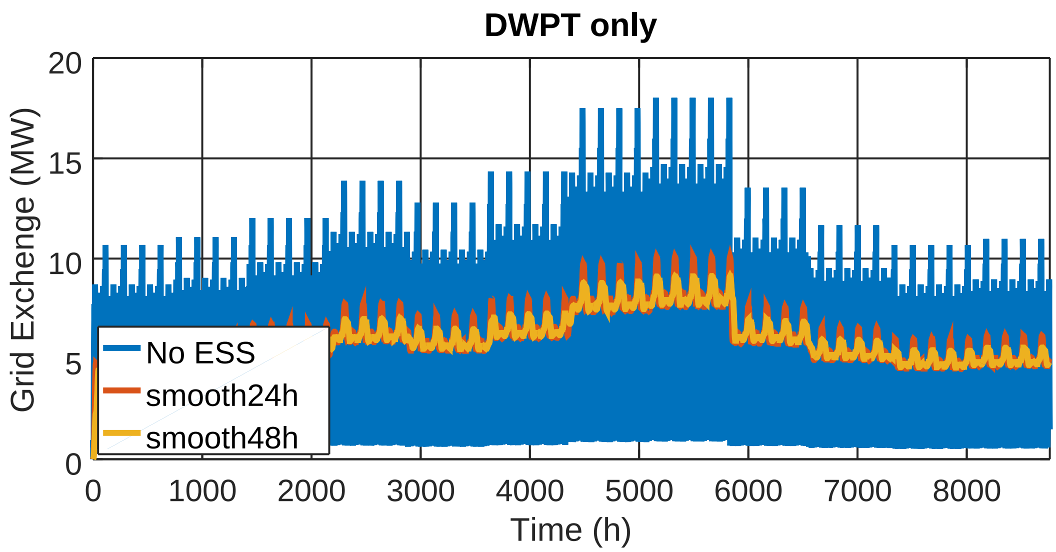
DWPT only
Grid Exchenge (MW)
20
15
10
5
0
0
1000
2000
3000
4000
5000
6000
7000
8000
Time (h)
No ESS
smooth24h
smooth48h